

# CIVIL ENGINEERING STUDIES

STRUCTURAL RESEARCH SERIES NO. 50



AD No. 11754

ASTIA FILE COPY

## EFFECT OF SMALL INITIAL IRREGULARITIES ON THE STRESSES IN CYLINDRICAL SHELLS

By

T. S. WU, L. E. GOODMAN

and

N. M. NEWMARK

Technical Report

to

OFFICE OF NAVAL RESEARCH

Contract N6ori-071(06), Task Order VI

Project NR-064-183

UNIVERSITY OF ILLINOIS  
URBANA, ILLINOIS

EFFECT OF SMALL INITIAL IRREGULARITIES ON  
THE STRESSES IN CYLINDRICAL SHELLS

by

T. S. Wu, L. E. Goodman and N. M. Newmark

A Technical Report  
Of A Cooperative Research Project

Sponsored by

THE OFFICE OF NAVAL RESEARCH

DEPARTMENT OF THE NAVY

and

THE DEPARTMENT OF CIVIL ENGINEERING

UNIVERSITY OF ILLINOIS

Contract N6ori - 07106, Task Order VI

Project NR-064-183

Urbana, Illinois  
7 April 1953

## TABLE OF CONTENTS

|  | Page |
|--|------|
| 1. INTRODUCTION . . . . .  | 1    |
| 1.1. General . . . . .   | 1    |
| 1.2. Acknowledgment . . . . .  | 5    |
| 2. CIRCULAR RING WITH SMALL INITIAL IRREGULARITIES . . .                     | 6    |
| 2.1. Recapitulation of Small-Deflection Theory . .                           | 6    |
| 2.1.1. Method of Analysis . . . . .  | 6    |
| 2.1.2. Illustrative Problems . . . . .                                       | 10   |
| 2.2. Large-Deflection Theory . . . . .                                       | 20   |
| 2.2.1. Method of Analysis . . . . .  | 20   |
| 2.2.2. Illustrative Problems . . . . .                                       | 34   |
| 2.3. Simplified Large-Deflection Theory . . . . .                            | 48   |
| 2.3.1. Method of Analysis . . . . .  | 48   |
| 2.3.2. Illustrative Problems. . . . .  | 53   |
| 3. CIRCULAR CYLINDRICAL SHELL WITH SMALL INITIAL<br>IRREGULARITIES . . . . . | 62   |
| 3.1. Basic Assumptions . . . . .   | 62   |
| 3.2. Fundamental Qualities . . . . .   | 65   |
| 3.3. Relations Between Stresses, Strains and<br>Displacements . . . . .      | 70   |
| 3.4. Equations of Equilibrium . . . . .                                      | 73   |
| 3.5. Method of Analysis . . . . .  | 76   |
| 3.6. Illustrative Problems . . . . .   | 84   |
| 4. CONCLUSIONS . . . . .   | 100  |
| 4.1. Summary . . . . .   | 100  |
| APPENDIX I. Nomenclature . . . . .   | 105  |
| BIBLIOGRAPHY . . . . .   | 109  |

# EFFECT OF SMALL INITIAL IRREGULARITIES ON THE STRESSES IN CYLINDRICAL SHELLS

## 1. INTRODUCTION

### 1.1. General

In the conventional small-deflection analysis of a thin circular cylinder under the action of uniform normal pressure, the internal stress developed in the tube is a constant circumferential force with no bending moment in either longitudinal or circumferential direction at any point. However, as is well known<sup>1</sup> (1, 2), if the uniform external pressure exceeds a certain limit known as the critical value, the cylinder will no longer maintain its circular shape. Buckling then occurs. In the problem which is under investigation in this manuscript it is assumed that the external pressure,  $p$ , is always less than this critical value,  $p_{cr.}$ , although the ratio  $p/p_{cr.}$  is not necessarily small compared with unity.

If the cross section of a cylinder deviates from the circular shape due to defects of manufacture, imperfect fabrication,

---

1. Numbers in parentheses, unless otherwise identified, refer to the Bibliography at the end of this report.

improper handling, or the action of external forces or shock, the strength of the tube is considerably reduced because bending moment is introduced. The most common imperfections in tubes are an initial ellipticity and local dents. Since the failure of cylinders under uniform external pressure depends very much upon the various kinds of imperfections in them, it seems quite important to investigate the effect of such imperfections on the strength of tubes.

When the initial irregularity is uniform along the length of the tube, the problem becomes a two-dimensional one and a method of analysis for a circular ring with initial irregularities can be applied to a tube by substituting the flexural rigidity of a shell,  $D = Eh^3/12(1 - \nu^2)$ , for the  $EI$  of a ring.

Theoretical investigations on the subject of a circular ring with initial irregularities have been made by M. Marbec (3), S. Timoshenko (4), M. A. Thuloup (5) and G. Salet (6). M. Marbec originated an elegant method for solving this problem, using small-deflection theory. However, when the uniform external pressure is not small compared with its critical value, the deflections of the ring axis resulting from deformations due to external loads are of great significance in the final result. This significance arises from the fact that in an irregular ring the axial stress contributes to the bending moment. This contribution is ignored in small-deflection theory.

A theory of thin shells has been well established for many years. A. E. H. Love (7) contributed an especially important part of the literature by making a mathematical study of the subject

and presenting it in a comprehensive manner. This theory has been subjected to many reviews, one of the most recent of which is that due to W. R. Osgood and J. A. Joseph (8). The expressions for change of curvature and the equations of equilibrium given in this paper differ slightly from those derived by Love. However, under the assumption of inextensibility of the middle surface of the shell, and neglecting terms of a non-linear nature, the results derived by Love and by Osgood and Joseph are identical. Among other investigators who have contributed to the theory of thin shells, H. Neuber (9), J. Barthelemy (10), A. L. Goldenweiser (11), V. Z. Vlasov (12), H. L. Langhaar (13) and P. S. Epstein (14) may be mentioned.

Although the theoretical background of the three-dimensional case has been developed, the application of the theory to the problem of a cylindrical shell with initial imperfections has scarcely been touched. This may be due to the complicated nature of the mathematical expressions for the relations between strains, changes of curvature and displacements, and equations of equilibrium. So far as the writers know, only one paper, concerning a shell of variable radius, written by E. F. Burmistrov (15), bears directly on the point in question. It is of the utmost practical importance, therefore, to develop a method of analysis, even if it is a very approximate one, to investigate the effect of initial irregularities on the strength of cylindrical shells.

The present investigation is undertaken with two objectives; firstly, to develop a method of analysis, based on large-deflection theory, for a circular ring with initial out-of-roundness and,

secondly, to solve a practical three-dimensional problem for a thin cylindrical shell with small initial irregularities.

The first method of analysis presented in this report for a circular ring with initial irregularities, in which both large deflection and extension of the central line of the ring axis are taken into consideration, is a numerical approach which is a combination of two well-known procedures. A method of successive approximations in conjunction with the numerical procedure of integration, due to N. M. Newmark (16) is used. This method, which is applicable whether or not the initial imperfection is small and under any loading condition, has great generality. Due to the fact that the procedure involves a considerable amount of numerical computation, a simplified method for predicting the maximum bending moment developed in a ring subjected to uniform pressure is developed. The simplified method is approximate, but it is direct. The results obtained by these two methods check extremely well.

A problem of a cylindrical shell with a dent varying in magnitude along the longitudinal axis of the cylinder is also solved in this dissertation for a uniform-pressure load. By assuming that the initial irregularity is small and that its square can be neglected, all fundamental quantities, such as curvatures, strain and stress components, which, in general, have very complicated mathematical expressions, are expressed as comparatively simple forms. Three governing displacement equations of equilibrium for the case of a circular cylindrical shell under uniform pressure are obtained. They contain correction terms due to the

assumed initial irregularities. These equations are then solved and the predictions of the analysis investigated from an engineering point of view.

#### 1.2. Acknowledgment

This investigation has been part of a research project in the Civil Engineering Department of the University of Illinois, sponsored by the Mechanics Branch, Office of Naval Research, Department of the Navy, under contract N6ori-71, Task Order VI. This report is based on a dissertation submitted to the Graduate Faculty of the University of Illinois by T. S. Wu, in partial fulfillment of the requirements for the degree of Doctor of Philosophy in Engineering, 1952.

## 2. CIRCULAR RING WITH SMALL INITIAL IRREGULARITIES

### 2.1. Recapitulation of Small-Deflection Theory

#### 2.1.1. Method of Analysis

In this theory several assumptions are made:

(1). The cross-sectional dimensions of the ring are assumed to be small in comparison with the unstrained radius of curvature. The stress distribution is, on any cross section then, nearly a linear one.

(2). The central line of the ring is regarded as inextensible. Any extension of the central line which might be produced by the given forces would be extremely small compared with the flexure actually produced.

(3). The uniform external pressure must be much less than the critical value and, therefore, the effect of the axial compressive force on the bending can be neglected.

(4). The deformations and displacements due to the action of external loads are very small compared with the dimensions of the ring concerned. Then the same dimensions can be used in the unstrained as in the strained state of the ring and the total deflections resulting from such deformations will usually be too small to modify the shape of the ring materially.

(5). The residual or initial stress due to the source of the imperfection is entirely disregarded.

Marbec's method, introduced in 1908, is the simplest and the most convenient one for the solution of the problem under investigation. It has also been derived, by R. Mayer (17) and

H. Neuber (18), using the method of arch analysis. It leads to the conclusion that in the case of a ring of any shape and of variable thickness, under the action of uniform pressure, the internal resisting forces and the internal bending moment acting at any point  $(x, y)$  on the ring are given by the expressions (Fig. 2.1.1.1):

$$H = -p(y - b), \quad V = p(x - a) \quad 2.1.1.1$$

and  $M = p(r_c^2 - \rho_c^2)/2 \quad 2.1.1.2$

where  $\rho_c^2 = (x - a)^2 + (y - b)^2$

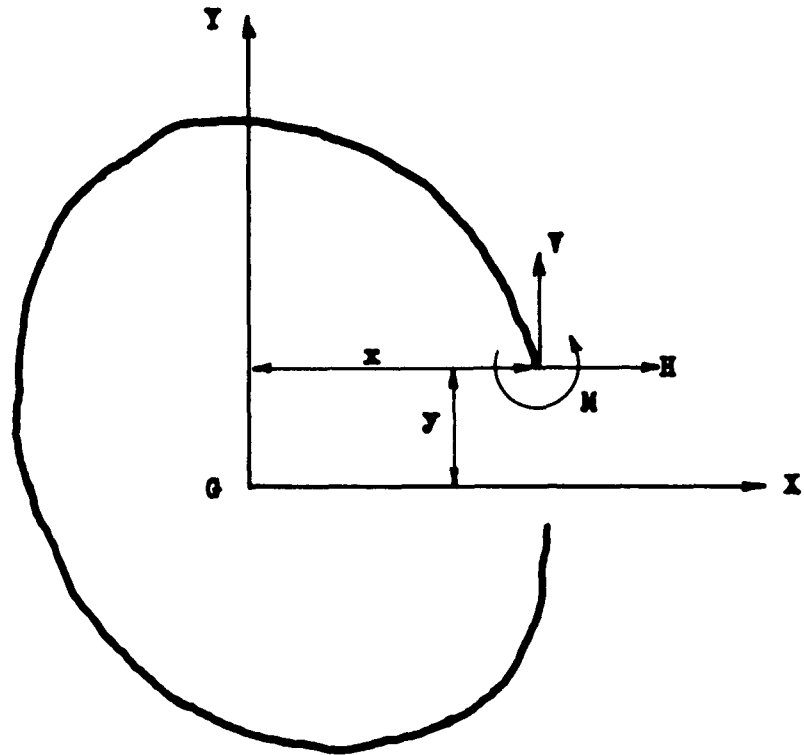
The symbols  $a$  and  $b$  represent the coordinates of the center of a "node" circle of radius  $r_c$ , and  $\rho_c$  is the distance from the point  $x, y$  to the point  $a, b$ . All coordinates are measured with respect to principal axes  $X, Y$  with origin at the centroid.

It can be seen that the bending moment at any point on the ring lying outside the node circle is positive; for points inside the node circle, bending moment is negative. The bending moment at any point on the node circle, i.e.  $\rho_c = r_c$ , is equal to zero; so that the node circle represents the funicular curve of the ring. The resultant of  $H$  and  $V$  is equal to  $p \times \rho_c$  and acts in a direction perpendicular to  $\rho_c$ .

The three unknown quantities  $a, b$  and  $r_c$  can be easily determined if the node circle is located. The coordinates of the center of the node circle with reference to the principal axes of a given shape of ring are:

$$a = [\int (x^2 + y^2) x ds / EI] / 2 [\int x^2 ds / EI] \quad 2.1.1.3$$

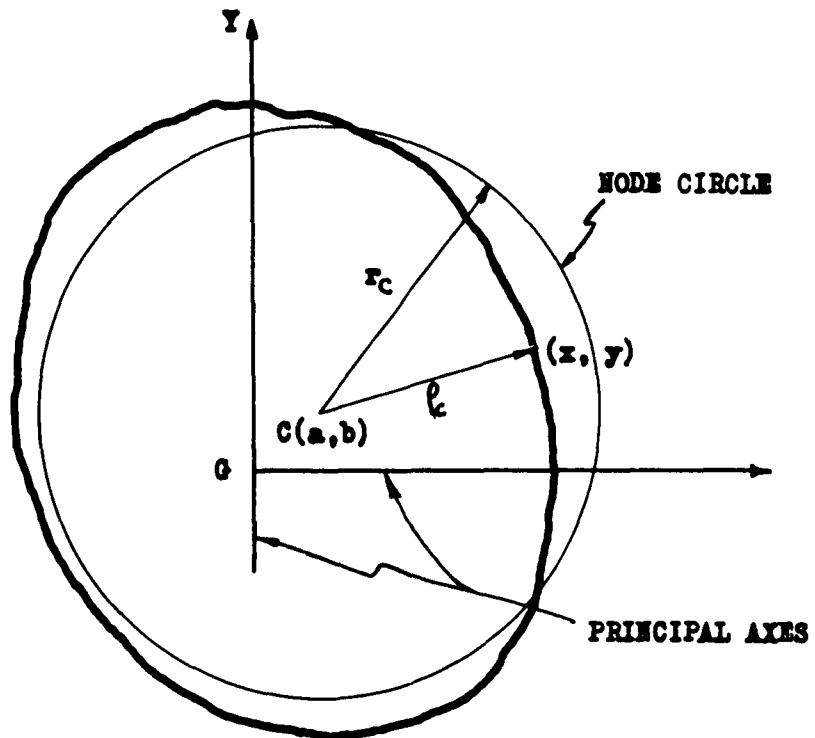
$$b = [\int (x^2 + y^2) y ds / EI] / 2 [\int y^2 ds / EI]$$



( a )

SIGN CONVENTIONS:

POSITIVE AS INDICATED



( b )

FIG. 2.1.1.1

NARDEC'S METHOD

The radius of the node circle is given by:

$$r_o^2 = (a^2 + b^2) + [\int (x^2 + y^2) ds / EI] / [\int ds / EI] \quad 2.1.1.4$$

All integrals are to be taken over the entire circumference of the ring.

It is evident that if the shape of a ring is symmetrical with respect to the x or y axis, a or b, respectively, will be equal to zero and, if the ring has two axes of symmetry, the center of the node circle C will coincide with the centroid G of the ring.

When the shape of a ring is known, the centroid of the given shape and its principal axes with reference to any arbitrary axes X' and Y' can be determined by the well-known expressions:

$$x'_G = [\int x' ds / EI] / [\int ds / EI] \quad 2.1.1.5$$

$$y'_G = [\int y' ds / EI] / [\int ds / EI]$$

$$\text{and } \tan 2\psi = [2 \int x' y' ds / EI] / \{ [\int (x')^2 ds / EI] - [\int (y')^2 ds / EI] \}$$

where  $\psi$  = angle between X and X' axes.

From the known coordinates (x, y) of any point on the ring with reference to its principal axes X and Y, the three quantities a, b, and  $r_o$  in Equations (2.1.1.3) and (2.1.1.4) can be evaluated by performing the integrations either analytically or numerically. Because of the complicated given shape of a ring, difficulty may be encountered in performing the integration of these quantities analytically. For this reason the numerical integration procedure due to N. M. Newmark (16), which yields quite accurate results

with a reasonable amount of work, is to be preferred in the majority of cases.

If the initial irregularity is very small, a further simplification can be made.

$$M = p [(r_c + \rho_c)/2] (r_c - \rho_c)$$

Since the initial irregularity is very small,  $r_c$  and  $\rho_c$  differ from  $R_0$  only by a very small amount and, therefore, it can be assumed that  $(r_c + \rho_c)/2$  is approximately equal to  $R_0$ . Then,

$$M \approx pR_0 (r_c - \rho_c) \quad 2.1.1.6$$

Since the axial force in a perfect circular thin ring is  $pR_0$ , Equation (2.1.1.6) indicates that for small initial irregularities the bending moment at any point is equal to this force multiplied by the irregularity at that point measured with respect to the node circle. The bending moment, then, bears a linear relationship to the irregularity measured with reference to the node circle. The area between the node circle and the ring axis represents the bending moment diagram for the ring. From a geometric point of view the area bounded by the ring axis and the funicular curve (which is a circle) balance each other.

### 2.1.2. Illustrative Problems

To illustrate the application of the Marbec method to a circular ring with initial irregularities under the action of a uniform external pressure, two numerical problems are worked out. The first is the case of an elliptical ring while the second concerns a circular ring having two symmetrical local dents.

(1). Elliptical Ring

The equation of an elliptical ring is expressed by:

$$x^2/(.99R_o)^2 + y^2/(1.01R_o)^2 = 1 \quad 2.1.2.1$$

Since the ellipse has two axes of symmetry, the center of the node circle and the centroid of the ellipse coincide (Fig. 2.1.2.1).

Both a and b are zero and Equation (2.1.1.4) becomes

$$r_c^2 = [\int (x^2 + y^2) ds / EI] / [\int ds / EI] \quad 2.1.2.2$$

In order to simplify the numerical integration, Equation (2.1.2.1) is transformed from Cartesian into polar coordinates.

$$\rho^2 = (1.01R_o)^2 / (k^2 \cos^2 \varphi + \sin^2 \varphi) \quad 2.1.2.3$$

$$\text{and} \quad r_c^2 = [\int B \rho^2 d\varphi / EI] / [\int B d\varphi / EI] \quad 2.1.2.4$$

in which  $k = 1.01/.99$

$$\text{and} \quad B = [\rho^2 + (d\rho/d\varphi)^2]^{1/2}$$

Because of the double symmetry only one quarter of the ring need be considered. To illustrate the numerical method six equal angular divisions are taken in the quarter ring. It is of advantage to take all the divisions equal when possible, however, this is not necessary. The numerical values of  $\rho$  and  $r_c$  computed from Equation (2.1.2.3) and (2.1.2.4) respectively are given in Table (2.1.2.1). The maximum axial force, bending moment and the fiber stresses due to this maximum axial force and bending moment are given in Table (2.1.2.4).

(2.). Circular Ring with Two Symmetrical Local Dents

A circular ring with two symmetrical local dents is shown in Fig. (2.1.2.2). The dented portion for  $-\varphi_o \leq \varphi \leq \varphi_o$  and

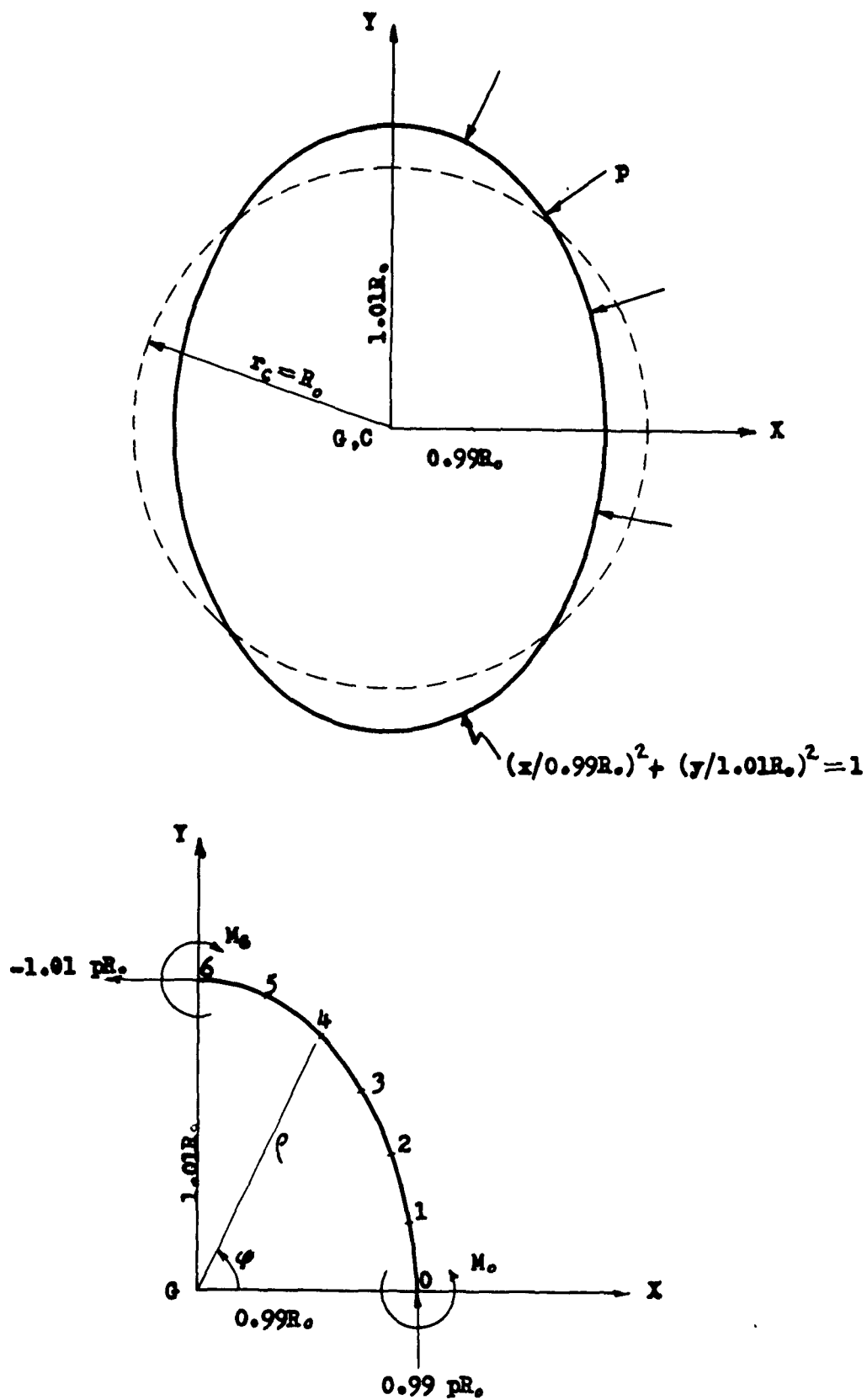


FIG. 2.1.2.1

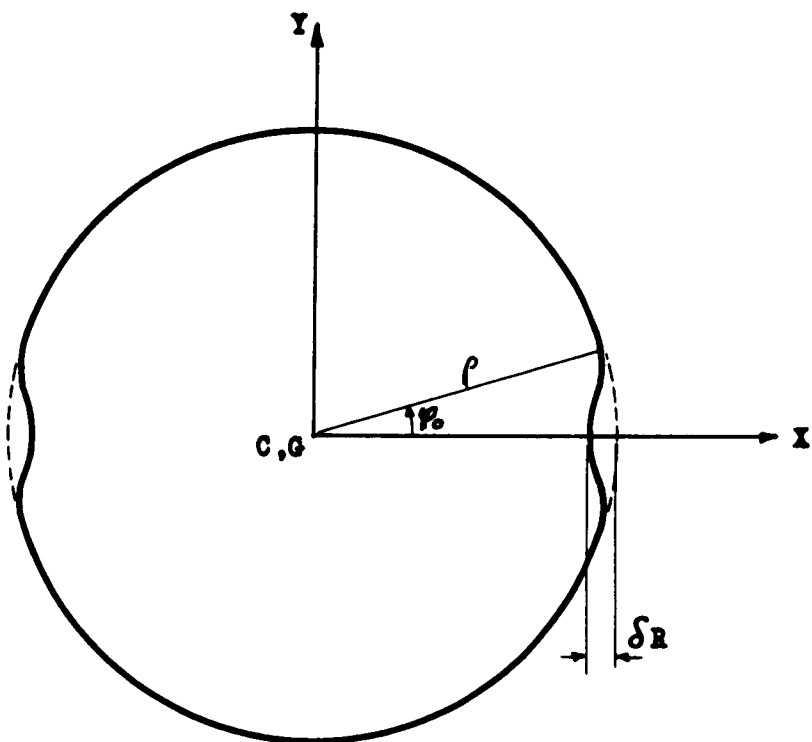
ELLIPTICAL RING

| Point  |          | $\varphi$                  | $\rho/R_0$ | $\rho^2/R_0^2$ | $B/R_0$  | $B\rho^2/R_0^3$ |          |                                  |   |   |   |   |          |
|--|----------|----------------------------|------------|----------------|----------|-----------------|----------|----------------------------------|---|---|---|---|----------|
| 0  |          | 0°                         | 0.990000   | 0.980100       | 0.990000 | 0.970299        |          |                                  |   |   |   |   |          |
| 1  |          | 15°                        | 0.991303   | 0.982681       | 0.991351 | 0.974182        |          |                                  |   |   |   |   |          |
| 2  |          | 30°                        | 0.994888   | 0.989803       | 0.995035 | 0.984888        |          |                                  |   |   |   |   |          |
| 3  |          | 45°                        | 0.999850   | 0.999699       | 1.000050 | 0.999749        |          |                                  |   |   |   |   |          |
| 4  |          | 60°                        | 1.004887   | 1.009797       | 1.005040 | 1.014887        |          |                                  |   |   |   |   |          |
| 5  |          | 75°                        | 1.008622   | 1.017319       | 1.008674 | 1.026143        |          |                                  |   |   |   |   |          |
| 6  |          | 90°                        | 1.010000   | 1.020100       | 1.010000 | 1.030301        |          |                                  |   |   |   |   |          |
| 6  |          | 5                          | 4          | 3              | 2        | 1               | 1        | 1                                | 1 | 1 | 1 | 1 | 0        |
| $\Delta\varphi$  | 1        | 1                          | 1          | 1              | 1        | 1               | 1        | 1                                | 1 | 1 | 1 | 1 | $\pi/12$ |
| $B/\text{EI}$  | 1.010000 | 1.008674                   | 1.005040   | 1.000050       | 0.985035 | 0.991351        | 0.990000 | $R_0/\text{EI}$                  |   |   |   |   |          |
| Conc.  | 6.05867  | 12.10178                   | 12.05913   | 12.00057       | 11.94175 | 11.89854        | 5.94135  | $R_0^3\Delta\varphi/12\text{EI}$ |   |   |   |   |          |
| "  | 0.132180 | 0.264020                   | 0.263089   | 0.261812       | 0.260529 | 0.259586        | 0.129620 | $R_0/\text{EI}$                  |   |   |   |   |          |
| $\sum B\Delta\varphi/\text{EI}$  | 0        | 1.570836 $R_0/\text{EI}$   |            |                |          |                 |          |                                  |   |   |   |   |          |
| $B\rho^2/\text{EI}$  | 1.030301 | 1.026143                   | 1.014887   | 0.999749       | 0.984888 | 0.974182        | 0.970299 | $R_0^3/\text{EI}$                |   |   |   |   |          |
| Conc.  | 6.17765  | 12.30662                   | 12.17476   | 11.99726       | 11.82281 | 11.69700        | 5.82568  | $R_0^3\Delta\varphi/12\text{EI}$ |   |   |   |   |          |
| "  | 0.134775 | 0.268489                   | 0.265612   | 0.261740       | 0.257934 | 0.255189        | 0.127097 | $R_0^3/\text{EI}$                |   |   |   |   |          |
| $\sum B\rho^2\Delta\varphi/\text{EI}$  | 0        | 1.570835 $R_0^3/\text{EI}$ |            |                |          |                 |          |                                  |   |   |   |   |          |
| $r_c^2 = (1.570835/1.570836)R_0^2 - 1.000000r_c^2, \quad r_c = 1.000000 R_0$ |          |                            |            |                |          |                 |          |                                  |   |   |   |   |          |

TABLE 2.1.2.1 ELLIPTICAL RING WITH ELLIPTICITY  $e=1 - (0.99/1.01)$

13

TABLE 2.1.2.1 ELLIPTICAL RING WITH ELLIPTICITY  $e=1 - (0.99/1.01)$



$$\text{For } \varphi < \varphi_0 \quad \rho = R_0 (1 - \delta \cos \frac{3\pi\varphi}{2\varphi_0})$$

$$\text{For } \varphi > \varphi_0 \quad \rho = R_0$$

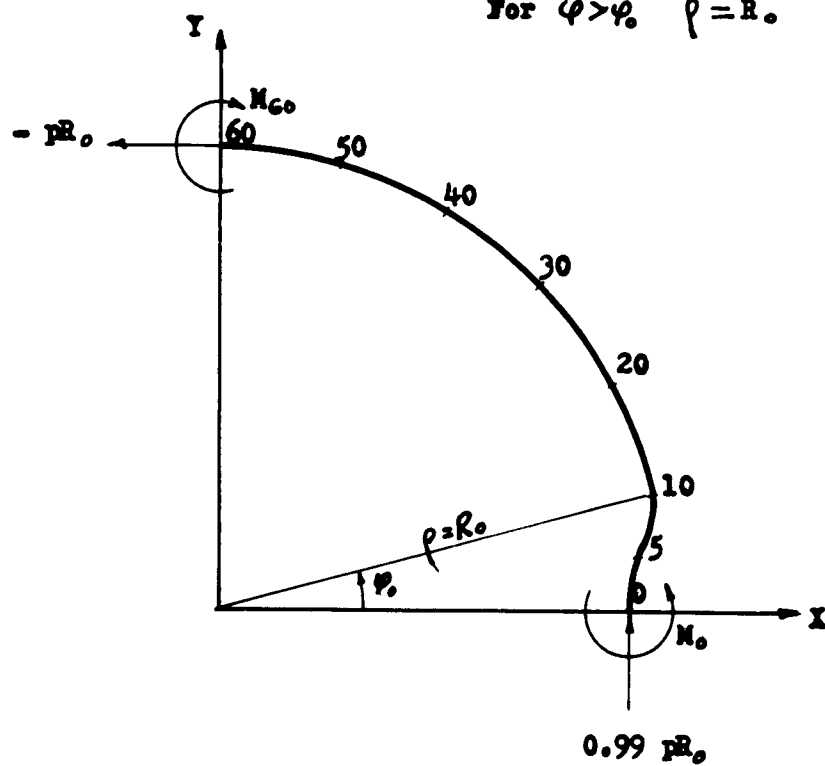


FIG. 2.1.2.2

CIRCULAR RING WITH TWO SYMMETRICAL DENTS

$\pi - \varphi_0 \leq \varphi \leq \pi + \varphi_0$  is defined by

$$\rho = R_0 (1 - \delta \cos^3 \pi \varphi / 2 \varphi_0) \quad 2.1.2.5$$

and for other values of  $\varphi$  ,  $\rho = R_0$  .

Here  $\delta$  and  $\varphi_0$  are two parameters which determine the depth of the dent and the angular area over which it extends.

As before, the ring has two axes of symmetry, a and b are equal to zero and  $r_0^2$  is given by Equation (2.1.2.4). One quarter of a ring with six equal angular divisions is again used. In order to take the effect of the dent into consideration, ten subdivisions are provided in the dented portion. For two cases  $\varphi_0 = 15^\circ$  ,  $\delta = 0.01$  and  $\varphi_0 = 15^\circ$  ,  $\delta = 0.1$  the numerical values of  $\rho$  and  $r_0$  computed from Equation (2.1.2.5) and (2.1.2.4) are given in Tables (2.1.2.2) and (2.1.2.3) respectively. The maximum axial force and bending moment and the fiber stresses for these two cases due to this maximum axial force and bending moment, are given in Table (2.1.2.4).

Examining the numerical results of these two illustrative problems shown in Table (2.1.2.4) it is interesting to note that, although the initial irregularity of the ring is very small (1/100 of the radius), the maximum fiber stress due to bending moment is from three to six times as great as that due to axial force. The maximum total fiber stress in a ring with an initial irregularity of this magnitude is magnified four to seven times that in a perfect circular ring for  $R_0/h = 50$  or 100. If the initial irregularity increases to 1/10 of the radius, the maximum total fiber stress is from 28 to 54 times that in a perfect circular

ring. This shows the great importance of initial irregularity from the point of view of safety in design.

The formula for bending moment given by Equation (2.1.1.2) is exact. The approximate formula for bending moment given by Equation (2.1.1.6) is only applicable to cases in which the initial irregularity is very small. When the initial irregularity of a ring ranges from  $1/100$  to  $1/10$  of the radius, the discrepancy between the 'exact' bending moment and the approximate one varies from 0.5% to 5%. For most practical cases, therefore, the approximate formula (Equation 2.1.1.6) can be used without introducing serious error.

In the above mentioned illustrative problems, it has been assumed that the ring under investigation has a uniform cross section so that the quantity  $EI$  is a constant and can be taken as unity in numerical calculations. If the thickness of a ring varies along its circumference, the average value of  $EI$  for every division in the numerical integration should be evaluated. The values of  $B$  and  $B\rho^2$  divided by the corresponding values of  $EI$  for the different divisions are then to be used in the integration. All other steps remain unchanged.



| Ring                           |                 |     | Initial Ellipticity<br>$e = 1 - (0.99/1.01)$ | Two Symmetrical Dents              |                                   |
|--------------------------------|-----------------|-----|--|------------------------------------|-----------------------------------|
|                                |                 |     |  | $\phi_0 = 15^\circ, \delta = 0.01$ | $\phi_0 = 15^\circ, \delta = 0.1$ |
| Point                          |                 |     | 6  | 0                                  | 0                                 |
| $H/pR_0$                       |                 |     | 1.010000                                     | 0                                  | 0                                 |
| $V/pR_0$                       |                 |     | 0  | 0.990000                           | 0.900000                          |
| $r_c/R_0$                      |                 |     | 1.000000                                     | 0.999296                           | 0.992901                          |
| $M/pR_0^2$                     |                 |     | 0.010050                                     | 0.009246                           | 0.087926                          |
| Approx. $M/pR_0^2$             |                 |     | 0.010000                                     | 0.009296                           | 0.092900                          |
| $\frac{\sigma_m}{p}$           |                 | 50  | 150.8  | 138.7                              | 1319                              |
|                                |                 | 100 | 603.0  | 554.8                              | 5276                              |
| $\frac{\sigma_N}{p}$           | $\frac{R_0}{h}$ | 50  | 50.50  | 50.00                              | 50                                |
|                                |                 | 100 | 101.0  | 100.0                              | 100                               |
| $\frac{\sum \sigma}{(pR_0/h)}$ |                 | 50  | 4.0  | 3.8                                | 27.3                              |
|                                |                 | 100 | 7.0  | 6.5                                | 53.7                              |

$\sigma_m$  = Fiber stress due to maximum bending moment

$\sigma_N$  = Fiber stress due to maximum axial force

$\sum \sigma$  = Total maximum fiber stress

$pR_0/h$  = Fiber stress due to axial force in perfect circular rings

TABLE 2.1.2.4

MAXIMUM STRESSES IN RINGS

## 2.2. Large-Deflection Theory

### 2.2.1. Method of Analysis

The method of analysis presented in this section for the stress analysis of a circular ring with initial irregularities subjected to uniform normal pressure is a numerical approach by means of which both large deflections and extension of the ring axis can be taken into consideration. It is also applicable to a ring of variable thickness under any loading condition.

In this investigation it is not assumed that the uniform normal pressure is small compared with its critical value. Two assumptions (1) and (5) of Article (2.1.1) are still used, however, in the present discussion.

When a ring is acted on by a system of external forces, there will always be a certain displacement of the ring axis. The relation between loads and displacements can be made clear by consideration of the physical behavior of the ring axis during deformation. The external forces induce in the ring internal stresses which, in turn, cause rotations as well as axial and shearing deformations throughout the ring axis. A deformation in any part of the ring axis is accompanied by a corresponding displacement of the ring axis, these two being interconnected by geometric relations. The effect of shear on displacement, in the case of a thin ring, is very small and will, therefore, be neglected in all the subsequent discussions. The displacements of the ring axis modify its original shape and consequently change the line of application of external loads. In a stable situation, the ring will reach a final equilibrium state.

In large-deflection theory, the deflection of the ring axis due to lengthening or shortening must be considered in setting up equations of equilibrium and equations of geometric continuity. Before the ring can be analyzed according to large-deflection theory, it is therefore necessary to set up the equations for deflections in terms of the known and unknown forces causing the deflection.

(1). Relation Between Deformation and Stresses

Fig. (2.2.1.1) shows an element of a planar curved ring in its final or deformed state. Under the action of external loads internal stresses, which are developed in the fibers, can be represented by a bending moment  $M$ , a normal force  $N$  acting through the centroidal axis on a cross section normal thereto and a shearing force  $Q$  acting parallel to the cross section.

The deformations, which are produced by the bending moment  $M$  and normal force  $N$ , consist of an extension of the ring axis and a rotation of the cross section. The bending moment is taken as positive when it decreases the initial curvature of a ring and the normal force is positive when it is tension. The angle change and deformation of the ring axis are considered as positive in the same sense as positive moment and normal force respectively.

In the case of a thin ring, the stress distribution over the cross section of the ring is nearly a linear one. Under these conditions, the centroidal axis coincides with the neutral axis of the ring. The extension of the ring axis due to rotation of the cross section produced by the bending moment is zero. The extension of the ring axis due to normal force is given by

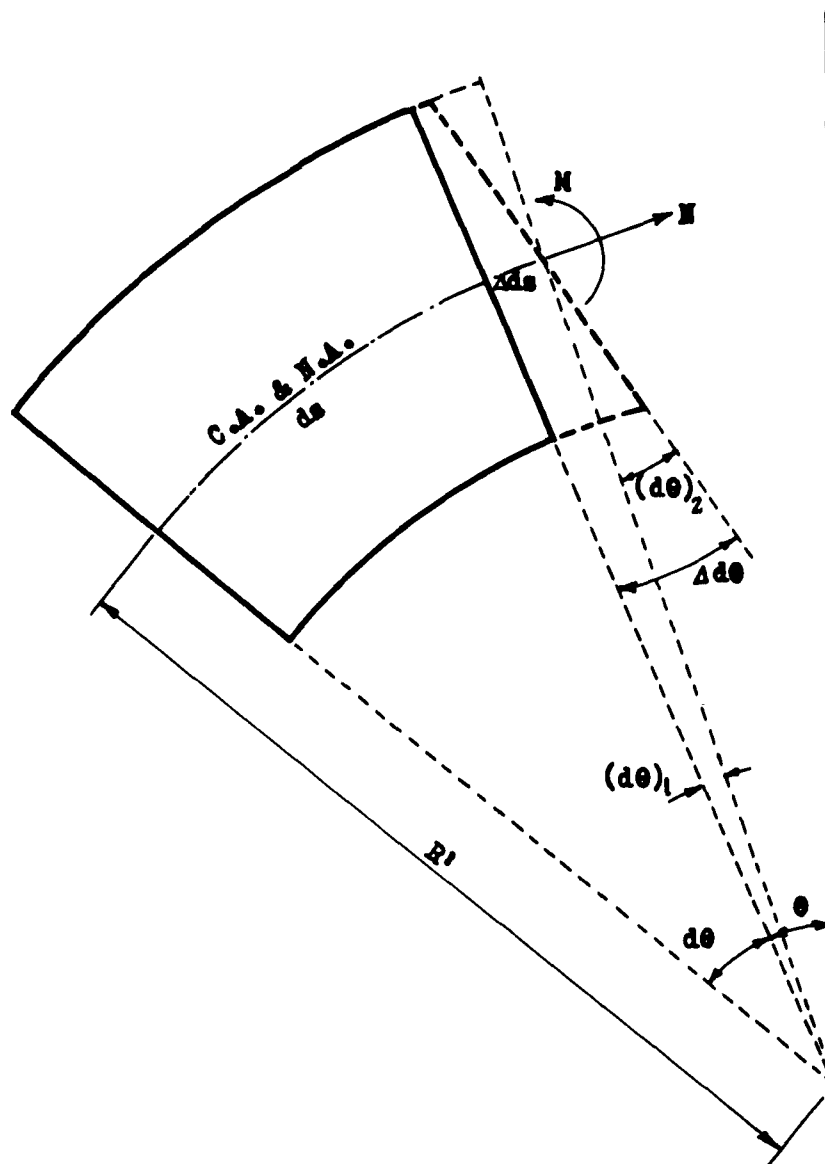


FIG. 2.2.1.1 DEFORMATIONS DUE TO INTERNAL STRESSES

$$\Delta ds = \epsilon ds = Nds/AE . \quad 2.2.1.1$$

The rotation of the cross section due to the extension of the ring axis can be expressed by

$$(\Delta d\theta)_1 = -\epsilon ds/R' = -Nds/AER' .$$

The rotation of the cross section due to bending moment is

$$(\Delta d\theta)_2 = Mds'/EI .$$

The total rotation is, then, equal to

$$\Delta d\theta = (Mds'/EI) - (\epsilon ds/R') . \quad 2.2.1.2$$

The curved length  $ds'$  and final curvature  $1/R'$  of an element in the deformed state can be found by following relations:

$$ds' = (1 + \epsilon) ds$$

$$\text{and} \quad (1/R') - (1/R) = (M/EI) - (\epsilon/R') \quad 2.2.1.3$$

Due to the fact that the value of  $\epsilon$  is very small compared with unity, an approximation which will not introduce appreciable error can be made by neglecting terms of higher order in  $\epsilon$ . Substituting Equations (2.2.1.3) into (2.2.1.2) we have

$$\Delta d\theta = (Mds/EI) - (\epsilon ds/R) . \quad 2.2.1.4$$

## (2). Relation Between Displacements and Deformations

In Fig. (2.2.1.2a),  $JJ_0$  represents the initial or undeformed state of an element of the ring axis. When it is acted by external loads,  $JJ_0$  will be deformed and displaced to  $J'J_0'$ . Due to the change in length  $\Delta ds$  and the change in slope  $\Delta\theta$  of the ring axis caused by deformation, there will be corresponding changes  $d\zeta$  and  $d\eta$  in the horizontal and vertical projection of the element respectively. As the deformations are small quantities

their effects on the total displacement may be considered independently and they can, therefore, be separately treated.

Let element  $JJ_0$  be shifted toward  $J'J_0$  until points  $J$  and  $J'$  coincide with each other (Fig. 2.2.1.2b). Let  $d\xi_1$  and  $d\eta_1$  be the deflections of element  $JJ_0$  due to extension of ring axis. Then,

$$d\xi_1 = \cos\theta \Delta ds = \epsilon \cos\theta ds \quad 2.2.1.5$$

$$d\eta_1 = \sin\theta \Delta ds = \epsilon \sin\theta ds$$

Let  $d\xi_2$  and  $d\eta_2$  be the deflections of  $JJ_0$  due to rotation of the element. When  $\Delta\theta$  is small, it can be assumed that  $\Delta J_0''J_0'J_1$  is similar to  $\Delta J_0'J'J_2$ . Then,

$$d\xi_2 = -\Delta\theta(dy + d\eta) \quad 2.2.1.6$$

$$d\eta_2 = \Delta\theta(dx + d\xi)$$

The total deflections, then, are given by

$$d\xi = -\Delta\theta(dy + d\eta) + \epsilon \cos\theta ds \quad 2.2.1.7$$

$$d\eta = \Delta\theta(dx + d\xi) + \epsilon \sin\theta ds$$

Consequently the rates of change of total deflection of the element  $JJ_0$  along  $ds$  are:

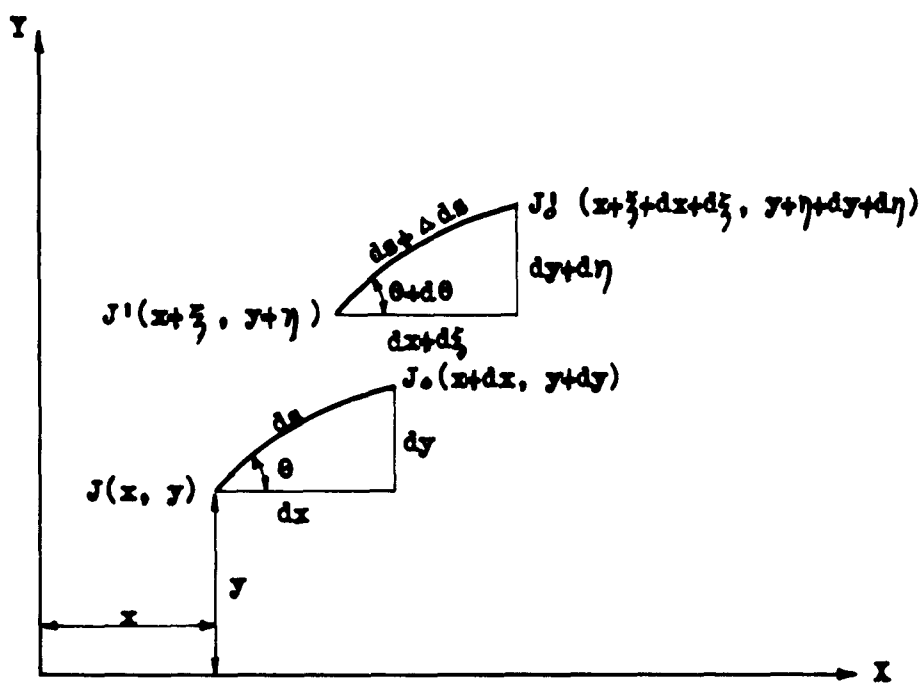
$$d\xi/ds = -\Delta\theta(\sin\theta + d\eta/ds) + \epsilon \cos\theta \quad 2.2.1.8$$

$$d\eta/ds = \Delta\theta(\cos\theta + d\xi/ds) + \epsilon \sin\theta$$

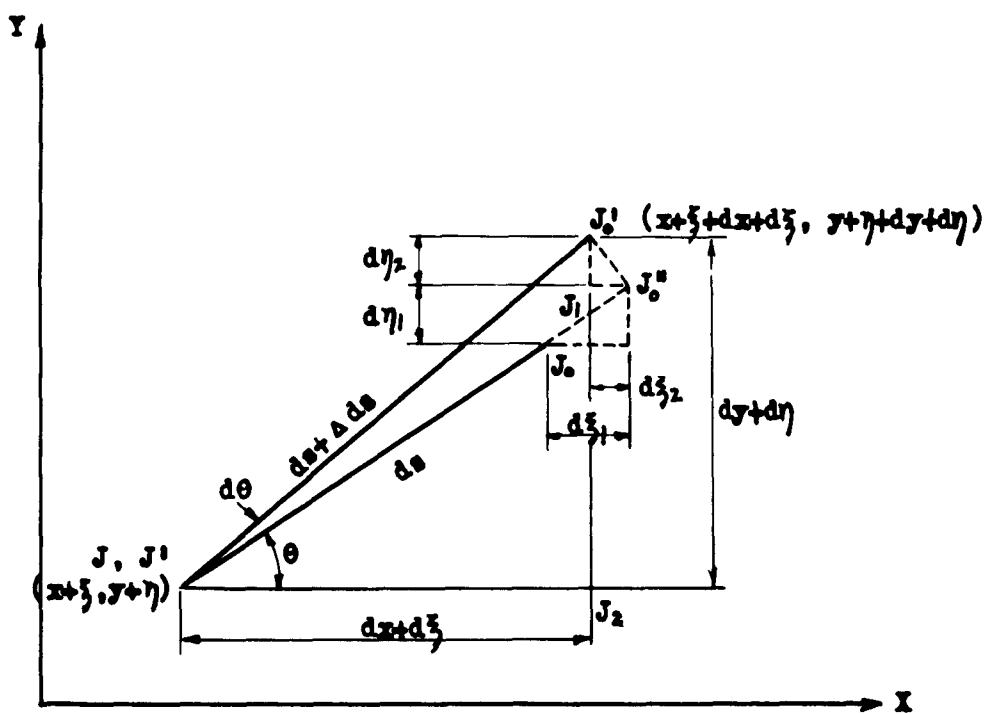
Solving the above two equations, we have

$$d\xi/ds = \{ -(1 + \epsilon)\Delta\theta \sin\theta - [(\Delta\theta)^2 - \epsilon] \cos\theta \} / [1 + (\Delta\theta)^2]$$

$$d\eta/ds = \{ (1 + \epsilon)\Delta\theta \cos\theta - [(\Delta\theta)^2 - \epsilon] \sin\theta \} / [1 + (\Delta\theta)^2]$$



( a )



( b )

FIG. 2.2.1.2

DISPLACEMENTS DUE TO DEFORMATIONS

The above two equations furnish the necessary relations between displacements and strains and rotations of an element of the ring axis. The term  $(\Delta\theta)^2$  which is usually disregarded in the small-deflection theory, will be included in the present investigation. In inextensible theory,  $\epsilon$  is taken equal to zero.

### (3). General Governing Equations

When a ring is subjected to external loads, it will deform and displace to its strained state. It is obvious that all external loads and internal forces, acting on any small element, must be in equilibrium and, furthermore, the displacements at any point due to the deformations must fulfill conditions of geometric continuity (conditions of compatibility).

The equations of equilibrium can be obtained by statics, but in order to establish the equations of compatibility the elastic deformation of the ring must be considered.

The rotation and displacements at a point  $J_0'$  measured with respect to a reference point  $J_1'$  are given by (Fig. 2.2.1.3):

$$\begin{aligned}\Delta\theta_{J_0'} &= \int_{J_1'}^{J_0'} d(\Delta\theta) \\ \xi_{J_0'} &= \int_{J_1'}^{J_0'} [-\Delta\theta (dy + d\eta) + \epsilon \cos\theta ds] \\ \eta_{J_0'} &= \int_{J_1'}^{J_0'} [\Delta\theta (dx + d\xi) + \epsilon \sin\theta ds]\end{aligned}\quad 2.2.1.10$$

On integrating the last two of Equations (2.2.1.10) by parts, they simplify to:

$$\begin{aligned}\xi_{J_0'} &= \int_{J_1'}^{J_0'} [(y + \eta) - (y_0 + \eta_0)] d(\Delta\theta) + \int_{J_1'}^{J_0'} \epsilon \cos\theta ds \\ \eta_{J_0'} &= \int_{J_1'}^{J_0'} [(x + \xi) - (x_0 + \xi_0)] d(\Delta\theta) + \int_{J_1'}^{J_0'} \epsilon \sin\theta ds\end{aligned}\quad \text{-----} 2.2.1.11$$

Since the ring is a closed one, points  $J_1'$  and  $J_0'$  can be chosen so as to be the same point. In order to provide geometrical continuity, the rotation and displacements at  $J_0'$  must be equal to zero. Substituting Equations (2.2.1.2) into the first equation of (2.2.1.9) and (2.2.1.11) and equating the rotation and displacements to zero, we have

$$\Delta\theta = \int M \frac{ds}{EI} - \int \frac{\epsilon ds}{R} = 0$$

$$\xi = \int M[(y+\eta) - (y_0+\eta_0)] \frac{ds}{EI} - \int \epsilon[(y+\eta) - (y_0+\eta_0)] \frac{ds}{R} + \int \epsilon \cos\theta ds = 0$$

$$\eta = \int M[(x_0+\xi_0) - (x+\xi)] \frac{ds}{EI} - \int \epsilon[(x_0+\xi_0) - (x+\xi)] \frac{ds}{R} + \int \epsilon \sin\theta ds = 0.$$

----- 2.2.1.12

The above three equations represent the conditions of compatibility.

Let the ring now be cut at point  $J_0'$ . Internal forces  $H_0$ ,  $V_0$  and  $M_0$  must exist at  $J_0'$  to produce continuity at that point (Fig. 2.2.1.3). The bending moment at any point  $J'$  can be written as

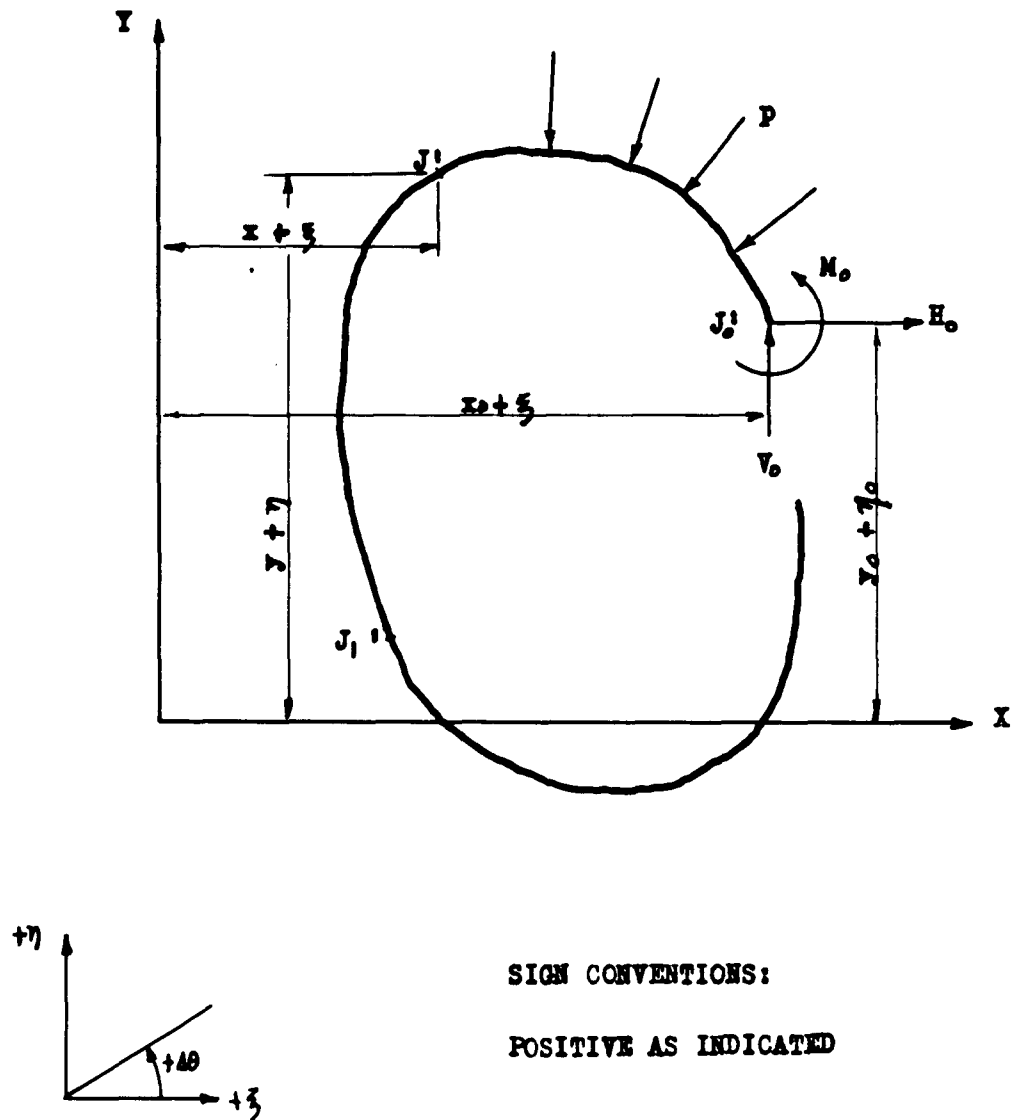
$$M = M_0 + H_0[(y+\eta) - (y_0+\eta_0)] + V_0[(x_0+\xi_0) - (x+\xi)] + m_s + \Delta m_s. \quad 2.2.1.13$$

In the case of a ring subjected to uniform external pressure, the static moment and its increments due to deflection of the ring axis will be:

$$m_s = -\frac{P}{2}[(x_0-x)^2 + (y-y_0)^2]$$

2.2.1.14

$$\Delta m_s = -p[(x_0-x)(\xi_0-\xi) + (y-y_0)(\eta-\eta_0) + \frac{1}{2}(\xi_0-\xi)^2 + \frac{1}{2}(\eta-\eta_0)^2]$$



SIGN CONVENTIONS:

POSITIVE AS INDICATED

FIG. 2.2.1.3

INTERNAL FORCES AT POINT  $J_1$

By substituting Equations (2.2.1.13) into (2.2.1.12) they become

$$\begin{aligned}\Delta\theta &= M_0 \int \frac{ds}{EI} + H_0 \int [(y-y_0) + (\eta-\eta_0)] \frac{ds}{EI} + V_0 \int [(x_0-x) + (\xi_0-\xi)] \frac{ds}{EI} \\ &\quad + \int m_s \frac{ds}{EI} + \int \Delta m_s \frac{ds}{EI} - \int \frac{\epsilon ds}{R} = 0 \\ \xi &= M_0 \int [(y-y_0) + (\eta-\eta_0)] \frac{ds}{EI} + H_0 \int [(y-y_0) + (\eta-\eta_0)]^2 \frac{ds}{EI} \\ &\quad + V_0 \int [(y-y_0) + (\eta-\eta_0)][(x_0-x) + (\xi_0-\xi)] \frac{ds}{EI} + \int m_s [(y-y_0) + (\eta-\eta_0)] \frac{ds}{EI} \\ &\quad + \int \Delta m_s [(y-y_0) + (\eta-\eta_0)] \frac{ds}{EI} - \int \epsilon [(y-y_0) + (\eta-\eta_0)] \frac{ds}{R} + \int \epsilon \cos \theta ds = 0 \\ \eta &= M_0 \int [(x_0-x) + (\xi_0-\xi)] \frac{ds}{EI} + H_0 \int [(x_0-x) + (\xi_0-\xi)][(y-y_0) + (\eta-\eta_0)] \frac{ds}{EI} \\ &\quad + V_0 \int [(x_0-x) + (\xi_0-\xi)] \frac{ds}{EI} + \int m_s [(x_0-x) + (\xi_0-\xi)] \frac{ds}{EI} \\ &\quad + \int \Delta m_s [(x_0-x) + (\xi_0-\xi)] \frac{ds}{EI} - \int \epsilon [(x_0-x) + (\xi_0-\xi)] \frac{ds}{R} + \int \epsilon \sin \theta ds = 0.\end{aligned}$$

----- 2.2.1.15

Equations (2.2.1.15), which furnish the conditions of geometrical continuity at any point, contain three unknown forces,  $H_0$ ,  $V_0$  and  $M_0$ , and two unknown displacements,  $\xi$  and  $\eta$ . Equations (2.2.1.9) furnish additional relations between forces and displacement components. These five independent equations are sufficient to determine the five unknowns. Any forces and deflection configurations which satisfy Equations (2.2.1.15) and (2.2.1.9) will automatically satisfy the equations of equilibrium and compatibility equations. It can be seen that if the displacements  $\xi$  and  $\eta$  and the extension  $\epsilon$  of the ring axis are neglected in Equations (2.2.1.15) these equations reduce to

well-known arch formulas.

Equations (2.2.1.15) and (2.2.1.9) which take the extension and deflection of the ring axis into consideration are applicable to a ring of any shape and subjected to any loading condition. In the present investigation, only uniform normal pressure is of interest.

When the uniform pressure acting on the ring is internal, a negative value of  $p$  is to be used in Equations (2.2.1.15).

From equations (2.2.1.15), it can be seen that all the integrals have physical meanings. In the first equation,

$\int ds/EI$  represents the angle-change between two points due to  $M_o = 1$

$\int [(\alpha_o - \alpha) + (\xi - \xi_o)] ds/EI$  represents the angle-change between two points due to  $V_o = 1$

$\int [(\gamma - \gamma_o) + (\eta - \eta_o)] ds/EI$  represents the angle-change between two points due to  $H_o = 1$

$\int (m_s + \Delta m_s) ds/EI$  represents the angle-change between two points due to  $m_s$

$\int \epsilon ds/R$  represents the angle-change between two points due to  $\epsilon$ . (angle-change = change in slope)

The quantities in the second and third equations represent the horizontal and vertical components of deflection between two points due to forces, static moment and the extension of the ring axis.

Due to the complexity of these two sets of equations, it is difficult to obtain an analytical solution for a general case. For this reason, a numerical approach which serves as a useful

tool to attack problems of this nature is suggested.

#### (4). Numerical Method

The method presented in this dissertation for the stress analysis of a circular ring with initial out-of-roundness under uniform normal pressure analyzed by large-deflection theory is a numerical procedure which, in turn, is a combination of two well-known procedures, namely, the numerical procedure of integration and the method of successive approximations due to N. M. Newmark (16).

The general processes of analysis can be summarized in the following steps:

(i). Divide the ring into a number of equal divisions along the curved length. As mentioned previously, in order to simplify the numerical integration, it is preferable to have equal angular divisions.

(ii). Evaluate all physical quantities such as slope, curvature, curved length factor ( $ds/d\varphi$ ), static moment, etc. at all division points. They will be encountered in the numerical integration. Most of these quantities can be readily calculated from the given equation of the ring. The static moment depends upon the loading condition as well as the geometrical shape of the ring.

(iii). Assume two deflection configurations,  $\xi$  and  $\eta$ , and neglect  $\epsilon$  in the first approximation.

(iv). All integrals in Equations (2.2.1.15) can now be evaluated numerically.

(v). Solve for forces  $H_0$ ,  $V_0$  and bending moment  $M_0$  by means of Equations (2.2.1.15).

(vi). From  $H_0$  and  $V_0$ , compute  $N$  and, in turn,  $\epsilon$  at all division points. Evaluate  $\int \epsilon ds/R$ .

(vii). Calculate the total angle-change,  $\Delta\theta$ , by integrating Equations (2.2.1.9). In solving actual problems the total angle-change at any two specified points can be obtained by summing up all components of angle change, due to forces, static moment and the extension of the ring axis, from the integrals in the first equation of (2.2.1.15) which have been evaluated in (iv).

(viii). Two derived deflection configurations,  $\xi$  and  $\eta$ , can be obtained by integration from Equation (2.2.1.9).

(ix). Repeat the procedures until the derived and assumed deflection configurations agree with each other.

In the case of a ring symmetrical about one axis (which is usually taken as one of the coordinate axes) only half of the ring has to be considered. The horizontal shearing forces at the two ends of the axis of symmetry are equal to zero. Since the vertical tangents at two ends remain vertical after deformation, the relative angle-change at one end with respect to the other is zero. Furthermore, the relative vertical displacement of one end with respect to the other is also zero. Two equations of geometrical continuity are sufficient to solve for the two unknowns.

When the ring has two axes of symmetry only one quadrant need be taken into consideration. Due to symmetry the shear at

both ends must be zero and the axial force can be expressed in terms of the known ordinate and unknown deflection of either end. The only unknown remaining is the bending moment which can be determined from the condition that the angle-change at one end with respect to the other end is zero.

The accuracy of the numerical integration, which determines the accuracy of the final result, depends greatly upon the nature of the function to be integrated and the number of divisions chosen along the ring axis. The more divisions chosen, the more accurate will the final result be. On the other hand more numerical computations are required. For most practical problems, six divisions in one quadrant of a ring will give reasonably accurate results. The equivalent concentration formulae due to N. M. Newmark (16) will yield quite accurate results with a reasonable amount of work.

The rate of convergence of the method of solution, which is an iterative procedure, depends on the correctness of the assumed deflection configuration and on the magnitude of the external pressure. A deflection configuration which can be used to hasten the convergence of the solution is obtained by multiplying the deflections determined by the small-deflection theory by the magnification factor  $1/(1 - p/p_{cr})$ . The same technique can be applied to a ring under internal pressure in which case the factor is  $1/(1 + p/p_{cr})$ . For some problems, the assumed deflections obtained in this manner will be very close to the correct ones. If the external pressure is much less than its critical value, the solution will converge rapidly whereas, if the external

pressure approaches its critical value, the rate of convergence is slower, as would be expected. For most cases a very accurate result can be achieved through four cycles of iteration.

### 2.2.2. Illustrative Problems

In order to illustrate the application of this numerical method to practical problems, circular rings with various kinds of imperfection are analyzed in this article.

In large-deflection theory, the magnitude of the uniform pressure acting on the ring must be specified. We consider the ring to be subjected to the action of a uniform external pressure of magnitude  $p = 1.5EI/R_o^3$  for all illustrative examples. This implies  $p/p_{cr.} = 0.5$ .

#### (1) Elliptical Ring

The elliptical ring, with ellipticity,  $e$ , equal to 1 - (0.99/1.01), illustrated in Article (2.1.2) (Fig. 2.1.2.1) will be more accurately analyzed using large-deflection theory.

Since the ring has two axes of symmetry, only one quadrant, taken with six equal angular divisions, need be investigated. It is evident that the tangents at division points 0 and 6 will remain vertical and horizontal respectively after straining. The total angle-change at point 0 with respect to point 6 is therefore equal to zero. Then,

$$M_o \int \frac{ds}{EI} + V_o \int [(x_o - x) + (\xi_o - \xi)] \frac{ds}{EI} + \int m_s \frac{ds}{EI} + \int \Delta m_s \frac{ds}{EI} - \int \frac{\epsilon ds}{R} = 0$$

From statics, the following relations can be written:

$$H_0 = 0, \quad H_6 = -p(y_6 + \eta_6)$$

and  $V_0 = p(x_0 + \xi_0), \quad V_6 = 0$

The integrals  $\int ds/EI$ ,  $\int m_s ds/EI$  and  $\int (x_0 - x) ds/EI$  in Equation (2.2.1.16) are constants and the others are function of  $\xi$  and  $\eta$ . Once the deflections  $\xi$  and  $\eta$  are either assumed or known, the forces  $H_6$ ,  $V_0$  and bending moment  $M_0$  can be easily found.

The slope of the tangent at any point on the ellipse (Fig. 2.2.1.4) is given by

$$\tan \theta = dy/dx = -(0.99/1.01)^2 x/y.$$

The values of  $\sin \theta$  and  $\cos \theta$  at division points which are required in integrating Equation (2.2.1.9) can be evaluated readily.

In case the extension of the ring axis is to be included in the investigation, one more numerical constant must be computed. The computed constant used in the present example,  $pR_0/EA = 0.0005$ , is based on these data:  $p = 30$  lbs per in.,  $R_0 = 50$  in.,  $h = 1$  in. and  $E = 30 \times 10^6$  lbs per sq. in. In the case of a thin ring, the stability effect usually predominates and the effect of extension of the ring axis is extremely small in comparison to that produced by flexure.

The initial curvature at any point is given by the expression

$$(1/R) = [ \rho^2 + 2 \left( \frac{d\rho}{d\phi} \right)^2 - \rho \frac{d^2\rho}{d\phi^2} ] / [ \rho^2 + \left( \frac{d\rho}{d\phi} \right)^2 ]^{3/2}.$$

The values of  $1/R$  at division points are necessary for performing

the integration  $\int \epsilon ds/R$ . The axial force  $N$  for use in computing  $\epsilon$  (Fig. 2.2.1.4) is given by  $N = -V \sin \theta + H \cos \theta$ .

As previously mentioned, the assumed deflection configuration which is used in the first approximation can be obtained by multiplying the deflection predicted by small-deflection theory by a magnification factor  $1/(1 - p/p_{cr.})$ . The lowest critical pressure for a circular ring under uniform external pressure is equal to  $3EI/R_0^3$ . In the present case the magnification factor is 2. After the bending moments and the forces  $H$  and  $V$  at division points have been calculated by Marbec's method [neglecting the terms  $(\Delta \theta)^2$  and  $\epsilon$ ] the angle-change  $\Delta \theta$  and the deflections  $\xi$  and  $\eta$  of small-deflection theory can be obtained by means of Equations (2.2.1.4) and (2.2.1.9) respectively. Multiplying these deflections by 2, a set of so-called 'magnified deflections' are obtained. These 'magnified' small-deflections are a very good approximation to the true or large deflections.

The numerical data involved in this method of analysis and comparisons of the results obtained by large-deflection and small-deflection theories are tabulated in Table (2.2.2.1).

From the analysis of this problem, it can be seen that the effect of the extensibility of the ring axis is extremely small.

## (2). Ring Having Shape of Third Buckling Mode

A ring having an irregularity corresponding to the shape of the third buckling mode of a circular tube is given by the expression

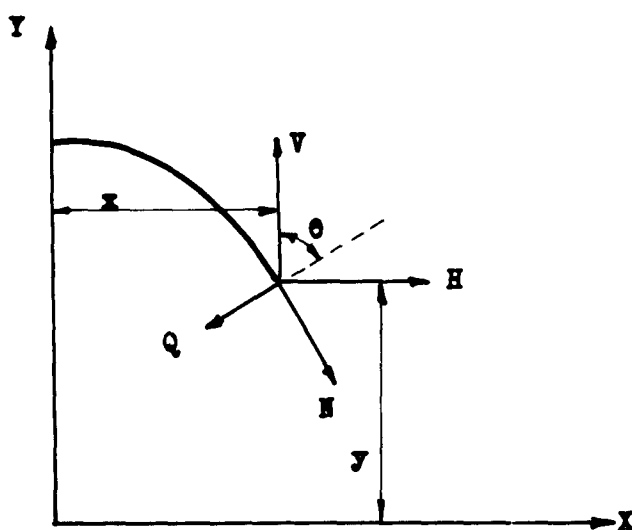
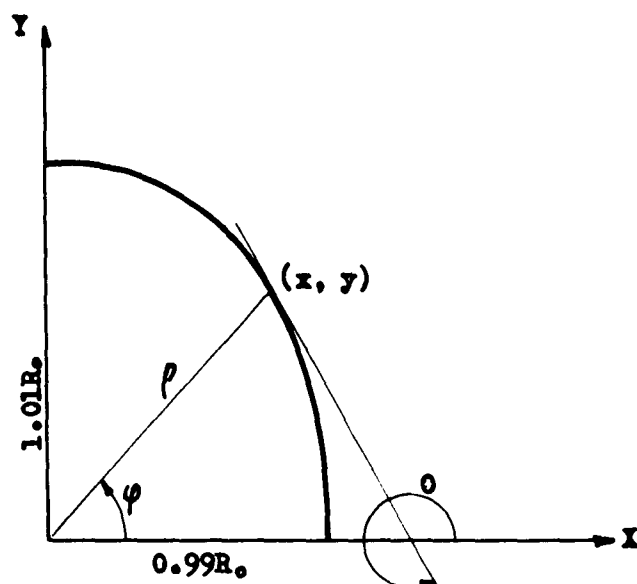


FIG. 2.2.1.4

ELLIPTICAL RING

| Point | slno     | cos $\theta$ | $1/R$<br>$R_0'$ | $\rho$<br>$R_0$ | $\tau$<br>$R_0$ | $\gamma$<br>$R_0$ | $m_2$<br>$R_0^2$ | $B$<br>$R_0$ | $A\theta_{\theta_0}=1$<br>$R_0/R_1$ | $B_{\theta_0}$<br>$R_0^2$ | $\Delta\theta_{\theta_0}$<br>$R_0^2$ | $7$<br>$R_0$ | $\Delta m_2$<br>$R_0^2$ | $B(\frac{\gamma_0-1}{R_0^2})$<br>$R_0^2/R_1$ | $A\theta_{\theta_0}=1$<br>$R_0^2/R_1$ | $B_{\theta_0}$<br>$R_0^2$ | $\Delta\theta_{\theta_0}$<br>$R_0^2$ | $\epsilon$     | $B/C$          | $A\theta_0$    |                |         |         |
|-------|----------|--------------|-----------------|-----------------|-----------------|-------------------|------------------|--------------|-------------------------------------|---------------------------|--------------------------------------|--------------|-------------------------|--|---------------------------------------|---------------------------|--------------------------------------|----------------|----------------|----------------|----------------|---------|---------|
| 0     | -1       | 0            | .970033         | .990000         | .930000         | 0                 | 0                | .990000      | 1.570804                            | 0                         | .567636                              | 0            | 0                       | 0  | 0                                     | .008864                   | 0                                    | $\sim 0.00816$ | $\sim 0.00010$ | $\sim 0.00047$ | .000079        |         |         |
| 1     | -968423  | .264713      | .973896         | .991303         | .937525         | .256568           | -.073441         | .991351      | 1.31153                             | .032194                   | .564815                              | .033152      | -.574682                | -.009190                                     | .000152                               | .000013                   | -.000793                             | .000880        | -.000013       | $\sim 0.00815$ | $\sim 0.00049$ | .000066 |         |
| 2     | -.874471 | .483079      | .984506         | .994888         | .861599         | .497444           | -.131969         | .995035      | 1.05156                             | .127764                   | .545219                              | .131314      | -.545253                | .006773                                      | .001131                               | .000169                   | .003251                              | .000291        | -.000148       | $\sim 0.00799$ | $\sim 0.00048$ | .000054 |         |
| 3     | -.721103 | .652828      | .999151         | .999850         | .707080         | .707000           | -.289569         | 1.00005      | .790413                             | .283014                   | .4492664                             | .289984      | -.500595                | -.007744                                     | .003268                               | .000568                   | .006246                              | .007047        | -.000568       | $\sim 0.00711$ | $\sim 0.00050$ | .000041 |         |
| 4     | -.515071 | .857147      | 1.01447         | 1.00489         | .502443         | .870257           | -.497530         | 1.00504      | .527933                             | -.490014                  | .392467                              | .500037      | .3398142                | -.001371                                     | .006117                               | .001177                   | .008663                              | .005076        | $\sim 0.01183$ | $\sim 0.00479$ | $\sim 0.00050$ | .000028 |         |
| 5     | -.268634 | .963242      | 1.02613         | 1.00662         | .261051         | .974254           | -.7440269        | 1.00867      | .264298                             | .773273                   | .232696                              | .7446691     | -.235527                | .000211                                      | .008598                               | .001333                   | .009863                              | .002627        | -.001346       | $\sim 0.00124$ | $\sim 0.01680$ | .000053 | .000014 |
| 6     | 0        | 1            | 1.03051         | 1.01000         | 0               | 1.01000           | 1.00010          | 1.01000      | 0                                   | .999900                   | 0                                    | -.101010     | 0                       | 0  | .009427                               | .000274                   | -.010090                             | 0              | .000277        | 0              | $\sim 0.01943$ | .000053 | 0       |

$$1.570836(R_M/MI) + (.99 - .009990)(PR^3/MI) + (-.577589 - .008864)(PR^3/MI) + .000079 = 0$$

$$M_{\odot} = .019577 \text{ PR}^2, \quad V_{\odot} = .980010 \text{ PR}, \quad H_{\odot} = 0$$

[illegible]

### TABLE 2.2.2.1

ELLIPTICAL RING WITH ELLIPTICITY  $e=1 - (0.99/1.01)$

$$\rho = R_o(1 - \delta \cos 6\varphi).$$

The shape is shown in Fig. 2.2.1.5. Two cases  $\delta = 0.01$  and  $\delta = 0.1$  are investigated. Since the ring is symmetrical with respect to both X and Y axes, only one quadrant need be investigated. Six equal angular divisions are used, as in previous examples.

The extension of the ring axis is assumed to be negligible in this example. The governing equation, then, becomes

$$M_o \int \frac{ds}{EI} + V_o \int [(x_o - x) + (\xi_o - \xi)] \frac{ds}{EI} + \int m_s \frac{ds}{EI} + \int \Delta m_s \frac{ds}{EI} = 0.$$

The curved length factor,  $B = ds/d\varphi$ , is given by

$$B = R_o(1 + 36\delta^2 - 2\delta \cos 6\varphi - 35\delta^2 \cos^2 6\varphi)^{\frac{1}{2}}.$$

The slope of the tangent to the ring axis at any point is expressed by the formula

$$\tan \theta = (1 - \delta \cos 6\varphi + 6\delta \sin 6\varphi \tan 6\varphi) / [6\delta \sin 6\varphi - (1 - \delta \cos 6\varphi) \tan 6\varphi].$$

For  $\delta = 0.01$ , the numerical data are tabulated in Table (2.2.2.2a). The final results for bending moment and deflection for both cases  $\delta = 0.01$  and  $\delta = 0.1$  are shown in Table (2.2.2.2b).

### (3). Circular Ring Having Two Symmetrical Dents

The circular ring having two symmetrical dents examined in Article (2.1.2) is re-analyzed using large-deflection theory in this article. Cases  $\varphi_o = 15^\circ$ ,  $\delta = 0.01$  and  $\varphi_o = 15^\circ$ ,  $\delta = 0.1$  under external and internal pressure are investigated. It is assumed that the extension of the ring axis is negligible.

The slope of the tangent to the ring axis at any point is

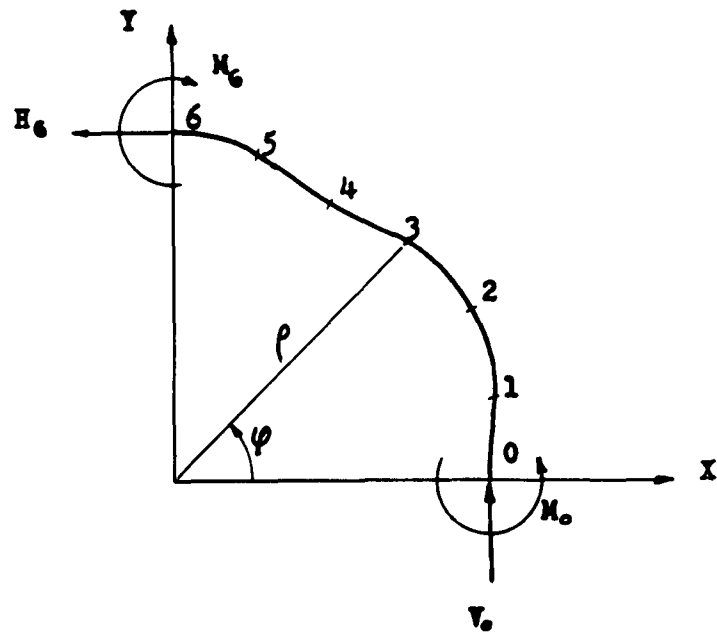
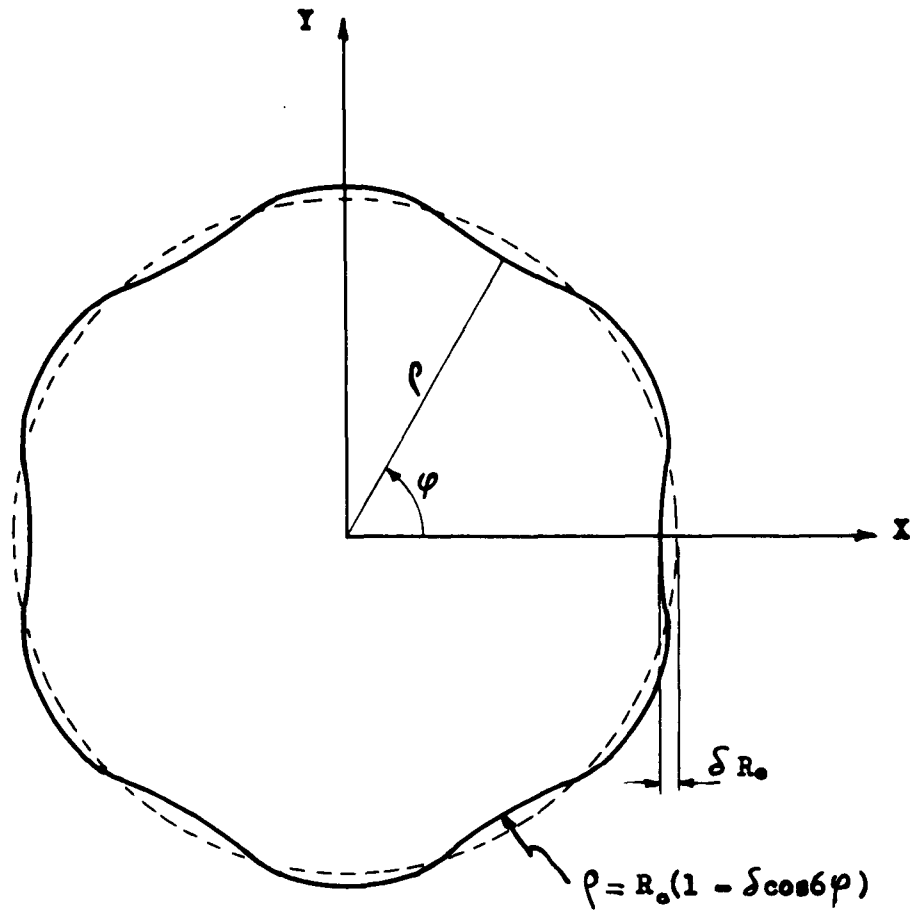


FIG. 2.2.1.5 RING HAVING THIRD BUCKLING MODE SHAPE



given by:

$$\text{for } \varphi < \varphi_0 \quad \tan \theta = (\rho + \frac{d\rho}{d\varphi} \tan \varphi) / (\frac{d\rho}{d\varphi} - \rho \tan \varphi)$$

$$\text{and } \varphi > \varphi_0 \quad \tan \theta = -x/y$$

Due to symmetry only six equal angular divisions in one quadrant of the ring (with ten subdivisions in the dented portion) need be investigated.

If the pressure acting on the ring is internal, the governing equations can be written as follows:

$$H_0 = 0, \quad H_6 = p(y_0 + \eta_0)$$

$$V_0 = -p(x_0 + \xi_0), \quad V_6 = 0$$

and

$$M_0 \int \frac{ds}{EI} + V_0 \int [(x_0 - x) + (\xi_0 - \xi)] \frac{ds}{EI} - \int m_s \frac{ds}{EI} - \int \Delta m_s \frac{ds}{EI} = 0$$

For rings such that the depth of the indentation is one-hundredth of the nominal radius,  $\delta = 0.01$ , subjected to external and internal pressure, numerical data are given in Tables (2.2.2.3) to (2.2.2.5) and the bending moments and deflections for all cases are tabulated in Tables (2.2.2.4b) and (2.2.2.5b). The bending moments and deflections of a ring under internal pressure in small-deflection theory are not given in the table. For small-deflection theory the distinction between internal and external pressure merely creates a change in sign.

It is quite interesting to note that the influence of deflection of the ring axis on the final bending moment and deflection is different for rings having various kinds of imperfections. For an elliptical ring having an ellipticity equal to 0.01, both the bending moments and deflections at division points

increase 100% compared with those given by small-deflection theory for  $p/p_{cr} = 0.5$ . On the other hand, in the case of a ring whose shape corresponds to the third buckling mode, the maximum bending moment is only a few percent greater than that obtained by Marbec's method. The deflection component, either horizontal or vertical, calculated from large-deflection equations also is unaffected. For the ring having two symmetrical dents, the maximum bending moment in the ring increases 17% for  $\delta = 0.01$  and 10% for  $\delta = 0.1$ . However, the horizontal deflection increases about 75% and the vertical deflection is about 110% greater than that predicated by small-deflection theory.

If the ring is acted on by internal pressure instead of external pressure, the axial tensile force developed in the ring tends to reduce the deflection produced by the internal pressure. Therefore, consideration of the deflection of the ring axis in the large-deflection theory will result in bending moments and deflections less than those predicted by small-deflection theory. In the analysis of the ring having two symmetrical dents, for cases  $\delta = 0.01$  and  $\delta = 0.1$ , the horizontal and vertical deflections are about 25% to 30% and 35% to 40% respectively less than those in the small-deflection case. The maximum bending moment drops off about 6% for  $\delta = 0.01$  and 12% for  $\delta = 0.1$ .

From the numerical data of illustrative problems analyzed by the large-deflection equations, besides noting that the extension of the ring axis is extremely small and can be neglected in the analysis, it is also worthwhile to point out that the changes of lines of application of uniformly distributed external

loads (due to the deflection of the ring axis) do not materially affect the magnitude of the bending moment. The effect of axial forces in the ring is the only essential one which does play a significant part in the final determination of bending moment and deflection. That effect is great

when (a)  $p / p_{cr}$  is large, say greater than 0.2.

and (b) The irregularity resembles the oval shape of the lowest bucking mode of a circular ring.

TABLE 2.2.2.3 CIRCULAR RING HAVING TWO SYMMETRICAL LOCAL DENTS ( INTERNAL PRESSURE )

For  $\varphi < 15^\circ$   $\rho = R_o(1 - \delta \cos^3 \varphi)$   
 $\varphi > 15^\circ$   $\rho = R_o$

| Point | sin $\theta$ | cos $\theta$ | $\varphi$ | $\rho$<br>$R_o$ | $x$<br>$R_o$ | $y$<br>$R_o$ | $m_z$<br>$R_o^2$ | $B$<br>$R_o$ | $A\theta \rho_{\theta=1}$<br>$R_o^2/MI$ | $B(x_o-x)$<br>$R_o^2$ | $A\theta \rho_{\theta=1}$<br>$R_o^2/MI$ | $Bm_z$<br>$R_o^2$ | $\Delta\theta m_z$<br>$R_o^2/MI$ | $\xi$<br>$R_o$ | $\eta$<br>$R_o$ | $\Delta m_z$<br>$R_o^2$ | $B(\xi_o-\xi)$<br>$R_o^2$ | $\Delta\theta \rho_{\theta=1}$<br>$R_o^2/MI$ | $Bm_z$<br>$R_o^2$ | $\Delta\theta m_z$<br>$R_o^2/MI$ |
|-------|--------------|--------------|-----------|-----------------|--------------|--------------|------------------|--------------|---|-----------------------|---|-------------------|----------------------------------|----------------|-----------------|-------------------------|---------------------------|--|-------------------|----------------------------------|
| 0     | -1           | 0            | 0         | .990000         | .990000      | 0            | 0                | .990000      | 1.569952                                | 0                     | .561969                                 | 0                 | -.570869                         | -.001657       | 0               | 0                       | 0                         | -.001703                                     | 0                 | .000054                          |
| 1     | -.999999     | -.001549     | 1.5       | .990365         | .990025      | .025925      | -.000336         | .990746      | 1.544027                                | -.000025              | .561969                                 | -.000333          | -.570866                         | -.001653       | -.000000        | -.000000                | -.000005                  | -.001703                                     | -.000000          | .000054                          |
| 2     | -.999999     | .001655      | 3.0       | .991398         | .990039      | .051886      | -.001346         | .992673      | 1.518065                                | -.000039              | .561970                                 | -.001334          | -.570845                         | -.001636       | "               | "                       | -.000021                  | -.001703                                     | "                 | -.000054                         |
| 3     | -.999912     | .013294      | 4.5       | .992926         | .989866      | .077904      | -.003035         | .995044      | 1.492046                                | .00134                | .561969                                 | -.003013          | -.570790                         | -.001610       | "               | "                       | -.000047                  | -.001702                                     | "                 | .000054                          |
| 4     | -.999035     | .043928      | 6.0       | .994705         | .989256      | .103975      | -.005406         | .997112      | 1.465968                                | .00740                | .561959                                 | -.005377          | -.570682                         | -.001576       | .000001         | "                       | -.000081                  | -.001700                                     | "                 | .000054                          |
| 5     | -.997748     | .067071      | 7.5       | .996464         | .987940      | .130065      | -.008461         | .998495      | 1.439844                                | .02053                | .561924                                 | -.008431          | -.570502                         | -.001535       | .000003         | "                       | -.000122                  | -.001698                                     | "                 | .000054                          |
| 6     | -.993345     | .115179      | 9.0       | .997969         | .985683      | .156117      | -.012196         | .999237      | 1.413693                                | .004309               | .561843                                 | -.012171          | -.570234                         | -.001489       | .000007         | "                       | -.000168                  | -.001694                                     | "                 | .000054                          |
| 7     | -.988743     | .149621      | 10.5      | .999064         | .982335      | .182065      | -.016603         | .999611      | 1.387527                                | .007658               | .561689                                 | -.016588          | -.569859                         | -.001441       | .000014         | -.000001                | -.000216                  | -.001689                                     | -.000001          | .000054                          |
| 8     | -.981416     | .191891      | 12.0      | .999705         | .977859      | .207850      | -.021675         | .999839      | 1.361355                                | .012137               | .561432                                 | -.021668          | -.569360                         | -.001391       | .000022         | -.000001                | -.000266                  | -.001683                                     | -.000001          | .000054                          |
| 9     | -.973376     | .229213      | 13.5      | .999962         | .972333      | .233436      | -.027402         | .999971      | 1.335177                                | .017667               | .561044                                 | -.027401          | -.568719                         | -.001341       | .000033         | -.000002                | -.000316                  | -.001675                                     | -.000002          | .000054                          |
| 10    | -.965926     | .258819      | 15.0      | 1               | .965926      | .258819      | -.033783         | 1            | 1.308977                                | .024074               | .560500                                 | -.033783          | -.567919                         | -.001290       | .000046         | -.000003                | -.000367                  | -.001666                                     | -.000003          | .000054                          |
| 20    | -.866025     | .500000      | 30.0      | 1               | .866025      | .500000      | -.132685         | 1            | 1.047198                                | .123975               | .542408                                 | -.132685          | -.547403                         | -.000794       | .000253         | -.000020                | -.000863                  | -.001503                                     | -.000020          | .000057                          |
| 30    | -.707107     | .707107      | 45.0      | 1               | .707107      | .707107      | -.290014         | 1            | .785398                                 | .282893               | .490318                                 | -.290014          | -.493230                         | -.000385       | .000564         | -.000040                | -.001272                  | -.001221                                     | -.000040          | .000065                          |
| 40    | -.500000     | .866025      | 60.0      | 1               | .500000      | .866025      | -.495050         | 1            | .523599                                 | .490000               | .390004                                 | -.495050          | -.391354                         | -.000126       | .000895         | -.000027                | -.001531                  | -.000851                                     | -.000027          | .000076                          |
| 50    | -.258819     | .965926      | 75.0      | 1               | .258819      | .965926      | -.733819         | 1            | .261799                                 | .731181               | .230756                                 | -.733819          | -.231054                         | -.000017       | .001147         | .000090                 | -.001640                  | -.000433                                     | .000090           | .000071                          |
| 60    | 0            | 1            | 90.0      | 1               | 0            | 1            | -.990050         | 1            | 0                                       | .990000               | 0                                       | -.990050          | 0                                | 0              | .001225         | .000413                 | -.001657                  | 0  | .000413           | 0                                |

$\varphi_o = 15^\circ$  &  $\delta = 0.01$

| Point | $\Delta\theta$ | $\frac{1}{r^2} \frac{d\theta}{d\varphi}$ | $\frac{d\theta}{d\varphi} \cos\theta$ | $\frac{d\theta}{d\varphi} \sin\theta$ | $\frac{d\theta}{d\varphi}$ | Point    | Large-Deflection Theory<br>$\varphi_0 = 15^\circ$ & $\delta = 0.1$ |            |           |           |            |           | Small-Deflection Theory<br>$\varphi_0 = 15^\circ$ & $\delta = 0.1$ |            |           |           |            |           |          |  |  |  |  |  |  |  |  |
|-------|----------------|--|---------------------------------------|---------------------------------------|----------------------------|----------|--|------------|-----------|-----------|------------|-----------|--|------------|-----------|-----------|------------|-----------|----------|--|--|--|--|--|--|--|--|
|       |                |  |                                       |                                       |                            |          | $\xi/R_0$  | $\eta/R_0$ | $M/R_0^2$ | $\xi/R_0$ | $\eta/R_0$ | $M/R_0^2$ | $\xi/R_0$  | $\eta/R_0$ | $M/R_0^2$ | $\xi/R_0$ | $\eta/R_0$ | $M/R_0^2$ |          |  |  |  |  |  |  |  |  |
| 0     | 0              | 1  | 0                                     | 0                                     | 0                          | 0        | -.001641   | 0          | .010864   | -.017560  | 0          | .101637   | -.000940   | 0          | .009249   | -.010140  | 0          | .007926   |          |  |  |  |  |  |  |  |  |
| 1     | -.000418       | .999999                                  | -.000418                              | .000001                               | -.000414                   | .000001  | 1  | -.001637   | -.000000  | .010498   | -.017524   | -.000008  | .098374  | -.000936   | -.000000  | .008887   | -.010110   | -.000007  | .008636  |  |  |  |  |  |  |  |  |
| 2     | -.000809       | .999999                                  | -.000809                              | -.000001                              | -.000803                   | -.000001 | 2  | -.001621   | -.000000  | .009459   | -.017392   | -.000062  | .089037  | -.000923   | -.000000  | .007864   | -.009997   | -.000052  | .075250  |  |  |  |  |  |  |  |  |
| 3     | -.001150       | .999999                                  | -.001150                              | -.000014                              | -.001145                   | -.000014 | 3  | -.001595   | .000000   | .007917   | -.017165   | -.000190  | .074990  | -.000901   | .000000   | .006347   | -.009805   | -.000158  | .661161  |  |  |  |  |  |  |  |  |
| 4     | -.001426       | .999998                                  | -.001425                              | -.000061                              | -.001421                   | -.000060 | 4  | -.001561   | .000001   | .006115   | -.016843   | -.000383  | .058296  | -.000873   | .000001   | .004580   | -.009535   | -.000316  | .044475  |  |  |  |  |  |  |  |  |
| 5     | -.001631       | .999997                                  | -.001628                              | -.000107                              | -.001625                   | -.000107 | 5  | -.001521   | .000003   | .004321   | -.016440   | -.000606  | .041382  | -.000840   | .000003   | .002828   | -.009202   | -.000493  | .027657  |  |  |  |  |  |  |  |  |
| 6     | -.001770       | .999997                                  | -.001759                              | -.000201                              | -.001757                   | -.000201 | 6  | -.001477   | .000007   | .002773   | -.015978   | -.000802  | .026545  | -.000805   | .000006   | .001327   | -.008832   | -.000643  | .013028  |  |  |  |  |  |  |  |  |
| 7     | -.001860       | .999997                                  | -.001840                              | -.000275                              | -.001839                   | -.000275 | 7  | -.001430   | .000013   | .001627   | -.015485   | -.000924  | .015431  | -.000768   | .000011   | .000234   | -.008447   | -.000731  | .002240  |  |  |  |  |  |  |  |  |
| 8     | -.001905       | .999996                                  | -.001871                              | -.000362                              | -.001870                   | -.000362 | 8  | -.001381   | .000022   | .000931   | -.014983   | -.000957  | .008632  | -.000731   | .000017   | -.000406  | -.008068   | -.000749  | -.004128 |  |  |  |  |  |  |  |  |
| 9     | -.001935       | .999996                                  | -.001884                              | -.000440                              | -.001884                   | -.000440 | 9  | -.001332   | .000032   | .000615   | -.014483   | -.000904  | .005553  | -.000695   | .000025   | -.000663  | -.007705   | -.000703  | -.006697 |  |  |  |  |  |  |  |  |
| 10    | -.001957       | .999996                                  | -.001891                              | -.000503                              | -.001891                   | -.000503 | 10   | -.001282   | .000045   | .000517   | -.013985   | -.000796  | .017545  | -.000660   | .000034   | -.000702  | -.007354   | -.000620  | -.007074 |  |  |  |  |  |  |  |  |
| 20    | -.002031       | .999996                                  | -.001761                              | -.001012                              | -.001761                   | -.001012 | 20   | -.000797   | .000248   | -.000143  | -.008802   | .001288   | -.002073   | -.000361   | .000156   | -.000701  | -.004133   | .000732   | -.007074 |  |  |  |  |  |  |  |  |
| 30    | -.001836       | .999997                                  | -.001301                              | -.001296                              | -.001301                   | -.001296 | 30   | -.000391   | .000556   | -.000826  | -.004296   | .004564   | -.009622   | -.000160   | .000308   | -.000701  | -.001811   | .002875   | -.007074 |  |  |  |  |  |  |  |  |
| 40    | -.001388       | .999998                                  | -.000695                              | -.001207                              | -.000695                   | -.001201 | 40   | -.000130   | .000892   | -.001417  | -.001423   | .008125   | -.015370   | -.000049   | .000450   | -.000701  | -.000557   | .004079   | -.007074 |  |  |  |  |  |  |  |  |
| 50    | -.000745       | .999999                                  | -.000193                              | -.000719                              | -.000193                   | -.000719 | 50   | -.000018   | .001150   | -.001816  | -.000194   | .010876   | -.019527   | -.000006   | .000549   | -.000701  | -.000072   | .005202   | -.007074 |  |  |  |  |  |  |  |  |
| 60    | 0              | 1  | 0                                     | 0                                     | 0                          | 0        | 60   | 0          | .001231   | -.001941  | 0          | .011741   | -.020823   | 0          | .000579   | -.000701  | 0          | .005540   | -.007074 |  |  |  |  |  |  |  |  |

1.569952  $M_0 + (.99 - .001641)(.561969 - .001679) R_0^2 + (-.570869 + .000045) R_0^3 = 0$

$M_0 = .010864 R_0^2$ ,  $V_0 = .988359 R_0$ ,  $R_0 = 0$

(a)  $\varphi = 15^\circ$  &  $\delta = 0.01$

(b)

TABLE 2.2.2.4

CIRCULAR RING HAVING TWO SYMMETRICAL LOCAL DENTS (EXTERNAL PRESSURE)

For  $\varphi < 15^\circ$   $\rho = R_0(1 - \delta \cos^3 6\varphi)$   
 For  $\varphi > 15^\circ$   $\rho = R_0$



## 2.3. Simplified Large-Deflection Theory

### 2.3.1. Method of Analysis

Due to the fact that the numerical method devised for the large-deflection analysis of a circular ring having initial irregularities requires a considerable amount of numerical work, it has seemed necessary to develop a simplified method by means of which a rapid analysis of such problems can be made. In the case of a circular ring having initial out-of-roundness under the action of uniform normal pressure, either external or internal, a simplification is effected by using the bending moments predicted by the small-deflection theory and multiplying them by factors proportional to the relative amplitudes of the various buckling modes present in the original imperfect shape. The maximum bending moments calculated by this rapid method of analysis agree quite satisfactorily with the results obtained from the numerical solution of the large-deflection equations.

The basic concept of the method of analysis presented in this article is not entirely new. From the elementary theory of bending it is well known that if a beam is submitted to the action of lateral loads alone the deflection of the beam and the stress produced are proportional to the magnitudes of the loads. Small changes in the positions of the loads have only a small effect on deflections and stresses. Small deflections do not materially affect the bending moment in the beam and in the calculation of these quantities it is the usual practice to neglect entirely the deflections of the beam resulting from the action

of external loads.

In case axial and lateral loads act simultaneously, conditions are entirely different. The stresses and deflections are no longer proportional to the magnitude of the longitudinal force. A slight eccentricity in the application of the axial load or a slight deviation of the axis of the beam from a straight form may have a substantial effect on the deflections of the beam and on the stresses in it. The effect of small lateral deflections of the beam is no longer negligible and must be considered in the calculation of bending moments. When the magnitude of the axial compressive force approaches a certain limiting value, usually designated the 'critical' load, the deflection becomes very sensitive to small changes in the position of the point of application or in the magnitude of the axial load.

When a straight bar is under the simultaneous action of lateral and axial loads, the maximum bending moment or deflection is correctly obtained by using the bending moment or deflection produced by lateral loads alone multiplied by a certain factor. The value of this factor depends only on the magnitude of the ratio of axial load to its critical value. It approaches unity as the compressive force becomes smaller and smaller. It increases indefinitely when the compressive force approaches the critical value. Without introducing serious error, the factor can be replaced by a well-known simple form,  $1/(1 - p/p_{cr})$ .

A ring subjected to the action of uniform pressure corresponds to the case of a curved beam under the simultaneous

action of lateral and axial loads the latter of which is unknown in magnitude and varies along the ring axis. Although the ring problem is more complicated than the case of a straight bar, the fundamental idea is still valid. Due to the presence of axial forces in the ring, small deflections of the ring axis, resulting from the action of external pressure, have an important effect on the final deflections and bending moments. We can say that the maximum bending moment or maximum deflection which is produced by the action of uniform pressure, can be obtained by multiplying the bending moment or deflection obtained from small-deflection theory by certain factors. The problem is how to determine the magnitudes of these factors and the way they are to be used.

Any closed curve defined by  $\rho = R_0 [1 - f(\varphi)]$  can be expanded in a Fourier series (19) of buckling mode shapes, as follows:

$$\rho = R_0 \left[ \left(1 - \frac{a_0}{2}\right) - \sum_{n=1,2,\dots}^{\infty} (a_n \cos n\varphi + b_n \sin n\varphi) \right] \quad 2.3.1.1$$

where

$$\begin{aligned} \frac{a_0}{2} &= \frac{1}{2\pi} \int_{-\pi}^{\pi} f(\varphi) d\varphi \\ a_n &= \frac{1}{\pi} \int_{-\pi}^{\pi} f(\varphi) \cos n\varphi d\varphi \\ b_n &= \frac{1}{\pi} \int_{-\pi}^{\pi} f(\varphi) \sin n\varphi d\varphi \end{aligned}$$

If the curve is symmetrical with respect to one coordinate axis, Equation (2.3.1.1) becomes

$$\rho = R_0 \left[ \left(1 - \frac{a_0}{2}\right) - \sum_{n=1,2,\dots}^{\infty} a_n \cos n\varphi \right]. \quad 2.3.1.2$$

In the case of a curve having two axes of symmetry, the odd modes in Equation (2.3.1.2) disappear.

This equation implies that a ring of any shape is equivalent to a sum of rings having the shapes of buckling modes. The bending moment for each mode shape can readily be determined by Marbec's method and the sum of the bending moments will be the total bending moment developed in the given ring. Considering the effect of deflection of the ring axis resulting from external pressure, the maximum bending moment developed in the ring can be obtained by summing up all the bending moments of the buckling mode shapes present in the original imperfect form multiplied by their proper magnification factors.

The critical pressure for a circular ring under uniform pressure, for each buckling mode shape, can be found by the formula:

$$p_{cr.} = (n^2 - 1)EI/R_0^3 \quad \text{for } n = 2, 3, 4, \text{ ----} \quad 2.3.1.3$$

The magnification factor for each buckling mode shape is therefore expressed by

$$F(n) = 1/(1 - p/p_{cr.}) = [1 - \lambda/(n^2 - 1)]^{-1} \quad 2.3.1.4$$

where  $\lambda = pR_0^3/EI$ .

The magnification factor given by Equation (2.3.1.4) is to be used in the simplified method.

For a given value of  $\lambda$  the magnification factor approaches unity for higher values of  $n$ , the mode order. For most practical cases, the magnification factors of a few of the lower order components are of importance; the others can be taken as

unity. The problem, then, is reduced to the determination of the bending moment predicted by small-deflection theory and a few components of the bending moment for the lower mode shapes.

If the ring has a shape which corresponds to a pure buckling mode, the bending moment in the ring involves only the one component of that mode. The maximum bending moment predicted by this rapid method of analysis is obtained by using the bending moment for the small-deflection case multiplied by one magnification factor corresponding to the particular buckling mode in question. If this mode is a higher one, the factor is approximately equal to unity; therefore, the maximum bending moment predicted by this method will differ very slightly from the bending moment predicted by small-deflection theory. This was observed to be the case for the ring treated as example (2) in Article (2.2.1) (see Table 2.2.2.2).

If the initial irregularity of a ring is very small, a further simplification can be made. As mentioned in Article (2.1.1), the bending moment at any point on a ring is equal to a constant force (the axial force in a perfect circular ring) multiplied by the amplitude of the irregularity at that point measured with respect to the node circle. The node circle is such that the areas, on either side of the ring, bounded by the ring axis and the node circle balance each other. Now in the Fourier expansion, the quantity  $R_o(1 - a_o/2)$  has a physical significance. The term  $a_o/2$  which is  $(1/2\pi) \int_{-\pi}^{\pi} f(\varphi) d\varphi$  represents a correction which will equalize the positive and negative areas bounded by the given curve  $f(\varphi)$  and a reference curve. In other

words, the radius of the node circle is  $R_o(1 - a_o/2)$ .

The expression  $\sum a_n \cos(n\varphi)$ , which is equal to  $R_o(1 - a_o/2) - \rho$ , also has a physical meaning. The coefficient of the expression,  $a_n$ , for different values of  $n$  will give the amplitude of the imperfection as far as the corresponding buckling mode shape is concerned. This quantity, for small imperfections, is proportional to the magnitude of the bending moment. In view of this simplification, even the small-deflection analysis is unnecessary and the only work required is that of expanding the given shape of the ring into a Fourier series. The coefficient of the zero'th mode then defines the radius of the node circle and the coefficient of the  $n$ 'th mode determines the bending moment in that mode.

The technique mentioned in this article is also applicable to the case of a ring subjected to the internal pressure. The 'magnification' factor, which is  $1/(1 + p/p_{cr})$  in this case, is less than unity.

### 2.3.2. Illustrative Problems

In order to illustrate the application of the simplified method of analysis developed in Article (2.3.1) to a practical problem, the same numerical examples given in Article (2.2.2) are reworked.

#### (1). Elliptical Ring (Fig. 2.1.2.1)

The ellipse  $(x/0.99R_o)^2 + (y/1.01R_o)^2 = 1$  differs very slightly from the lowest buckling mode shape,  $\rho = R_o(1 - 0.01\cos 2\varphi)$ . The bending moment in the elliptical ring is the sum of moments

for each of the mode shapes. The lowest, of course, predominates because it has both the largest  $a_n$  and the largest magnification factor. For simplicity, all other modes can be neglected without introducing appreciable error. The bending moment at point 6 predicted by the rapid method of analysis developed in this dissertation is simply the bending moment predicted by small-deflection theory multiplied by the magnification factor for the lowest mode. In other symbols,

$$M_6 = -.010050 R_o \times p R_o \times 1/(1 - 1/2) = -.020100 p R_o^2$$

This may be compared with a value of  $-.019829 p R_o^2$  obtained by the 'exact' large-deflection analysis. Since, however, the initial imperfection of the ring is very small the bending moment for small-deflection theory need not even be calculated. It may be considered that the expression  $\rho = R_o(1 - 0.01 \cos 2\varphi)$  describes the ellipse  $(x/0.99R_o)^2 + (y/1.01R_o)^2 = 1$ . Comparing two expressions

$$\rho = R_o \left[ \left(1 - \frac{a_0}{2}\right) - \sum a_n \cos n\varphi \right] \quad \text{and} \quad \rho = R_o (1 - 0.01 \cos 2\varphi)$$

it is evident that  $a_0 = 0$ ,  $a_2 = 0.01$ , and all other  $a_n = 0$ . It may be seen that the radius of the node circle is  $R_o$  and the irregularity at point 6 measured with respect to the node circle is equal to  $-0.01R_o$ . The axial force in a perfect circular ring is  $pR_o$  so that the approximate maximum bending moment at point 6 can be calculated as follows:

$$M_6 = -0.01 R_o \times p R_o \times 1/(1 - 1/2) = -0.0200 p R_o^2$$

(2). Ring Having Shape of Third Buckling Mode (Fig. 2.2.1.5)

Since the ring has a pure buckling mode shape, the bending moment developed in this ring contains only a single component. Using Marbec's method for the small-deflection analysis the following results are obtained:

$$\text{For } \delta = 0.01, \quad r_c = 1.000075 R_o, \quad M_o = 0.010025 pR_o^2$$

$$\text{and for } \delta = 0.1, \quad r_c = 1.006901 R_o, \quad M_o = 0.101925 pR_o^2$$

The magnification factor for the third buckling mode shape is  $1/(1 - 1.5/35) = 70/67$ . The maximum bending moment (at point 0) predicted by the simplified method is

$$\text{for } \delta = 0.01, \quad M_o = 0.010025 R_o \times pR_o \times 70/67 = 0.010474 pR_o^2$$

$$\text{and for } \delta = 0.1, \quad M_o = 0.101925 R_o \times pR_o \times 70/67 = 0.106488 pR_o^2$$

Since the initial irregularity is quite small, the approximate method can be applied. We do not even have to know the results of a small-deflection analysis. The equation of the ring is at once in the form of a Fourier series, with  $a_o$  equal to zero. The irregularity at point 0 with reference to the node circle equal to  $\delta R_o$ . Then,

$$\text{for } \delta = 0.01, \quad M_o = 0.01 R_o \times pR_o \times 70/67 = 0.010448 pR_o^2$$

$$\text{and for } \delta = 0.1, \quad M_o = 0.1 R_o \times pR_o \times 70/67 = 0.104478 pR_o^2$$

In this case the tedious 'exact' analysis (Table 2.2.2.2) yielded;

$$\text{For } \delta = 0.01, \quad M_o = 0.010339 pR_o^2$$

$$\text{and for } \delta = 0.1, \quad M_o = 0.104280 pR_o^2$$

(3). Ring Having Two Symmetrical Dents

The shape of a ring having two symmetrical dents is given by the expression (Fig. 2.1.2.2):

$$\rho = R_0 [1 - \delta \cos^3(\pi\varphi/2\varphi_0)] \quad \text{for } -\varphi_0 \leq \varphi \leq \varphi_0$$

$$\rho = R_0 \quad \text{for } \varphi_0 \leq \varphi \leq \pi - \varphi_0$$

$$\rho = R_0 [1 - \delta \cos^3(\varphi - \pi)\pi/2\varphi_0] \quad \text{for } \pi - \varphi_0 \leq \varphi \leq \pi + \varphi_0$$

$$\rho = R_0 \quad \text{for } \pi + \varphi_0 \leq \varphi \leq 2\pi - \varphi_0$$

Due to the symmetry of the ring with respect to two axes, the Fourier series expanded for this ring is given by Equation (2.3.1.5)

$$\rho = R_0 \left[ \left(1 - \frac{a_0}{2}\right) - \sum_{n=2,4,\dots}^{\infty} a_n \cos n\varphi \right] \quad 2.3.1.5$$

in which

$$\begin{aligned} \frac{a_0}{2} &= \frac{1}{2\pi} \left[ \int_{-\varphi_0}^{2\pi-\varphi_0} R_0 d\varphi - \delta R_0 \int_{-\varphi_0}^{\varphi_0} \cos^3 \frac{\pi\varphi}{2\varphi_0} d\varphi - \delta R_0 \int_{\pi-\varphi_0}^{\pi+\varphi_0} \cos^3 \frac{\pi}{2\varphi_0} (\varphi - \pi) d\varphi \right] \\ a_n &= \frac{1}{\pi} \left[ \int_{-\varphi_0}^{2\pi-\varphi_0} R_0 \cos n\varphi d\varphi - \delta R_0 \int_{-\varphi_0}^{\varphi_0} \cos^3 \frac{\pi\varphi}{2\varphi_0} \cos n\varphi d\varphi \right. \\ &\quad \left. - \delta R_0 \int_{\pi-\varphi_0}^{\pi+\varphi_0} \cos^3 \frac{\pi}{2\varphi_0} (\varphi - \pi) \cos n\varphi d\varphi \right]. \end{aligned}$$

Therefore

$$\frac{a_0}{2} = R_0 \left( 1 - \frac{8\delta}{3\pi} \cdot \frac{\varphi_0}{\pi} \right)$$

and

$$a_n = -\frac{48\delta R_0}{\pi} \cdot \frac{\varphi_0}{\pi} \cdot \frac{\cos n\varphi_0}{\left(1 - \frac{4n^2\varphi_0^2}{\pi^2}\right) \left(9 - \frac{4n^2\varphi_0^2}{\pi^2}\right)} \quad \text{for } n = 2, 4, \dots$$

The Fourier series of the ring is

$$\rho = R_0 \left[ \left(1 - \frac{8\delta}{3\pi} \cdot \frac{\varphi_0}{\pi}\right) - \frac{48}{\pi} \cdot \frac{\varphi_0}{\pi} \sum_{n=2,4,\dots}^{\infty} \frac{\cos n\varphi_0}{\left(1 - \frac{4n^2\varphi_0^2}{\pi^2}\right) \left(9 - \frac{4n^2\varphi_0^2}{\pi^2}\right)} \cos n\varphi \right].$$

(1).  $\varphi_0 = 15^\circ$  and  $\delta = 0.01$

By substituting  $\varphi_0 = 15^\circ$  and  $\delta = 0.01$  into Equation (2.3.1.6), we have

$$\rho = R_0 \left[ (1 - 0.000707) - 0.012732 \sum_{n=2,4,\dots}^{\infty} \frac{\cos \frac{n\pi}{12}}{(1 - \frac{n^2}{36})(9 - \frac{n^2}{36})} \cos n\varphi \right] \quad 2.3.1.7$$

Setting  $n=2, 4, \dots$  in Equation (2.3.1.7), the expression for each mode shape in the ring is readily obtained. For instance,

$$\rho^{(2)} = R_0 (0.999293 - 0.001396 \cos 2\varphi)$$

$$\rho^{(4)} = R_0 (0.999293 - 0.001339 \cos 4\varphi)$$

$$\rho^{(6)} = R_0 (0.999293 - 0.001250 \cos 6\varphi)$$

-----

A single problem is now resolved into a set of problems, each of which is independent of the others and can be solved separately. The bending moments, at point 0, for the first three mode shapes analyzed by Marbec's method are as follows:

$$M_0^{(2)} = 0.001394 \, pR_0^2$$

$$M_0^{(4)} = 0.001338 \, pR_0^2$$

$$M_0^{(6)} = 0.001248 \, pR_0^2$$

The summation of  $M_0^{(n)}$  must be equal to  $.009246 \, pR_0^2$ , the bending moment at point 0 of the ring, which has been computed in Article (2.1.2) by small-deflection theory. Hence,

$$M_0^{(8)} + M_0^{(10)} + M_0^{(12)} + \text{-----} = 0.005266 \, pR_0^2$$

The magnification factors for these modes are

$$F^{(2)} = 2, \quad F^{(4)} = 10/9, \quad F^{(6)} = 70/67 \quad \text{and} \quad F^{(8)} = F^{(10)} = \dots = 1.$$

Since, for higher mode shapes, the magnification factor approaches unity, the bending moment at point O predicted by the simplified method will be

$$\begin{aligned} M_o &= (.001394 \times 2 + .001338 \times 10/9 + .001248 \times 70/67 + 0.005266) pR_o^2 \\ &= (.002788 + .001486 + .001304 + .005266) pR_o^2 \\ &= .010844 pR_o^2. \end{aligned}$$

If only the first component of bending moment were considered, the maximum bending moment at point O would be computed as

$$\begin{aligned} M_o &= (.001394 \times 2 + .007852) pR_o^2 \\ &= 0.010640 pR_o^2. \end{aligned}$$

The discrepancy between these two results is about 2%.

Since  $\delta$  is very small, a further simplification can be made. This device, as in previous examples, makes it unnecessary to know the results of a small-deflection analysis in advance.

For  $\varphi = 0$ , Equation (2.3.1.7) reduces to

$$\begin{aligned} \rho &= R_o [1 - 0.000707 - (0.001395 + 0.001339 + 0.001250 + \dots)] \\ &= R_o (0.999293 - 0.009293). \end{aligned}$$

It has been pointed out that  $0.999293 R_o$  can be taken as the radius of the node circle and the coefficients  $0.001395 R_o$ , --- can be considered as the amplitudes of the irregularity for corresponding mode shapes, at point O, measured with respect to the node circle. The approximate bending moment at point O in the small-deflection case is given by the term  $0.009293 pR_o^2$ . The approximate maximum bending moment at point O analyzed by the simplified method is

$$\begin{aligned}
 M_o &= (0.001395 \times 2 + 0.001339 \times 10/9 + 0.001250 \times 70/67 + \dots) pR_o^2 \\
 &= (0.002790 + 0.001488 + 0.001306 + 0.005309 + \dots) pR_o^2 \\
 &= 0.010893 pR_o^2.
 \end{aligned}$$

$$(11). \quad \varphi_o = 15^\circ \quad \text{and} \quad \delta = 0.1$$

In the case  $\varphi_o = 15^\circ$ ,  $\delta = 0.1$ , the mode shapes of the ring are

$$\rho^{(2)} = R_o (0.992926 - 0.013956 \cos 2\varphi)$$

$$\rho^{(4)} = R_o (0.992926 - 0.013394 \cos 4\varphi)$$

-----

The bending moments at point 0 for the first two mode shapes (analyzed by Marbec's method) are

$$M_o^{(2)} = 0.013905 pR_o^2$$

$$M_o^{(4)} = 0.013344 pR_o^2$$

and the total bending moment at point 0 which was computed in Article (2.1.2) for the small-deflection case is equal to  $0.087926 pR_o^2$ .

Then, the maximum bending moment at point 0 is

$$\begin{aligned}
 M_o &= (0.013905 \times 2 + 0.013344 \times 10/9 + 0.060677) pR_o^2 \\
 &= 0.103313 pR_o^2.
 \end{aligned}$$

When the ring is acted on by internal pressure, a negative value of  $p$  must be used in computations. The magnification factor,  $1/(1 + p/p_{cr})$  is less than unity.

For  $\varphi_o = 15^\circ$  and  $\delta = 0.01$ , the maximum bending moment at point 0 predicted by the simplified method is

$$\begin{aligned}
 M_o &= -(0.001394 \times 2/3 + 0.001338 \times 10/11 + 0.001248 \times 70/73 \\
 &\quad + 0.005266) pR_o^2 \\
 &= -0.008608 pR_o^2.
 \end{aligned}$$

In the case  $\varphi_0 = 15^\circ$ ,  $\delta = 0.1$ , the maximum bending moment is equal to

$$\begin{aligned} M_0 &= -(0.013905 \times 2/3 + 0.013344 \times 10/11 + 0.060677) pR_0^2 \\ &= -0.082080 pR_0^2. \end{aligned}$$

The comparison of results for the illustrative problems analyzed by the different methods given in this dissertation are tabulated in Table (2.3.2.1).

| Ring Shape                             | Elliptical          | Third Buckling Mode<br>Shape | Two Symmetrical Local Dents |                                       |                                      |                                      |
|--|---------------------|------------------------------|-----------------------------|---------------------------------------|--------------------------------------|--------------------------------------|
| Pressure                               | External            | External                     | External                    | Internal                              | External                             | Internal                             |
| Amplitude of<br>Initial Irregularity   | $e=1 - (0.99/1.01)$ | $\delta=0.01$                | $\delta=0.1$                | $\varphi_0=15^\circ$<br>$\delta=0.01$ | $\varphi_0=15^\circ$<br>$\delta=0.1$ | $\varphi_0=15^\circ$<br>$\delta=0.1$ |
| Small-Deflection<br>Theory             | -0.010050           | 0.010025                     | 0.101925                    | 0.009246                              | 0.087926                             | -0.087926                            |
| "Exact" or Large-<br>Deflection Theory | -0.019829           | 0.010339                     | 0.104280                    | 0.010864                              | 0.101637                             | -0.080793                            |
| Simplified Large-<br>Deflection Theory | -0.020100           | 0.010474                     | 0.106488                    | 0.010844                              | 0.103313                             | -0.082080                            |

TABLE 2.3.2.1 SUMMARY OF MAXIMUM BENDING MOMENT  $\div PR_0^2$

### 3. CYLINDRICAL SHELL HAVING SMALL INITIAL IRREGULARITIES

#### 3.1. Basic Assumptions

The method introduced in the preceding chapters for the analysis of a circular ring having small initial irregularities and subjected to a uniform pressure can also be applied to the case of a thin cylindrical shell provided that the initial imperfection is uniform along the length of the shell. It is only necessary to substitute the flexural rigidity,  $D = Eh^3/12(1 - \nu^2)$ , for  $EI$ . A natural question arises as to the limits of the validity of this procedure when applied to localized dents in cylindrical shells. This question has been answered (at least partially) by the solution of the shell equations for a dent varying in magnitude along the longitudinal axis of the cylinder.

The middle surface of the shell under consideration is assumed to be defined by the equation:

$$\rho = R_0[1 - \delta(\cos mx)(\cos n\varphi)] \quad 3.1.1$$

where  $\delta$ ,  $m$ , and  $n$  are parameters which determine the geometrical shape of the shell.

The shell deviates from its original circular shape by an amount  $\delta \cos(mx)$  and has a cross section similar to the  $n$ 'th

buckling mode shape. Its variation along the longitudinal axis may be specified by the wave length in that direction,  $2L = 2\pi/m$ . When the wave length,  $2L$ , is large compared with the mean radius,  $R_0$ , of the cylindrical shell ( $L/R_0 \gg 1$ ) the situation approaches the two-dimensional case of a cylindrical shell having a cross section similar to the  $n$ 'th mode shape all along its length. If the wave length is small ( $L/R_0 \ll 1$ ) the dent in the cylindrical shell is highly localized and the shell has a corrugated surface. The results to be developed are based on a theory which does not hold for very highly localized dents so that results must <sup>not</sup> be pressed to this limit. When the parameter  $n$  is zero the shell has a circular cross-section having different diameters at different sections along the length. This last case has been considered by E. F. Burmistrov (16).

In all the subsequent discussions the following basic assumptions are made:

- (1). The initial irregularity of the shell is so small that second and higher order terms in  $\delta$  can be neglected.
- (2). The square of the quantity  $(m\delta R_0)$  is negligible compared with unity, i.e. the wave length of the dent in the longitudinal direction is large in comparison with the mean radius of the cylindrical shell.
- (3). The square of the quantity  $(n\delta)$  must also be small compared with unity, i.e. the shell must have the cross section of one of the lower mode shapes.
- (4). The shell is a thin shell; its thickness is so small as compared with its initial radii of curvature,  $R_x$  and  $R_\varphi$ ,

that the quantities  $h/R_\chi$  and  $h/R_\varphi$  can be disregarded.

(5). The method of analysis is based on a small-deflection theory in which extension of the middle surface of the shell is neglected.

(6). The normal forces  $N_\chi$  ,  $N_\varphi$  and shear  $N_{\chi\varphi}$  must be small in comparison with their critical values.

### 3.2. Fundamental Quantities

As is conventional in developing the governing equations for a cylindrical shell, we consider a small element formed by two pairs of adjacent planes which are normal to the middle surface of the shell and which contain its principal curvatures. The location of this element is defined by the coordinate  $x$  and the angle  $\varphi$ . The coordinate axes  $X$  and  $Y$  tangent at  $O$  to the lines of principal curvature and the axis  $Z$  normal to the middle surface are shown in Fig. (3.2.1). The curved length of the infinitesimal element is

$$(ds)^2 = A^2(dx)^2 + B^2(d\varphi)^2. \quad 3.2.1$$

If the middle surface of the shell is given by  $\rho = \rho(x, \varphi)$ , the symbols  $A$  and  $B$  represent the expressions:

$$A = [1 + (d\rho/dx)^2]^{\frac{1}{2}} \quad \text{and} \quad B = [\rho^2 + (d\rho/d\varphi)^2]^{\frac{1}{2}} \quad 3.2.2$$

The principal curvatures of the surface are

$$(1/R_x) = -\rho(d^2\rho/dx^2)/A^3B$$

$$\text{and} \quad (1/R_\varphi) = [\rho^2 + 2(d\rho/d\varphi)^2 - \rho(d^2\rho/d\varphi^2)]/AB^3. \quad 3.2.3$$

In the case of the shell given by Equation (3.1.1) (neglecting the second and higher order quantities  $m\delta R_0$  and  $n\delta$ ), Equations (3.2.2) and (3.2.3) become

$$A = 1, \quad B = R_0(1 - \delta \cos mx \cos n\varphi),$$

$$(1/R_x) = -m^2 \delta R_0 \cos mx \cos n\varphi, \quad 3.2.4$$

$$\text{and} \quad (1/R_\varphi) = [1 - (n^2 - 1)\delta \cos mx \cos n\varphi]/R_0.$$

Only first-order terms in the (small) deformation  $\delta$  have been retained in the foregoing expressions. It is later shown that

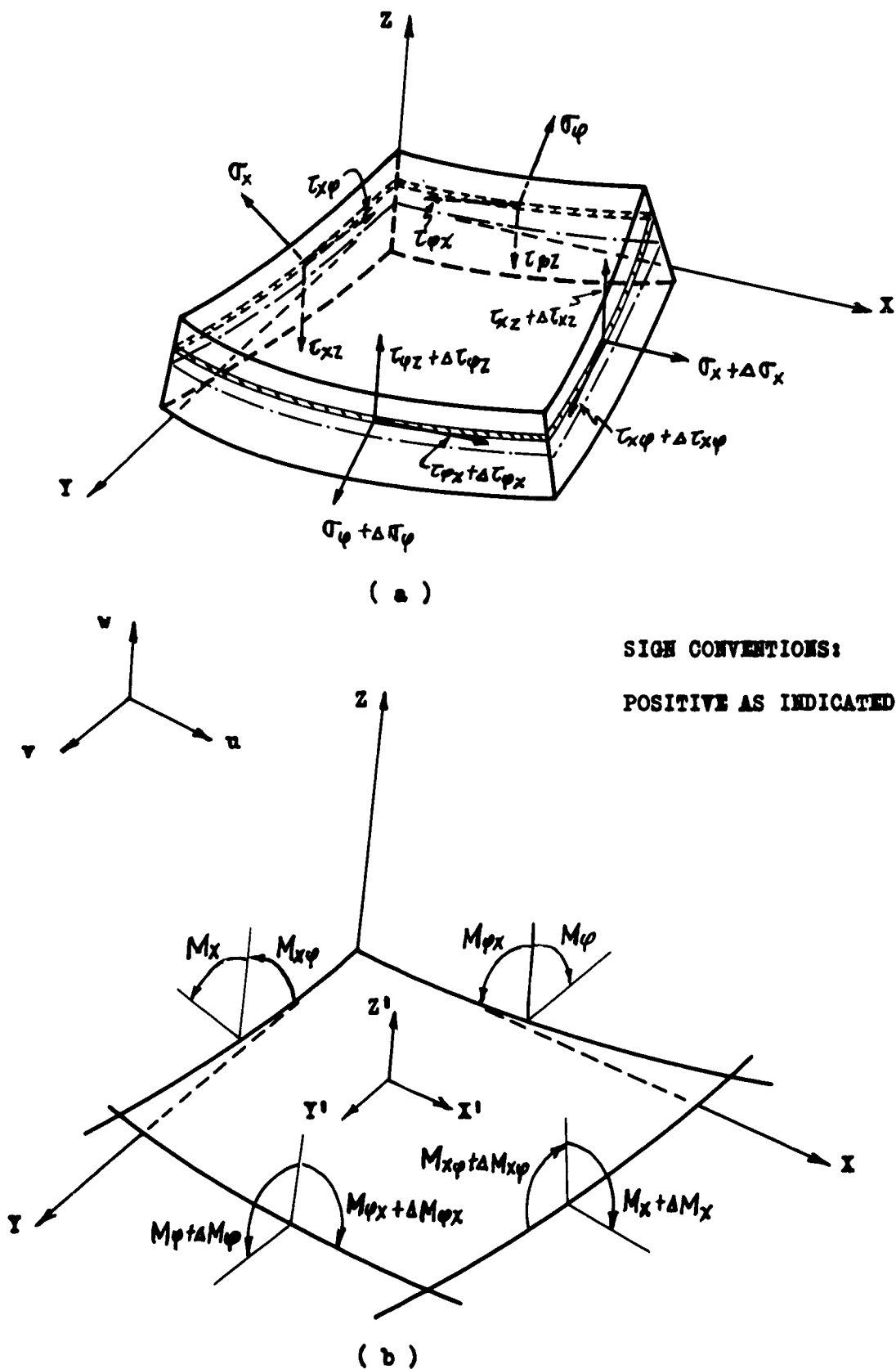


FIG. 3.2.1

SHELL ELEMENT

the stresses due to a dent whose cross-sectional profile is not a perfect circle depend on these terms. On the other hand, in the case investigated by Burmistrov (16), where the cross-section of the shell is always a perfect circle and only the radius varies, the second-order terms must be retained. In this case the first-order terms in  $\delta$  cancel and without the second-order terms the solution reduces to that for a perfect circular cylinder.

In order to analyze the equilibrium of the element, the stresses acting on the plane faces are resolved in the directions of the coordinate axes (Fig. 3.2.1a). The normal stress is taken as positive when it produces tension. The positive directions of the components of shearing stress are taken as the positive directions of the coordinate axes if a tensile stress on the same side would have the positive direction of the corresponding axis. If the tensile stress has a direction opposite to the positive axis, the positive direction of the shearing stress components should be reversed. The bending moments are taken as positive when they tend to decrease the initial curvatures. The positive directions of twisting moment are indicated in Fig. (3.2.1b).

The resultant normal and shearing forces (per unit length of the normal section) in the longitudinal and circumferential directions shown in Fig. (3.2.1a) are:

$$N_x = \int_{-h/2}^{h/2} \sigma_x (1 - z/R_\varphi) dz$$

$$N_\varphi = \int_{-h/2}^{h/2} \sigma_\varphi (1 - z/R_x) dz$$

$$N_{x\varphi} = \int_{-h/2}^{h/2} \tau_{x\varphi} (1 - z/R_{\varphi}) dz$$

$$N_{\varphi x} = \int_{-h/2}^{h/2} \tau_{\varphi x} (1 - z/R_x) dz$$

$$Q_x = \int_{-h/2}^{h/2} \tau_{xz} (1 - z/R_{\varphi}) dz$$

3.2.5

$$Q_{\varphi} = \int_{-h/2}^{h/2} \tau_{\varphi z} (1 - z/R_x) dz$$

Due to the fact that the curvatures of the shell in the longitudinal and circumferential directions are different, the shearing forces  $N_{x\varphi}$  and  $N_{\varphi x}$  are generally not exactly equal to each other, although it is still true that  $\tau_{x\varphi} = \tau_{\varphi x}$ .

The bending and twisting moments (per unit length of the normal sections) are given by the expressions:

$$M_x = \int_{-h/2}^{h/2} \sigma_x z (1 - z/R_{\varphi}) dz, \quad M_{\varphi} = \int_{-h/2}^{h/2} \sigma_{\varphi} z (1 - z/R_x) dz$$

3.2.6

$$M_{x\varphi} = \int_{-h/2}^{h/2} \tau_{x\varphi} z (1 - z/R_{\varphi}) dz, \quad M_{\varphi x} = \int_{-h/2}^{h/2} \tau_{\varphi x} z (1 - z/R_x) dz$$

Since the thickness of a thin shell is small in comparison with the radii of the curvature, the terms  $z/R_x$  and  $z/R_{\varphi}$  in Equations (3.2.5) and (3.2.6) disappear in the evaluation of the resultant normal forces, shears and bending moments. Then  $N_{x\varphi}$  is equal to  $N_{\varphi x}$ .

Using Hooke's law and neglecting the terms  $z/R_x$  and  $z/R_{\varphi}$ , the relations between direct stresses and strains at any

point are as follows:

$$\begin{aligned}\sigma_x &= E(1-\nu^2)^{-1}(\epsilon_x + \nu\epsilon_\varphi) \\ \sigma_\varphi &= E(1-\nu^2)^{-1}(\epsilon_\varphi + \nu\epsilon_x)\end{aligned}\quad 3.2.7$$

and

$$\tau_{x\varphi} = \tau_{\varphi x} = E(1+\nu)^{-1}\gamma_{x\varphi}/2$$

Similarly, the elastic relations between stresses at any point, at a distance  $z$  from the middle surface, and changes of curvature are given by:

$$\begin{aligned}\sigma_x &= -Ez(1-\nu^2)^{-1}(\chi_x + \nu\chi_\varphi) \\ \sigma_\varphi &= -Ez(1-\nu^2)^{-1}(\chi_\varphi + \nu\chi_x)\end{aligned}\quad 3.2.8$$

and

$$\tau_{x\varphi} = \tau_{\varphi x} = -Ez(1+\nu)^{-1}\chi_{x\varphi}$$

Substituting Equations (3.2.7) and (3.2.8) into (3.2.5) and (3.2.6) respectively, the normal forces and moments reduce to:

$$\begin{aligned}N_x &= K(\epsilon_x + \nu\epsilon_\varphi) \\ N_\varphi &= K(\epsilon_\varphi + \nu\epsilon_x) \\ N_{x\varphi} &= K(1-\nu)\gamma_{x\varphi}/2 \\ M_x &= -D(\chi_x + \nu\chi_\varphi) \\ M_\varphi &= -D(\chi_\varphi + \nu\chi_x)\end{aligned}\quad 3.2.9$$

and

$$M_{x\varphi} = -M_{\varphi x} = D(1-\nu)\chi_{x\varphi}$$

where

$$K = (1-\nu^2)/Eh$$

### 3.3. Relations Between Stresses, Strains and Displacements

In investigating the relations between strains, changes of curvature, and displacements, the deformation of an element must be considered. In Love's "Mathematical Theory of Elasticity" (7), relationships of this type are developed. Recently, expressions for these relations, in which the changes of curvature differ slightly from those derived by Love, have been published by W. R. Osgood and J. A. Joseph (8). However, with the assumption that the middle surface of the shell is inextensible, the expressions for changes of curvature derived by Love and by Osgood and Joseph agree. In the present investigation, expressions for changes of curvature in the form derived by Osgood and Joseph will be used. The relations between strains and displacements are given by following expressions:

$$\epsilon_x = \frac{1}{A} \frac{\partial u}{\partial x} + \frac{v}{AB} \frac{\partial A}{\partial \varphi} - \frac{\omega}{R_x}$$

$$\epsilon_\varphi = \frac{1}{B} \frac{\partial v}{\partial \varphi} + \frac{u}{AB} \frac{\partial B}{\partial x} - \frac{\omega}{R_\varphi}$$

$$\gamma_{x\varphi} = \frac{1}{A} \frac{\partial v}{\partial x} - \frac{v}{AB} \frac{\partial B}{\partial x} - \frac{u}{AB} \frac{\partial A}{\partial \varphi} + \frac{1}{B} \frac{\partial u}{\partial \varphi}$$

$$\chi_x = \frac{u}{A} \frac{\partial}{\partial x} \left( \frac{1}{R_x} \right) + \left( \frac{1}{R_\varphi} - \frac{1}{R_x} \right) \frac{v}{AB} \frac{\partial A}{\partial \varphi} + \frac{1}{A^2} \frac{\partial^2 \omega}{\partial \varphi^2} + \frac{1}{AB^2} \frac{\partial A}{\partial \varphi} \frac{\partial \omega}{\partial \varphi} \\ + \frac{1}{A} \frac{\partial}{\partial x} \left( \frac{1}{A} \right) \frac{\partial \omega}{\partial x} + \frac{\omega}{R_x^2}$$

$$\chi_\varphi = \left( \frac{1}{R_x} - \frac{1}{R_\varphi} \right) \frac{u}{AB} \frac{\partial B}{\partial x} + \frac{v}{B} \frac{\partial}{\partial \varphi} \left( \frac{1}{R_\varphi} \right) + \frac{1}{A^2 B} \frac{\partial B}{\partial x} \frac{\partial \omega}{\partial x} + \frac{1}{B^2} \frac{\partial^2 \omega}{\partial \varphi^2} \\ + \frac{1}{B} \frac{\partial}{\partial \varphi} \left( \frac{1}{B} \right) \frac{\partial \omega}{\partial \varphi} + \frac{\omega}{R_\varphi^2}$$

$$\begin{aligned} \chi_{x\varphi} = & \frac{u}{2B} \frac{\partial}{\partial \varphi} \left( \frac{1}{R_x} \right) + \frac{1}{2B} \left( \frac{1}{R_x} - \frac{1}{R_\varphi} \right) \frac{\partial u}{\partial \varphi} + \frac{v}{2A} \frac{\partial}{\partial x} \left( \frac{1}{R_\varphi} \right) + \frac{1}{2A} \left( \frac{1}{R_x} - \frac{1}{R_\varphi} \right) \frac{\partial v}{\partial x} \\ & + \frac{1}{AB} \frac{\partial^2 \omega}{\partial x \partial \varphi} - \frac{1}{A^2 B} \frac{\partial A}{\partial \varphi} \frac{\partial \omega}{\partial x} - \frac{1}{AB^2} \frac{\partial B}{\partial x} \frac{\partial \omega}{\partial \varphi} \end{aligned}$$

-----3.3.1

On substituting the known quantities  $A$ ,  $B$ ,  $1/R_x$  and  $1/R_\varphi$  given by Equations (3.2.4) and their derivatives with respect to the coordinates  $x$  and  $\varphi$  into Equations (3.3.1), these expressions reduce to:

$$\epsilon_x = \frac{\partial u}{\partial x} + \delta m^2 R_0 \omega \cos mx \cos n\varphi$$

$$\epsilon_\varphi = \frac{\partial v}{R_0 \partial \varphi} - \frac{\omega}{R_0} + \delta \cos mx \cos n\varphi \left( \frac{\partial v}{R_0 \partial \varphi} + \frac{\eta^2 - 1}{R_0} \omega \right) + \delta m u \sin mx \cos n\varphi$$

$$\gamma_{x\varphi} = \frac{\partial v}{\partial x} + \frac{\partial u}{R_0 \partial \varphi} + \delta \frac{\partial u}{R_0 \partial \varphi} \cos mx \cos n\varphi - \delta m v \sin mx \cos n\varphi$$

$$\chi_{xx} = \frac{\partial^2 \omega}{\partial x^2} + \delta m^3 R_0 u \sin mx \cos n\varphi$$

$$\begin{aligned} \chi_{\varphi\varphi} = & \frac{\partial^2 \omega}{R_0^2 \partial \varphi^2} + \frac{\omega}{R_0^2} + 2 \delta \cos mx \cos n\varphi \left[ \frac{\partial^2 \omega}{R_0^2 \partial \varphi^2} - (\eta^2 - 1) \frac{\omega}{R_0^2} \right] \\ & + \delta \sin mx \cos n\varphi \left( -\frac{m u}{R_0} + m \frac{\partial \omega}{\partial x} \right) + \delta \cos mx \sin n\varphi \left[ n(\eta^2 - 1) \frac{v}{R_0^2} - n \frac{\partial^2 \omega}{R_0^2 \partial \varphi^2} \right] \end{aligned}$$

$$\begin{aligned} \chi_{x\varphi} = & \frac{1}{R_0} \left( \frac{\partial^2 \omega}{\partial x \partial \varphi} + \frac{1}{2} \frac{\partial v}{\partial x} - \frac{1}{2 R_0} \frac{\partial u}{\partial \varphi} \right) \\ & + \delta \cos mx \cos n\varphi \left( \frac{\eta^2 - 2 - m^2 R_0^2}{2 R_0^2} \frac{\partial u}{\partial \varphi} - \frac{\eta^2 - 1 - m^2 R_0^2}{2 R_0} \frac{\partial v}{\partial x} + \frac{1}{R_0} \frac{\partial^2 \omega}{\partial x \partial \varphi} \right) \\ & + \delta \sin mx \cos n\varphi \left[ \frac{m(\eta^2 - 1)v}{2 R_0} - \frac{m}{R_0} \frac{\partial \omega}{\partial \varphi} \right] + \frac{\delta m^2 \eta u}{2} \cos mx \sin n\varphi \end{aligned}$$

-----3.3.2

Substituting Equations (3.3.2) into (3.2.9), we have

$$\begin{aligned}
 N_x &= K \left[ \frac{\partial u}{\partial x} + \frac{v}{R_0} \frac{\partial v}{\partial \varphi} - \frac{v}{R_0} \omega + \delta (m^2 R_0 + v \frac{n^2 - 1}{R_0}) \omega \cos mx \cos n\varphi \right. \\
 &\quad \left. + \delta v m u \sin mx \cos n\varphi + \dots \right] \\
 N_\varphi &= K \left[ \frac{1}{R_0} \frac{\partial v}{\partial \varphi} - \frac{\omega}{R_0} + v \frac{\partial u}{\partial x} + \delta \left( \frac{n^2 - 1}{R_0} + v m^2 R_0 \right) \omega \cos mx \cos n\varphi \right. \\
 &\quad \left. + \delta m u \sin mx \cos n\varphi + \dots \right] \\
 N_{x\varphi} &= K \left[ \frac{1-v}{2} \frac{\partial v}{\partial x} + \frac{1-v}{2R_0} \frac{\partial u}{\partial \varphi} + \dots \right] \\
 M_x &= -D \left[ \frac{\partial^2 \omega}{\partial x^2} + \frac{v}{R_0^2} \left( \frac{\partial^2 \omega}{\partial \varphi^2} + \omega \right) - 2\delta v (n^2 - 1) \frac{\omega}{R_0^2} \cos mx \cos n\varphi \right. \\
 &\quad \left. + \delta m (m^2 R_0^2 - v) \frac{u}{R_0} \sin mx \cos n\varphi + \dots \right] \\
 M_\varphi &= -D \left[ \frac{1}{R_0^2} \left( \frac{\partial^2 \omega}{\partial \varphi^2} + \omega \right) + v \frac{\partial^2 \omega}{\partial x^2} - 2\delta (n^2 - 1) \frac{\omega}{R_0} \cos mx \cos n\varphi \right. \\
 &\quad \left. + \delta m (v m^2 R_0^2 - 1) \frac{u}{R_0} \sin mx \cos n\varphi + \dots \right] \\
 M_{x\varphi} &= D \left[ \frac{1-v}{R_0} \frac{\partial^2 \omega}{\partial x \partial \varphi} + \frac{1-v}{2R_0} \frac{\partial v}{\partial x} - \frac{1-v}{2R_0^2} \frac{\partial u}{\partial \varphi} \right. \\
 &\quad \left. + \frac{1}{2} \delta m^2 n (1-v) u \cos mx \sin n\varphi + \dots \right].
 \end{aligned}$$

----- 3.3.3

The dotted lines in Equations (3.3.3) represent terms, which eventually vanish from the equations of equilibrium because they involve either (i) the product of  $\delta$  and  $v$ , (ii) the products of  $\delta$  and the derivatives of  $v$  and  $w$  with respect to  $x$  and  $\varphi$  or (iii) the products of  $\delta$  and the derivative of  $u$  with respect to  $\varphi$ .

### 3.4. Equations of Equilibrium

In the general theory of shells, the equations of equilibrium, which are formed by equating to zero the resultant and the resultant moment of all forces applied to an infinitely small element of a thin shell, have been derived by A. E. H. Love (7). Love's equations of equilibrium differ somewhat from those derived by W. R. Osgood and J. A. Joseph (8). If, however, the middle surface of the shell is assumed to be inextensible and two non-linear terms (small in the case under study) are neglected, the two sets of equations are identical. Due to the extremely complicated mathematical form and non-linear nature of the equations of equilibrium in the most general shell theory, assumptions have been made to simplify the problem. The most important one is that the forces  $N_x$ ,  $N_\varphi$  and  $N_{x\varphi}$  are very small in comparison with their critical values. Under these circumstances their effects on bending can be neglected. With this assumption all non-linear terms in the equations of equilibrium which contain the products of the resultant forces or resultant moments and either the small displacements  $u$ ,  $v$ ,  $w$  or their derivatives vanish. The equations of equilibrium are:

$$\frac{1}{A} \frac{\partial N_x}{\partial x} + \frac{1}{AB} \frac{\partial B}{\partial x} N_x + \frac{1}{B} \frac{\partial N_{x\varphi}}{\partial \varphi} + \frac{2}{AB} \frac{\partial A}{\partial \varphi} N_{x\varphi} - \frac{1}{AB} \frac{\partial B}{\partial x} N_\varphi - \frac{Q_x}{R_x} + X' = 0$$

$$\frac{1}{A} \frac{\partial N_{x\varphi}}{\partial x} + \frac{2}{AB} \frac{\partial B}{\partial x} N_{x\varphi} + \frac{1}{B} \frac{\partial N_\varphi}{\partial \varphi} + \frac{1}{AB} \frac{\partial A}{\partial \varphi} N_\varphi - \frac{1}{AB} \frac{\partial A}{\partial \varphi} N_x - \frac{Q_\varphi}{R_\varphi} + Y' = 0$$

$$\frac{1}{A} \frac{\partial Q_x}{\partial x} + \frac{1}{AB} \frac{\partial B}{\partial x} Q_x + \frac{1}{B} \frac{\partial Q_\varphi}{\partial \varphi} + \frac{1}{AB} \frac{\partial A}{\partial \varphi} Q_\varphi + \frac{N_x}{R_x} + \frac{N_\varphi}{R_\varphi} + Z' = 0$$

$$\frac{1}{A} \frac{\partial M_{xy}}{\partial x} + \frac{2}{AB} \frac{\partial B}{\partial x} M_{xy} - \frac{1}{B} \frac{\partial M_{xy}}{\partial \varphi} - \frac{1}{AB} \frac{\partial A}{\partial \varphi} M_{xy} + \frac{1}{AB} \frac{\partial A}{\partial \varphi} M_x + Q_{\varphi} = 0$$

$$\frac{1}{A} \frac{\partial M_x}{\partial x} + \frac{1}{AB} \frac{\partial B}{\partial x} M_x - \frac{1}{B} \frac{\partial M_{xy}}{\partial \varphi} - \frac{2}{AB} \frac{\partial A}{\partial \varphi} M_{xy} - \frac{1}{AB} \frac{\partial B}{\partial x} M_{xy} - Q_x = 0$$

-----3.4.1

By substituting Equations (3.2.4), (3.3.3) together with their derivatives into (3.4.1) and in this way eliminating  $Q_x$  and  $Q_{\varphi}$ , three equations in the dependent variables  $u$ ,  $v$  and  $w$  can be obtained.

$$\frac{\partial^2 u}{\partial x^2} + \frac{1-v}{2R_0} \frac{\partial^2 v}{\partial x \partial \varphi} + \frac{1-v}{2R_0^2} \frac{\partial^2 u}{\partial \varphi^2} - \frac{v}{R_0} \frac{\partial \omega}{\partial x} + \frac{X'}{K} + \delta [-m^2 R_0 + (1-n^2 v) \frac{m}{R_0}] \omega \sin mx \cos n \varphi$$

$$+ \delta m \frac{\partial u}{\partial x} \sin mx \cos n \varphi + \delta v m^2 u \cos mx \cos n \varphi + \text{-----} = 0$$

$$K \left( \frac{1-v}{2} \frac{\partial^2 v}{\partial x^2} + \frac{1+v}{2R_0} \frac{\partial^2 u}{\partial x \partial \varphi} + \frac{1}{R_0^2} \frac{\partial^2 v}{\partial \varphi^2} - \frac{1}{R_0^2} \frac{\partial \omega}{\partial \varphi} \right) + D \left( \frac{1}{R_0^4} \frac{\partial^3 \omega}{\partial \varphi^3} + \frac{1}{R_0^2} \frac{\partial^3 \omega}{\partial x^2 \partial \varphi} + \frac{1}{R_0^4} \frac{\partial \omega}{\partial \varphi} \right)$$

$$+ \frac{1-v}{2R_0^2} \frac{\partial^2 v}{\partial x^2} - \frac{1-v}{2R_0^2} \frac{\partial^2 u}{\partial x \partial \varphi} + Y'$$

$$+ \delta \cos mx \cos n \varphi \left\{ K \left[ -\frac{n(n^2-1)}{R_0^2} - v m^2 n \right] \omega + D \left[ \frac{2n(n^2-1)}{R_0^4} \omega + \frac{m^2 n (1-v)}{2R_0} \frac{\partial u}{\partial x} \right] \right\}$$

$$- \delta \sin mx \cos n \varphi \left\{ \frac{mn}{R_0} K + D \left[ \frac{m^2 n (1-v)}{2R_0} + \frac{mn (v m^2 R_0^2 - 12)}{R_0^3} \right] \right\} u + \text{-----} = 0$$

$$- D \left( \frac{\partial^4 \omega}{\partial x^4} + \frac{2}{R_0^2} \frac{\partial^4 \omega}{\partial x^2 \partial \varphi^2} + \frac{1}{R_0^4} \frac{\partial^4 \omega}{\partial \varphi^4} + \frac{1}{R_0^4} \frac{\partial^2 \omega}{\partial \varphi^2} + \frac{v}{R_0^2} \frac{\partial^2 \omega}{\partial x^2} - \frac{1-v}{R_0^2} \frac{\partial^3 v}{\partial x^2 \partial \varphi} - \frac{1-v}{R_0^3} \frac{\partial^3 u}{\partial x \partial \varphi^2} \right)$$

$$+ K \left( \frac{1}{R_0^2} \frac{\partial v}{\partial \varphi} - \frac{\omega}{R_0^2} + \frac{v}{R_0} \frac{\partial u}{\partial x} \right) + Z'$$

$$+ \delta \cos mx \cos n \varphi \left\{ D \left[ \frac{(-2vn^2 + v + 12)m^2}{R_0^2} \omega - \frac{2n^2(n^2-1)}{R_0^4} \omega \right. \right.$$

$$\left. - \frac{m^2(2m^2 R_0^2 - 2v + n^2 - v n^2)}{R_0} \frac{\partial u}{\partial x} \right] + K \left[ \frac{2(n^2-1)}{R_0^4} \omega + 2v m^2 \omega - \frac{m^2 R_0^2 + v n^2 - v}{R_0} \frac{\partial u}{\partial x} \right] \right\}$$

$$+ \delta \sin mx \cos n \varphi \left\{ D \left[ \frac{m^3(m^2 R_0^2 - \nu + n^2 - \nu n^2)}{R_0} + \frac{mn^2(\nu m^2 R_0^2 - 1)}{R_0^3} \right] + \frac{m}{R_0} K \right\} u$$

$$+ \text{-----} = 0$$

-----3.4.2

The three independent equations given by Equations (3.4.2) are sufficient to determine the three unknown displacement components. A solution which satisfies Equations (3.4.2) will satisfy the conditions of equilibrium and compatibility. From Equations (3.4.2), it can be seen that the terms which do not contain parameters  $\delta$ ,  $m$  and  $n$  will constitute a set of equations for a perfect circular cylindrical shell. Terms containing  $\delta$ ,  $m$  and  $n$  represent corrections due to the imperfections of the shell.

All terms represented by dotted lines in Equations (3.4.2) contain either (i), the products of  $\delta$  and  $v$  or (ii), the products of  $\delta$  and derivatives of  $v$  and  $w$  with respect to  $x$  and  $\varphi$ , or (iii), the products of  $\delta$  and derivatives of  $u$  with respect to  $\varphi$ .

### 3.5. Method of Analysis

As mentioned in the previous article, the governing equations for a cylindrical shell having initial irregularities consist of the equations for a perfect circular cylindrical shell plus the correction terms due to the imperfections of the shell. These terms contain the parameters  $\delta$ ,  $m$  and  $n$ . Now it is required to find displacement components which satisfy the governing equations and at the same time satisfy the boundary conditions of the given problem. The nature of the problem suggests trying a solution of the form

$$\begin{aligned} u &= U_0(x, \varphi) + \delta U_1(x, \varphi) \\ v &= V_0(x, \varphi) + \delta V_1(x, \varphi) \\ w &= W_0(x, \varphi) + \delta W_1(x, \varphi). \end{aligned} \tag{3.5.1}$$

Here  $U_0(x, \varphi)$ ,  $V_0(x, \varphi)$  and  $W_0(x, \varphi)$  are the solution for a perfect circular cylindrical shell and  $U_1(x, \varphi)$ ,  $V_1(x, \varphi)$  and  $W_1(x, \varphi)$  represent the corrections due to initial imperfections of the shell.

Substituting Equations (3.5.1) into (3.4.2) two sets of terms are encountered, one proportional to  $\delta$  and one independent of  $\delta$ . Each must vanish. On setting them equal to zero two sets of linear partial differential equations are obtained. The first group is given by Equations (3.5.2). They contain as dependent variables only  $U_0(x, \varphi)$ ,  $V_0(x, \varphi)$  and  $W_0(x, \varphi)$  which depend on the given external loading condition specified by  $X'$ ,  $Y'$ , and  $Z'$ .

These equations refer to the perfect circular cylindrical

shell.

$$\frac{\partial^2 U_0}{\partial x^2} + \frac{1+\nu}{2R_0} \frac{\partial^2 V_0}{\partial x \partial \varphi} + \frac{1-\nu}{2R_0^2} \frac{\partial^2 U_0}{\partial \varphi^2} - \frac{\nu}{R_0} \frac{\partial W_0}{\partial x} + \frac{X'}{K} = 0$$

$$F\left(\frac{1-\nu}{2} \frac{\partial^2 V_0}{\partial x^2} + \frac{1+\nu}{2R_0} \frac{\partial^2 U_0}{\partial x \partial \varphi} + \frac{1}{R_0^2} \frac{\partial^2 V_0}{\partial \varphi^2} - \frac{1}{R_0^2} \frac{\partial W_0}{\partial \varphi}\right) + \frac{1}{R_0^2} \frac{\partial^3 W_0}{\partial \varphi^3} + \frac{\partial^3 W_0}{\partial x^2 \partial \varphi} + \frac{1}{R_0^2} \frac{\partial W_0}{\partial \varphi} \\ + \frac{1-\nu}{2} \frac{\partial^2 V_0}{\partial x^2} - \frac{1-\nu}{2R_0} \frac{\partial^2 U_0}{\partial x \partial \varphi} + \frac{R_0^2}{D} Y' = 0$$

$$F\left(\frac{1}{R_0^2} \frac{\partial V_0}{\partial \varphi} - \frac{W_0}{R_0^2} + \frac{\nu}{R_0} \frac{\partial U_0}{\partial x}\right) - \left[R_0^2 \frac{\partial^4 W_0}{\partial x^4} + 2 \frac{\partial^4 W_0}{\partial x^2 \partial \varphi^2} + \frac{1}{R_0^2} \frac{\partial^4 W_0}{\partial \varphi^4} + \frac{1}{R_0^2} \frac{\partial^2 W_0}{\partial \varphi^2} \right. \\ \left. + \nu \frac{\partial^2 W_0}{\partial x^2} + (1-\nu) \frac{\partial^3 V_0}{\partial x^2 \partial \varphi} - \frac{1-\nu}{R_0} \frac{\partial^3 U_0}{\partial x \partial \varphi^2}\right] + \frac{R_0^2}{D} Z' = 0$$

-----3.5.2

The second set of equations contain  $U_1(x, \varphi)$ ,  $V_1(x, \varphi)$  and  $W_1(x, \varphi)$  as dependent variables. They depend only on the solution of the first set which give  $U_0(x, \varphi)$ ,  $V_0(x, \varphi)$  and  $W_0(x, \varphi)$ . This second set give the corrections due to the initial irregularity of the shell.

On introducing the assumption that the extension of the middle surface of the shell is negligibly small, (i.e.  $\epsilon_x = 0$ ,  $\epsilon_\varphi = 0$  and  $\gamma_{x\varphi} = 0$  in Equation 3.3.1), Equations (3.5.2) reduce to those given by S. Timoshenko (20).

If, now, a system of loads acting on the shell is symmetrical with respect to the plane  $x=0$  of the shell and symmetrical with respect to the axis  $\varphi=0$  in any plane of the cross section, the radial displacement at points  $+\varphi$  and  $-\varphi$  must be equal to each other and in the same direction, and the circumferential displacement at all points on the symmetry axis

must vanish. To satisfy these boundary conditions, Equations (3.5.1) can be taken in the form:

$$\begin{aligned} u &= U_0(x, \varphi) + \delta U_1(x) \cos n\varphi \\ v &= V_0(x, \varphi) + \delta V_1(x) \sin n\varphi \end{aligned} \quad 3.5.3$$

and  $w = W_0(x, \varphi) + \delta W_1(x) \cos n\varphi$

The longitudinal displacement  $u$  is chosen as a function of  $\cos n\varphi$  so that the variable  $\varphi$  in the second group of linear partial differential equations can be separated. Then, the second group of equations reduces to a set of linear ordinary differential equations, in the independent variable  $x$ .

$$\begin{aligned} & -\nu R_0 W_1' + \frac{n(1+\nu)}{2} R_0 V_1' + R_0^2 U_1'' - \frac{n(1-\nu)}{2} U_1 \\ & = [(m^2 R_0^2 - \nu n^2 - 1) m R_0 W_0 - m R_0^2 \frac{\partial U_0}{\partial x}] \sin mx - \nu m^2 R_0^2 U_0 \cos mx, \\ & -n R_0^2 W_1'' + n(F + n^2 - 1) W_1 + \frac{1-\nu}{2} (F+1) R_0^2 V_1'' - n^2 F V_1 - \frac{n}{2} [F(1+\nu) - (1-\nu)] R_0 U_1' \\ & = \left\{ F[n(n^2-1) + \nu n m^2 R_0^2] - 2n(n^2-1) \right\} W_0 \cos mx - \frac{1-\nu}{2} n m^2 R_0^3 \frac{\partial U_0}{\partial x} \cos mx \\ & \quad + \left[ F n m R_0 + \frac{n}{2} (1-\nu) m^3 R_0^3 + n(\nu m^2 R_0 - 1) m R_0 \right] U_0 \sin mx \\ & - R_0^4 W_1'''' + (2n^2 - \nu) R_0^2 W_1'' - (F + n^4 - n^2) W_1 - n(1-\nu) R_0^2 V_1'' + n F V_1 \\ & + [\nu F - n^2(1-\nu)] R_0 U_1' \\ & = \left\{ F[-2(n^2-1) - 2\nu m^2 R_0^2] + 2n^2(n^2-1) + (2\nu n^2 - \nu - 1) m^2 R_0^2 \right\} W_0 \cos mx \\ & \quad + \left[ F(m^2 R_0^2 + \nu n^2 - \nu) R_0 + (2m^2 R_0^2 - 2\nu + n^2 - \nu n^2) m^2 R_0^3 \right] \frac{\partial U_0}{\partial x} \cos mx \\ & \quad - [F m R_0 + (m^2 R_0^2 - \nu + n^2 - \nu n^2) m^3 R_0^3 + n^2(\nu m^2 R_0^2 - 1) m R_0] U_0 \sin mx \end{aligned}$$

When the external loads have been specified, Equations (3.5.2) can be solved and the solution  $U_o(x, \varphi)$ ,  $V_o(x, \varphi)$  and  $W_o(x, \varphi)$  used for solving Equations (3.5.4). However, the application of the general theory of bending of circular cylindrical shells in even the simplest cases may result in very complicated calculations. To make the theory applicable to the solution of practical problems some further simplifications in this theory are necessary.

The shell concerned is under the action of uniform external pressure. In equations (3.5.2),  $X'$  and  $Y'$  are equal to zero and  $Z'$  is equal to a constant,  $p$ . The solution for the case of a circular cylindrical shell subjected to uniform external pressure is well known.

When the shell is free to expand in a longitudinal direction at both ends we have as a solution of Equations (3.5.2)

$$U_o(x, \varphi) = (\nu p R_o / E h) x, \quad V_o(x, \varphi) = 0, \quad W_o(x, \varphi) = p R_o / E h$$

When the shell is restrained at its ends the approximate solution of Equations (3.5.2) is

$$U_o = 0, \quad V_o = 0, \quad W_o = w_o = (1 - \nu^2) p R_o / E h. \quad 3.5.5$$

The above solution is, of course, only correct at points distant from the supports. In the vicinity of the supports localized longitudinal bending occurs. Since interest centers in conditions at points remoted from the supports, it is satisfactory to use Equations (3.5.5) in Equations (3.5.4) for the determination of  $U_1$ ,  $V_1$ , and  $W_1$ . For a long shell the longitudinal

bending due to end restraint dies out rapidly (20).

Assuming now that  $U_1(x)$ ,  $V_1(x)$  and  $W_1(x)$  have the form:

$$\begin{aligned} U_1(x) &= \gamma_{mn} \sin(mx) \\ V_1(x) &= \beta_{mn} \cos(mx) \end{aligned} \quad 3.5.6$$

and  $W_1(x) = \alpha_{mn} \cos(mx)$

When  $x = 0$ ,  $U_1(x)$  satisfies the boundary condition that, due to the symmetry of the shell with respect to the plane  $x = 0$ ,  $u$  at  $x = 0$  must be equal to zero. Substituting Equations (3.5.6) into (3.5.4) and using  $U_0 = 0$ ,  $V_0 = 0$  and  $W_0 = w_0$ , the three simultaneous ordinary differential equations reduce to three simultaneous algebraic equations.

$$\begin{aligned} & \nu m R_0 \alpha_{mn} - \frac{1+\nu}{2} n m R_0 \beta_{mn} - \left[ m^2 R_0^2 + \frac{n^2(1-\nu)}{2} \right] \gamma_{mn} = \left[ m^3 R_0^3 + m R_0 (n^2 \nu - 1) \right] \omega_0; \\ & n \left[ m^2 R_0^2 + (F + n^2 - 1) \right] \alpha_{mn} - \left[ m^2 R_0^2 (F + 1) \frac{1-\nu}{2} + n^2 F \right] \beta_{mn} \\ & \quad - \frac{n m R_0}{2} [F(1+\nu) - (1-\nu)] \gamma_{mn} \\ & = \left\{ F[n(n^2 - 1) + \nu n m^2 R_0^2] - 2n(n^2 - 1) \right\} \omega_0, \\ & - \left[ m^4 R_0^4 + m^2 R_0^2 (2n^2 - \nu) + (F + n^4 - n^2) \right] \alpha_{mn} + n \left[ m^2 R_0^2 (1-\nu) + F \right] \beta_{mn} \\ & \quad + m R_0 [\nu F - n^2 (1-\nu)] \gamma_{mn} \\ & = \left\{ F[-2(n^2 - 1) - 2\nu m^2 R_0^2] + 2n^2(n^2 - 1) + m^2 R_0^2 (2\nu n^2 - \nu - 1) \right\} \omega_0 \end{aligned}$$

-----3.5.7

In the derivation of the relations between strains and displacements and of the equations of equilibrium, the extension of the middle surface of the shell was included. It can be seen that in Equations (3.5.7) the terms  $-2n(n^2 - 1)\omega_0$  and

$[2n^2(n^2 - 1) + m^2 R_o^2(2\nu n - \nu - 1)] w_o$  in the right hand sides of the second and third equations represent the effect of the extension of middle surface of the shell. In the case of a shell the value of  $F = 12(R_o/h)^2$  is very large. For simplicity in calculation, the terms corresponding to the effect of the extensibility of the middle surface of the shell can be neglected.

By disregarding these terms and solving Equations (3.5.7), the coefficients  $\alpha_{mn}$ ,  $\beta_{mn}$  and  $\gamma_{mn}$  in the displacement components are obtained.

$$\begin{aligned}\alpha_{mn} &= (C_2/C_1)(pR_o^4/D) \\ \beta_{mn} &= [nC_3/(1-\nu)C_1](pR_o^4/D) \\ \gamma_{mn} &= -[mR_o C_4/(1-\nu)C_1](pR_o^4/D)\end{aligned}\quad 3.5.8$$

where

$$C_1 = (1-\nu^2)m^4 R_o^4 F + m^8 R_o^8 + (4n^2 - \nu)m^6 R_o^6 + [6n^4 - n^2(5+\nu) + (1-\nu^2)]m^4 R_o^4$$

$$+ n^2(4n^2 - 3)(n^2 - 1)m^2 R_o^2 + n^4(n^2 - 1)^2 + \frac{1}{F}[m^8 R_o^8 + (n^2 - \nu)m^6 R_o^6$$

$$- n^2(n^2 + \nu - 1)m^4 R_o^4 - n^4(n^2 - 1)m^2 R_o^2]$$

$$C_2 = \nu m^6 R_o^6 + [n^2(3 + 2\nu - 2\nu^2) - 2 + \nu]m^4 R_o^4 + n^2[n^2(2 + \nu) - (3 - \nu)]m^2 R_o^2$$

$$+ n^4(n^2 - 1) + \frac{1}{F}\{[2n^2(1 - \nu) + \nu]m^6 R_o^6 + [n^2(1 + 2\nu - \nu^2) - 2 + \nu]m^4 R_o^4$$

$$- n^2[2n^2(1 - \nu) - n^2(2 - \nu) + 1]m^2 R_o^2\}$$

$$C_3 = (1 - \nu)(1 + 2\nu)m^4 R_o^4 + (1 - \nu)[2n^2(1 + \nu) - 3]m^2 R_o^2 + n^2(n^2 - 1)(1 - \nu)$$

$$\begin{aligned}
& + \frac{1}{F} \left\{ (1-\nu)m^8 R_0^8 - [2\nu n^2(1-\nu) - (1+\nu^2)] m^6 R_0^6 \right. \\
& - [4n^4(1-\nu^2) - 2n^2(4-3\nu)(1+\nu) + (1+\nu)(5-5\nu+2\nu^2)] m^4 R_0^4 \\
& - [2n^6(1-\nu)(2+\nu) - n^4(11-2\nu-7\nu^2) + n^2(13-7\nu-2\nu^2) - (5-5\nu+2\nu^2)] m^2 R_0^2 \\
& \left. - n^2(1-\nu)(n^6 - 4n^4 + 5n^2 - 2) \right\} \\
& + \frac{1}{F^2} \left\{ -(1-\nu)m^8 R_0^8 - (1-\nu)[\nu n^2 - (1+\nu)] m^6 R_0^6 + (1-\nu)[n^4 - n^2(1-\nu^2) - \nu] m^4 R_0^4 \right. \\
& \left. + (1-\nu)[\nu n^6 - n^4(1+\nu) + n^2] m^2 R_0^2 \right\}
\end{aligned}$$

$$\begin{aligned}
C_4 = & (1-\nu)(1-2\nu^2)m^4 R_0^4 - (1-\nu)(1-2\nu)m^2 R_0^2 + n^2(n^2-1)(1-\nu) \\
& + \frac{1}{F} \left\{ (1-\nu)m^8 R_0^8 + (1-\nu)[2n^2(2+\nu) - (1+\nu)] m^6 R_0^6 \right. \\
& + [4n^4(1-\nu^2) + 2n^2(4-3\nu-2\nu^2) + (1-\nu)(1+\nu-2\nu^2)] m^4 R_0^4 \\
& + [2\nu n^6(1-\nu) - n^4(5-6\nu-3\nu^2) + n^2(5-9\nu) - (1-\nu)(1-2\nu)] m^2 R_0^2 \\
& \left. - n^2[n^6(1-\nu) - 2n^4 + n^2(1+3\nu) - 2\nu] \right\} \\
& + \frac{1}{F^2} \left\{ (1-\nu)m^8 R_0^8 + (1-\nu)[\nu n^2 - (1+\nu)] m^6 R_0^6 \right. \\
& \left. - (1-\nu)[n^4 - n^2(1-\nu^2) - \nu] m^4 R_0^4 - (1-\nu)n^2[\nu n^4 - n^2(1+\nu) + 1] m^2 R_0^2 \right\}
\end{aligned}$$

When the deflected surface of the shell under the action of external loads has been determined, the internal forces and bending moments at any point of the shell can readily be found by means of Equations (3.3.3).

The bending moments,  $M_x$  and  $M_\varphi$ , in the longitudinal and circumferential directions respectively, are usually the determining factors in the failure of the thin shells. These bending moments at any point on the shell, have the following expressions respectively:

$$\begin{aligned}
 M_x = -\frac{D}{R_o^2} \{ & -\delta [m^2 R_o^2 + \nu(n^2 - 1)] \alpha_{mn} \cos mx \cos n\varphi \\
 & - 2\delta^2 \nu(2n^2 - 1) \alpha_{mn} \cos^2 mx \cos^2 n\varphi \\
 & + \delta^2 [m R_o (m^2 R_o^2 - \nu) \gamma_{mn} - \nu m^2 R_o^2 \alpha_{mn}] \sin^2 mx \cos^2 n\varphi \\
 & + \delta^2 [\nu n(n^2 - 1) \beta_{mn} + \nu n^2 \alpha_{mn}] \cos^2 mx \sin^2 n\varphi \}
 \end{aligned}$$

$$\begin{aligned}
 M_\varphi = -\frac{D}{R_o^2} \{ & -\delta [(n^2 - 1) + \nu m^2 R_o^2] \alpha_{mn} \cos mx \cos n\varphi \\
 & - 2\delta^2 (2n^2 - 1) \alpha_{mn} \cos^2 mx \cos^2 n\varphi \\
 & - \delta^2 [(1 - \nu m^2 R_o^2) m R_o \gamma_{mn} + m^2 R_o^2 \alpha_{mn}] \sin^2 mx \cos^2 n\varphi \\
 & + \delta^2 [n(n^2 - 1) \beta_{mn} + n^2 \alpha_{mn}] \cos^2 mx \sin^2 n\varphi \}
 \end{aligned}$$

-----3.5.9

### 3.6. Illustrative Problems

In the first illustrative problem, the surface of the cylindrical shell is defined by

$$\rho = R_0 [1 - \delta \cos(\pi x/L) \cos 2\varphi]. \quad 3.6.1$$

The cross section of the shell at  $x=0$  is a first buckling mode shape which is very close to an ellipse. At  $x = L/2$  the imperfection dies out and the cross-section is a circle. At a point one half wave-length along the longitudinal axis,  $x=L$ , the cross-section of the shell returns to its elliptical shape with a phase difference of 90 degrees. As the coordinate  $x$  increases, the cross-section approaches a circle again and when  $x$  is equal to one full wave-length the cross-section returns to its elliptical shape as at  $x=0$ .

Neglecting the extension of the middle surface of the shell, the displacement components are given by the following expressions:

$$\begin{aligned} u &= \delta \delta_{m2} \sin(\pi x/L) \cos 2\varphi \\ v &= \delta \beta_{m2} \cos(\pi x/L) \sin 2\varphi \\ w &= \delta \alpha_{m2} \cos(\pi x/L) \cos 2\varphi \end{aligned} \quad 3.6.2$$

and the values of  $C_s$  in Equations (3.5.8) are:

$$\begin{aligned} C_1 &= m^4 R_0^4 F + m^8 R_0^8 + 16 m^6 R_0^6 + 77 m^4 R_0^4 + 156 m^2 R_0^2 + 144 \\ &\quad + \frac{1}{F} (m^8 R_0^8 + 4 m^6 R_0^6 - 12 m^4 R_0^4 - 48 m^2 R_0^2) \\ C_2 &= 10 m^4 R_0^4 + 20 m^2 R_0^2 + 48 + \frac{1}{F} (8 m^6 R_0^6 + 2 m^4 R_0^4 - 100 m^2 R_0^2) \end{aligned}$$

$$C_3 = m^4 R_o^4 + 5m^2 R_o^2 + 12 + \frac{1}{F} (m^8 R_o^8 + m^6 R_o^6 - 37m^4 R_o^4 - 127m^2 R_o^2 - 72)$$

$$+ \frac{1}{F^2} (-m^8 R_o^8 + m^6 R_o^6 + 12m^4 R_o^4 - 12m^2 R_o^2)$$

$$C_4 = m^4 R_o^4 - m^2 R_o^2 + 12 + \frac{1}{F} (m^8 R_o^8 + 15m^6 R_o^6 + 33m^4 R_o^4 - 61m^2 R_o^2 - 144)$$

$$+ \frac{1}{F^2} (m^8 R_o^8 - m^6 R_o^6 - 12m^4 R_o^4 + 12m^2 R_o^2)$$

where  $m = \pi/L$ .

For the case of a thin shell, the magnitude of  $F$  is very large and the terms in  $1/F^2$  can be neglected in the calculation of these coefficients.

The bending moments, at any point, in the longitudinal and circumferential directions of the shell are given by:

$$M_x = -\frac{D}{R_o^2} (-\delta m^2 R_o^2 \alpha_{m2} \cos mx \cos 2\varphi + \delta^2 m^3 R_o^3 \gamma_{m2} \sin^2 mx \cos^2 2\varphi)$$

$$M_\varphi = -\frac{D}{R_o^2} [-3\delta \alpha_{m2} \cos mx \cos 2\varphi - 14\delta^2 \alpha_{m2} \cos^2 mx \cos^2 2\varphi \\ - \delta^2 (m R_o \gamma_{m2} + m^2 R_o^2 \alpha_{m2}) \sin^2 mx \cos^2 2\varphi \\ + \delta^2 (6\beta_{m2} + 4\alpha_{m2}) \cos^2 mx \sin^2 2\varphi]$$

-----3.6.3

The maximum bending moments in the longitudinal and circumferential directions occur at the point  $x=0$  and  $\varphi = 0$ . They are

$$\text{Max. } M_x = \delta m^2 \alpha_{m2} D$$

3.6.4

$$\text{Max. } M_\varphi = \delta (3 + 14\delta) \alpha_{m2} D/R_o^2$$

in which only the coefficient  $\alpha_{m2}$  appears.

The maximum bending moments  $M_x$  and  $M_\varphi$  at  $x=0$  and  $\varphi=0$  are plotted against the wave-length of the dent in the longitudinal direction for  $R_o/h$  ranging from 20 to 100 and  $\delta$  equal to .01 in Figs. (3.6.1) and (3.6.2).

For values of  $R_o/h=60$ ,  $L/R_o=10$  and  $\delta = 0.01$ , the variation of bending moments  $M_x$  and  $M_\varphi$  along the line  $\varphi = 0$  in the longitudinal direction of the shell are given in Figs. (3.6.3) and (3.6.4) respectively.

When  $m$  is equal to zero, the problem reduces to a two-dimensional one. The displacements in the circumferential and radial directions of an elliptical ring are given by:

$$v = \delta p R_o^4 \sin 2\varphi / 6D$$

and

$$w = \delta p R_o^4 \cos 2\varphi / 3D$$

The maximum bending moment at point of  $\varphi = 0$  is equal to

$$\text{Max. } M_\varphi = (3 + 14\delta) \delta p R_o^4 / 3.$$

In the case  $\delta = 0.01$ ,  $M_\varphi = 0.010467 p R_o^2$  which differs from the result obtained by Marbec's method by about 5%.

In the other extreme case  $m$  is infinitely large, i.e., the wave-length of the dent along the longitudinal axis of the shell approaches zero. In this case, the bending moments  $M_x$  and  $M_\varphi$  given by Equations (3.6.3) tend to become constant. However, when the dent is highly localized, the results of the solution given in the preceeding article are not reliable since the method of analysis is based on the assumption that the wave-length of the dent along the longitudinal axis of the shell is large compared with the mean radius of the shell.

Two other cases,  $n=2$ ,  $\nu=1/3$  and  $n=4$ ,  $\nu=1/3$  are also illustrated. The maximum bending moments  $M_x$  and  $M_\varphi$  at  $x=0$  and  $\varphi=0$  are similarly plotted against the wave-length of the imperfection for  $R_0/h$  ranging from 20 to 100 and  $\delta=0.01$ . By specifying  $R_0/h=60$ ,  $L/R_0=10$  and  $\delta=0.01$  as in the case of  $n=2$ ,  $\nu=0$ , the bending moments  $M_x$  and  $M_\varphi$  along the line  $\varphi=0$  can also be plotted. These curves are shown in Figs. (3.6.5) to (3.6.12).

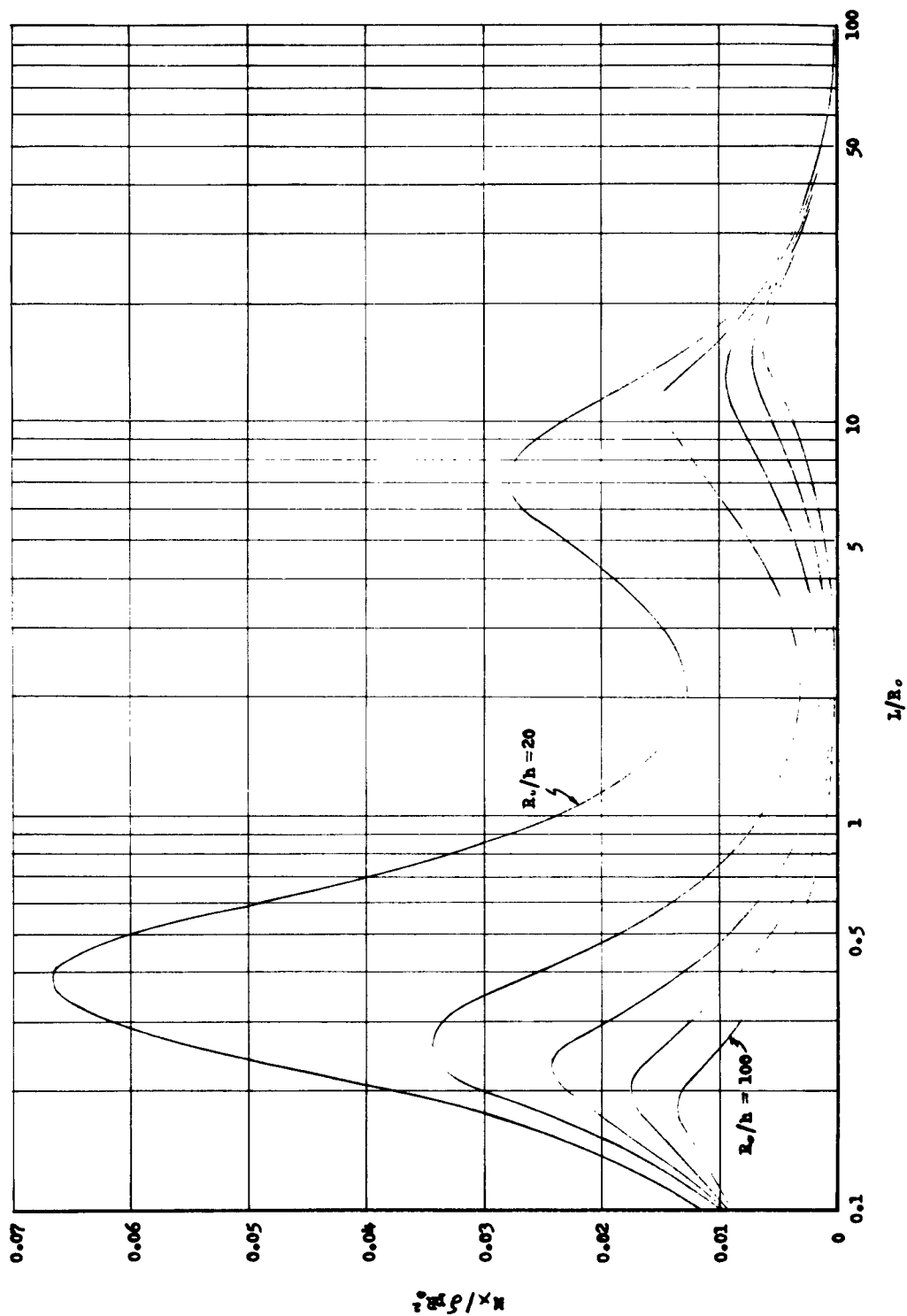
The foregoing curves show that, when the wave-length of the dent lies within a certain range, which depends on the value of  $R_0/h$ , bending moments in both the circumferential and the longitudinal directions are negligibly small and membrane stresses predominate. As the wave-length exceeds that range, the circumferential bending moment increases appreciably. If the wave-length increases still further, the circumferential bending moment increases until the solution is identical to the two-dimensional case.

On the other hand, when the wave-length decreases, bending moments increase over the intermediate wave-length at which membrane stresses predominate. The dent becomes more localized in character. The method of analysis, however, is not accurate in the vicinity of a highly localized dent.

Other things being equal, smaller values of  $R_0/h$  produce greater bending moments in shells having the same wave-length for the dent. In the case  $n=4$ , bending moments produced are larger than those for  $n=2$  if the wave-lengths of the dents and the values of  $R_0/h$  for these two cases are the same.

$$\rho = R_0 \left( 1 - \delta \cos \frac{\pi x}{L} \cos 2\varphi \right)$$

For  $\psi = 0$



$N_T$  at  $x = 0$  &  $\varphi = 0$

FIG. 3.6.1

$$\rho = R_0 \left( 1 - 0.01 \cos \frac{R_0}{L} \cos 2\varphi \right)$$

For  $\nu = 0$

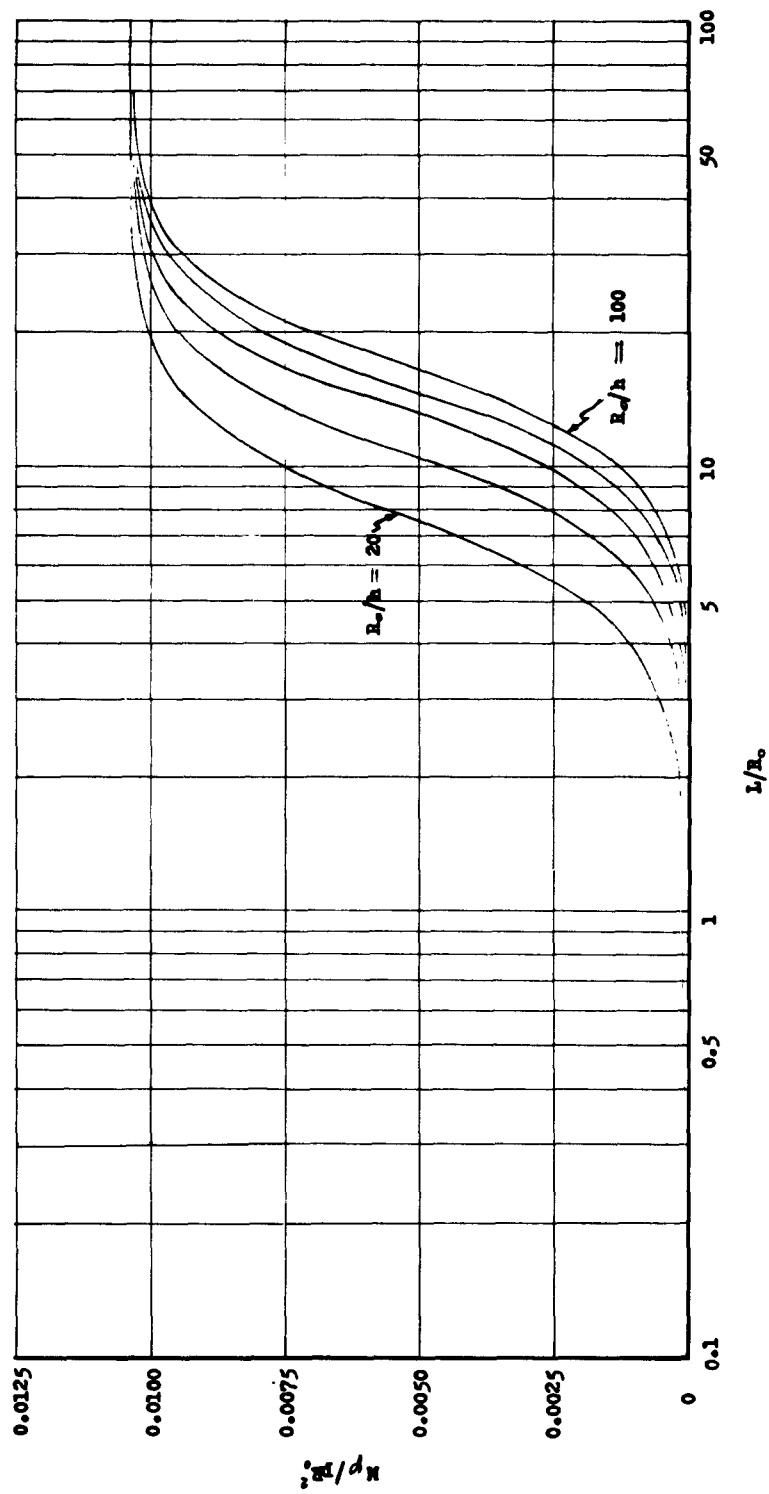
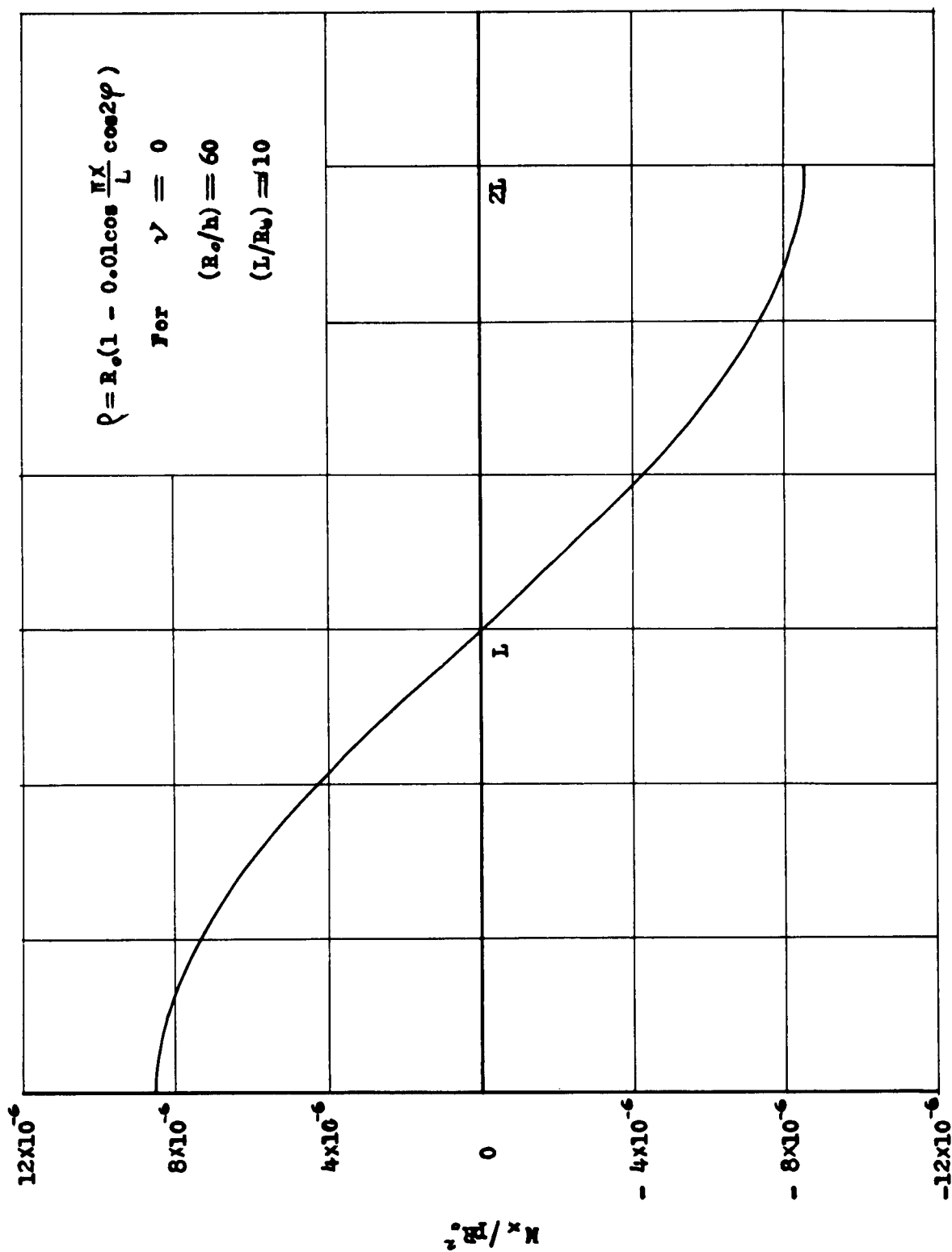
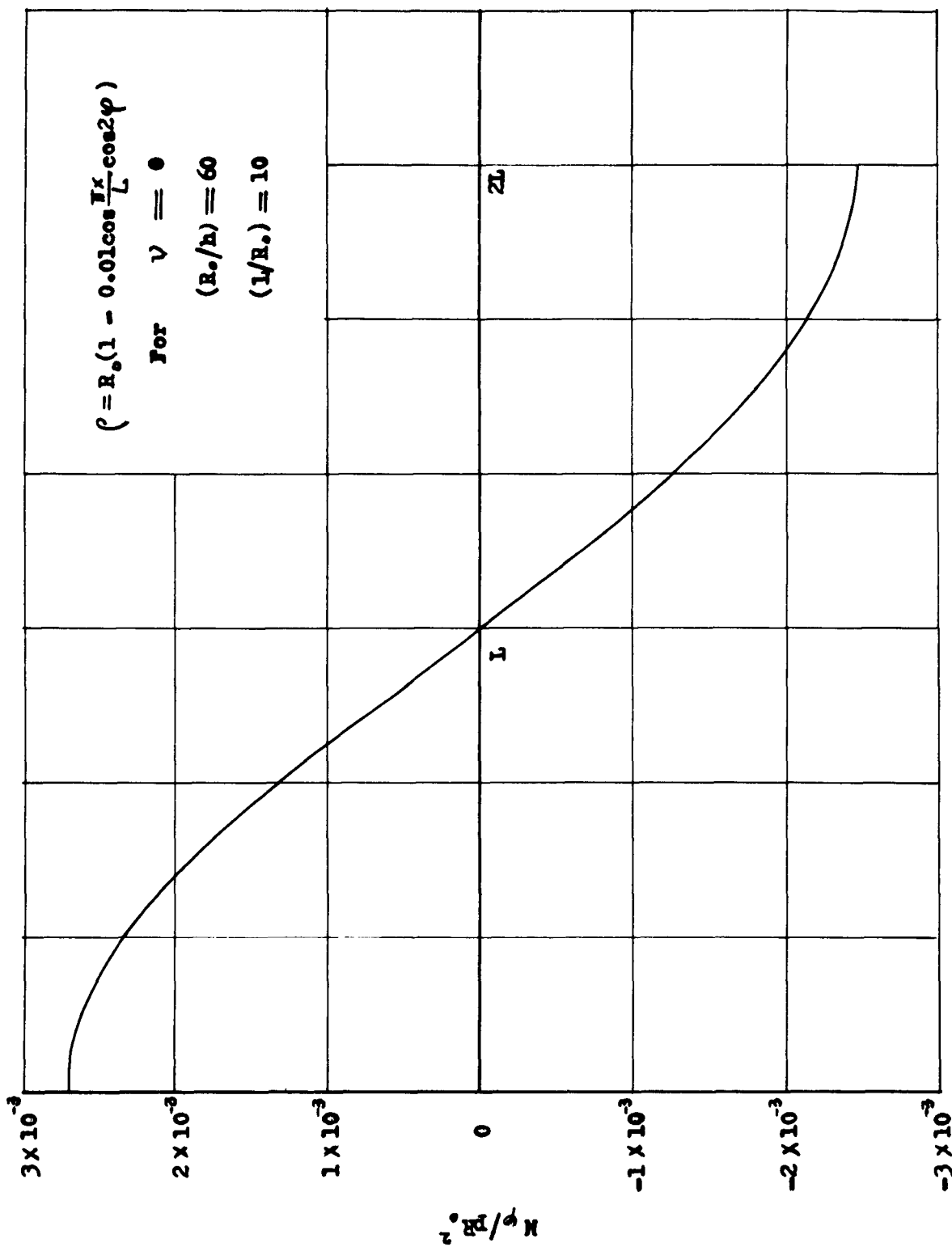


FIG. 3.6.2  $u_m$  at  $x = 0$  &  $\varphi = 0$

FIG. 3.6.3  $N_x$  at  $\varphi = 0$

FIG. 3.6.4  $M_\varphi$  at  $\varphi = 0$

$$\rho = R_0 \left( 1 - 0.01 \cos \frac{\pi X}{L} \cos 2\varphi \right)$$

For  $V = 1/3$

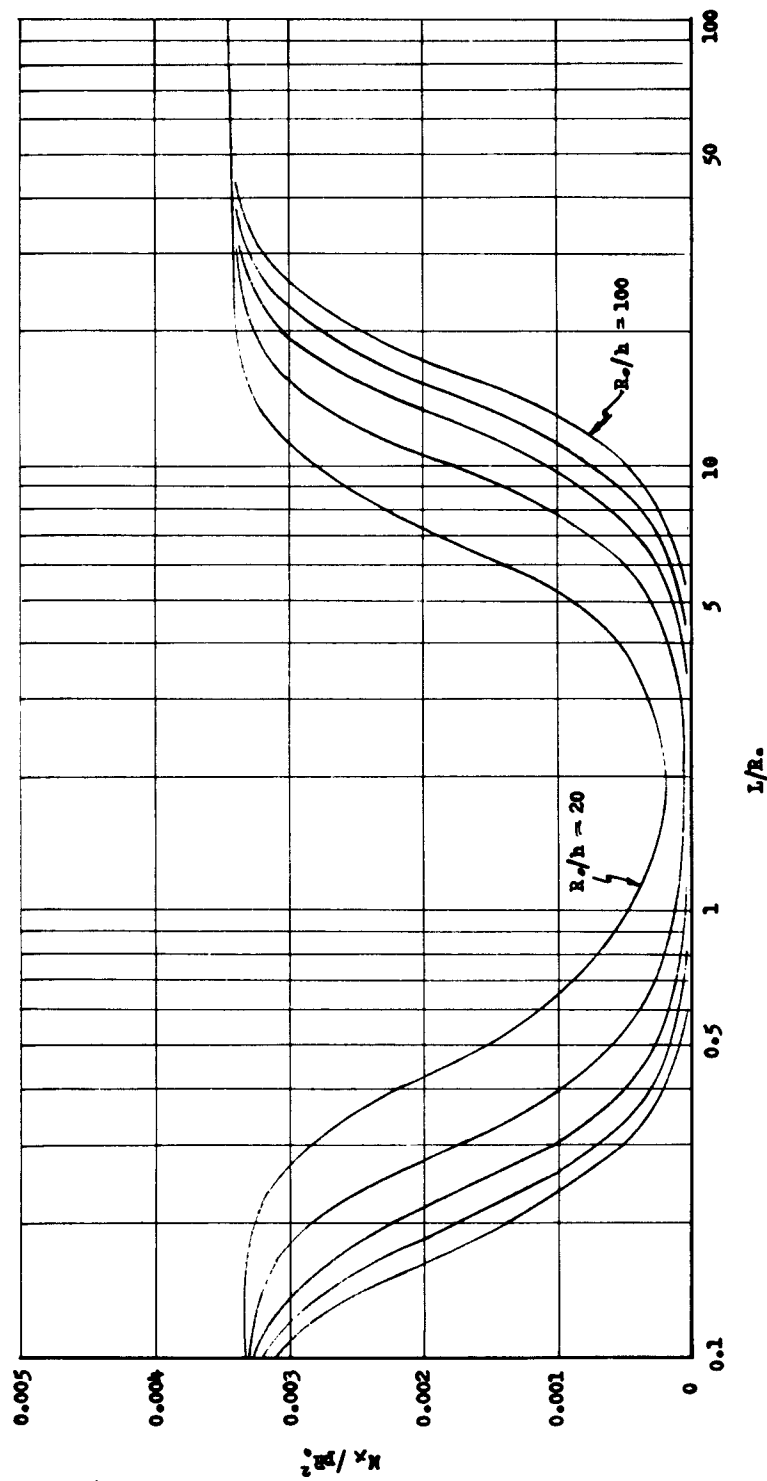


FIG. 3.6.5  $H_x$  at  $x = 0$   $\varphi = 0$

$$\rho = R \left( 1 - 0.01 \cos \frac{\pi Y}{L} \cos 2\varphi \right)$$

For  $\nu = 1/3$

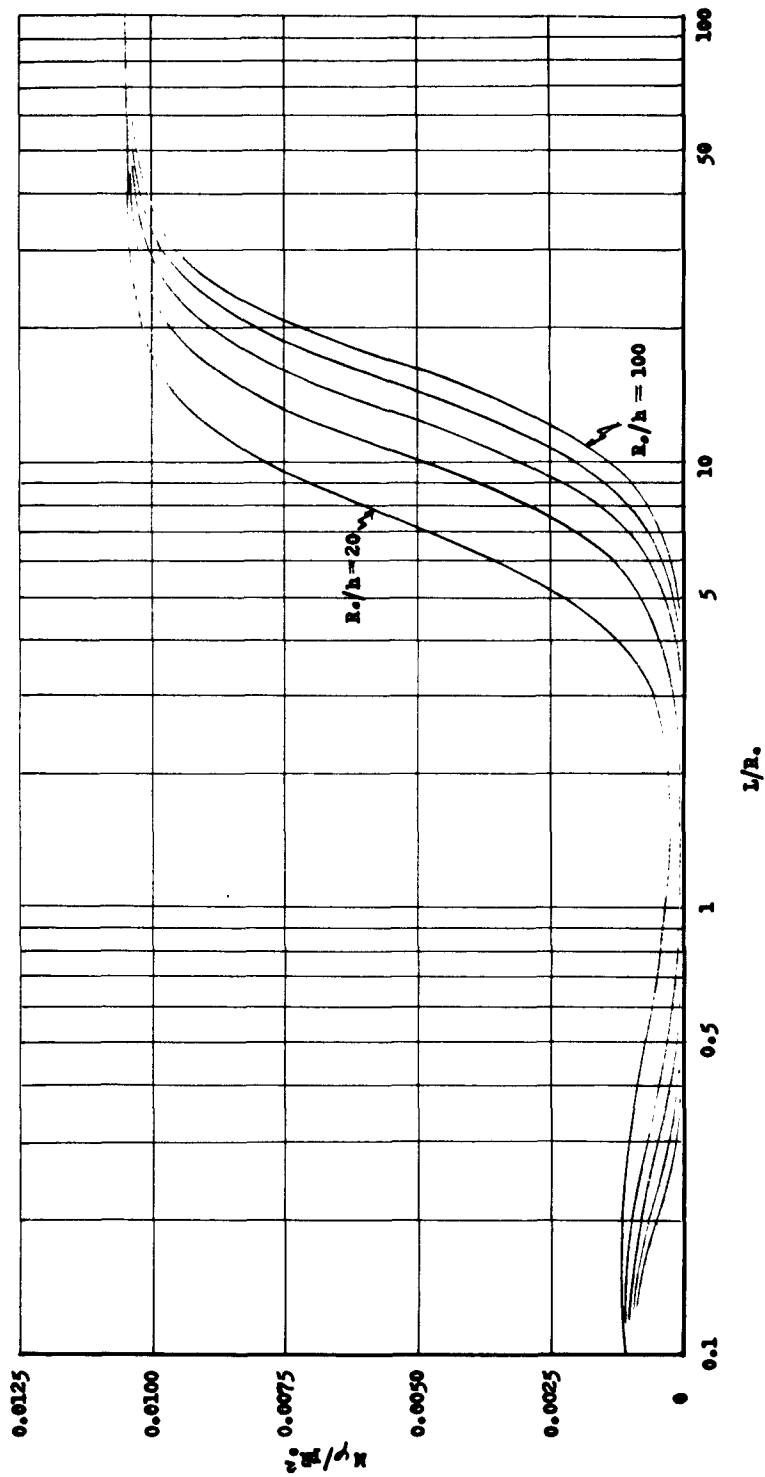


FIG. 3.6.6  $u/R_0$  at  $x=0$  &  $\varphi=0$

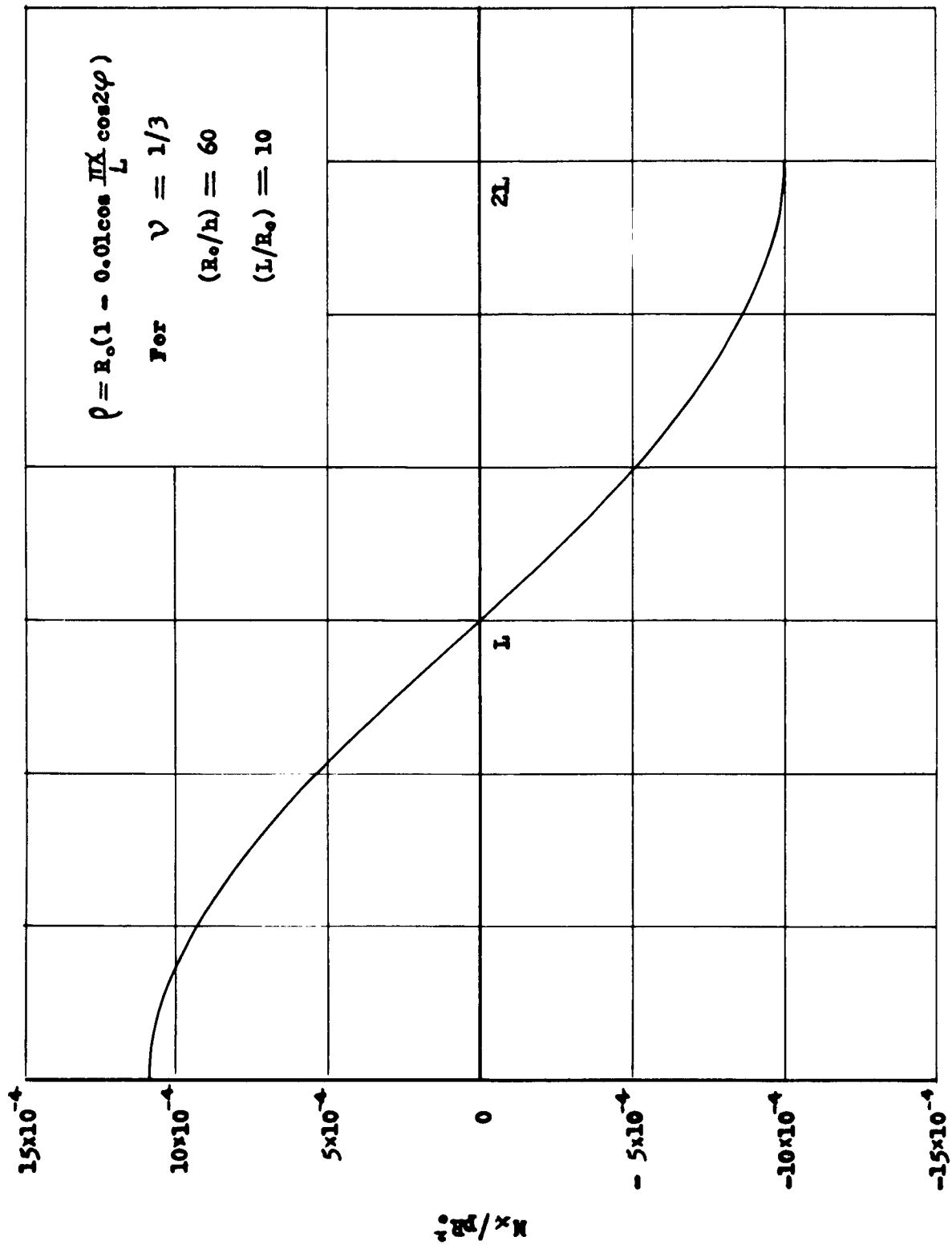
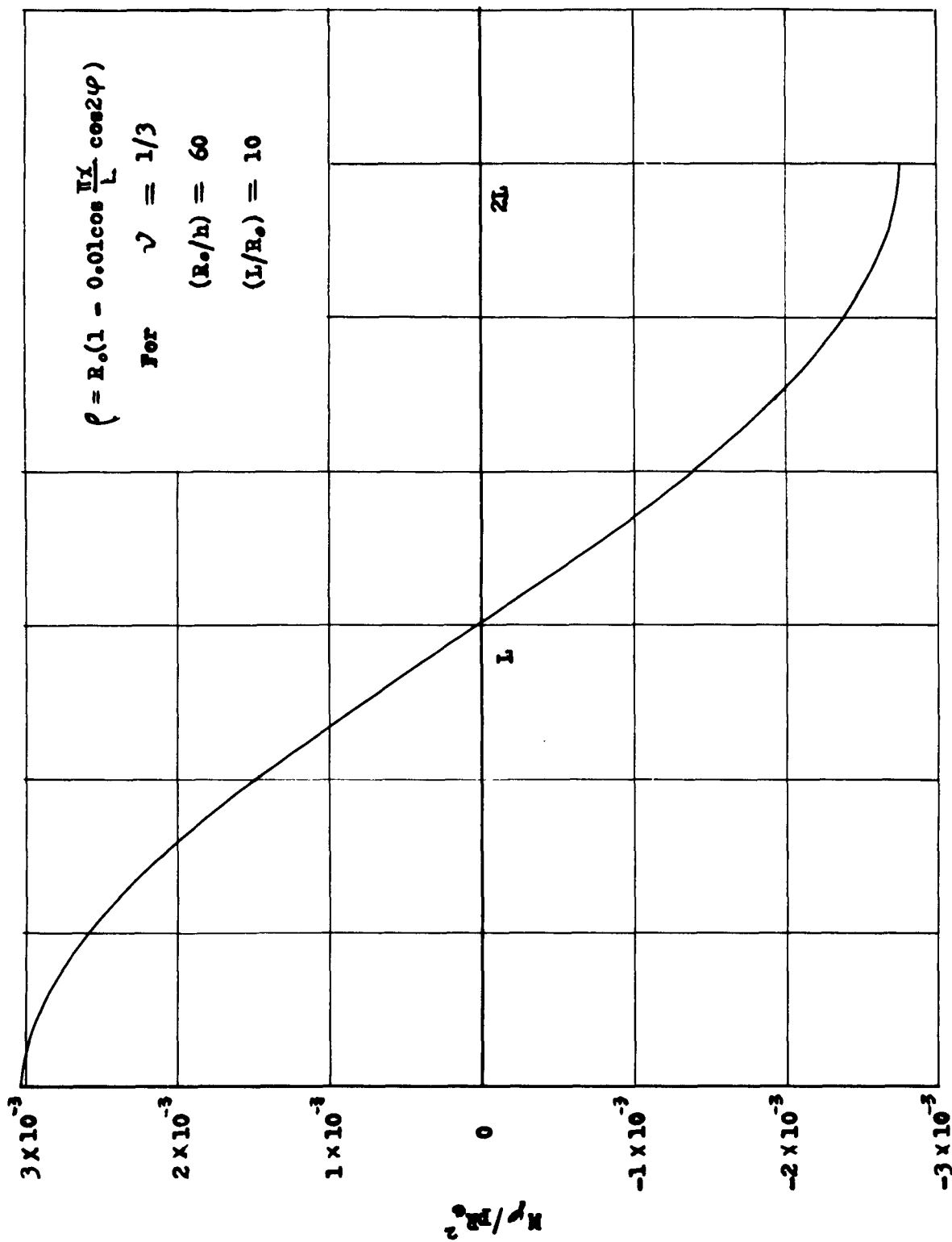


FIG. 3.6.7  $M_x$  at  $\varphi = 0$

FIG. 3.6.8  $w^0$  at  $\varphi=0$

$$\rho = R \sqrt{1 - 0.01 \cos \frac{R}{L} \cosh 4\varphi}$$

For  $\nu = 1/3$

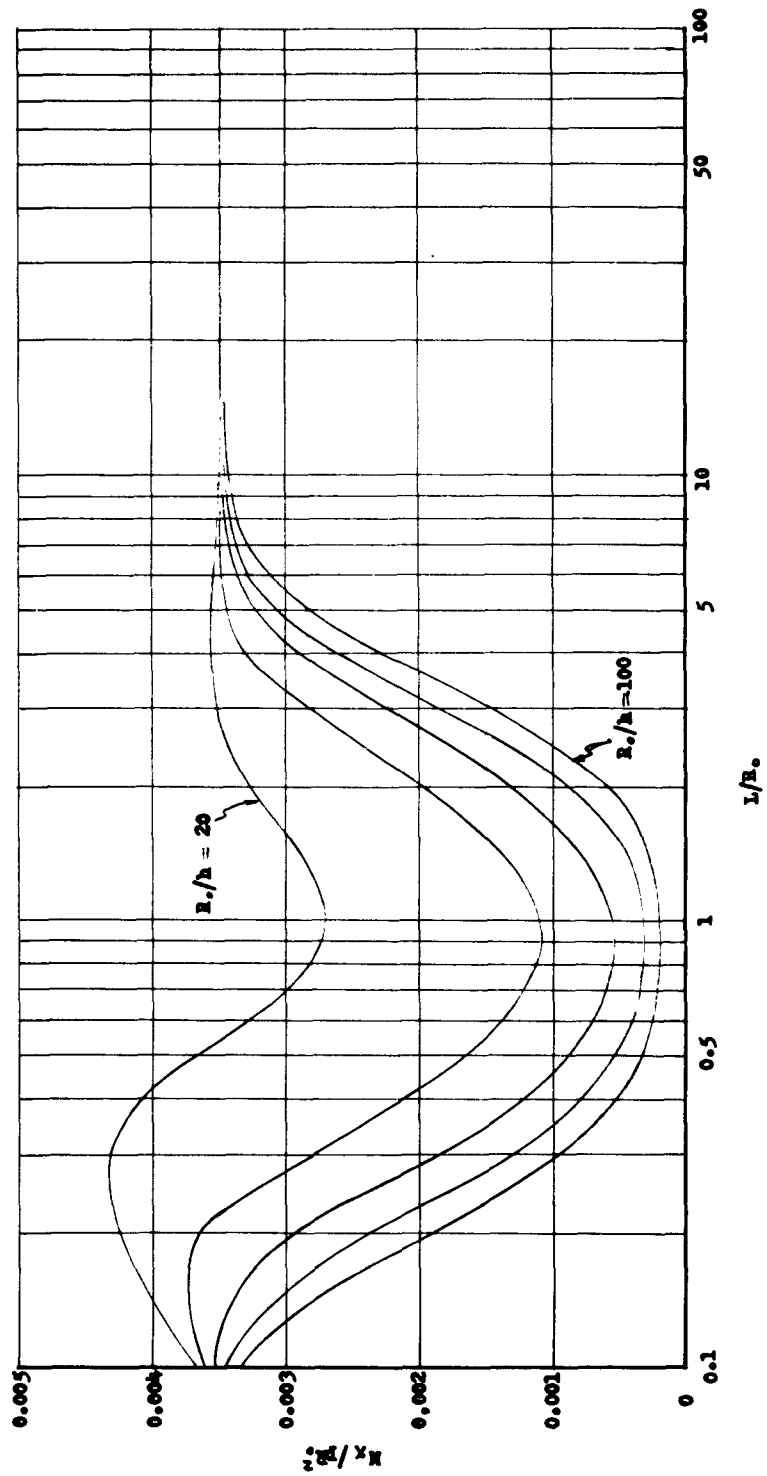


FIG. 3.6.9  $N_x$  at  $x = 0$   $\varphi = 0$

$$\rho = R_0 \left( 1 - 0.01 \cos \frac{\pi x}{L} \cos \phi \right)$$

For  $\nu = 1/3$

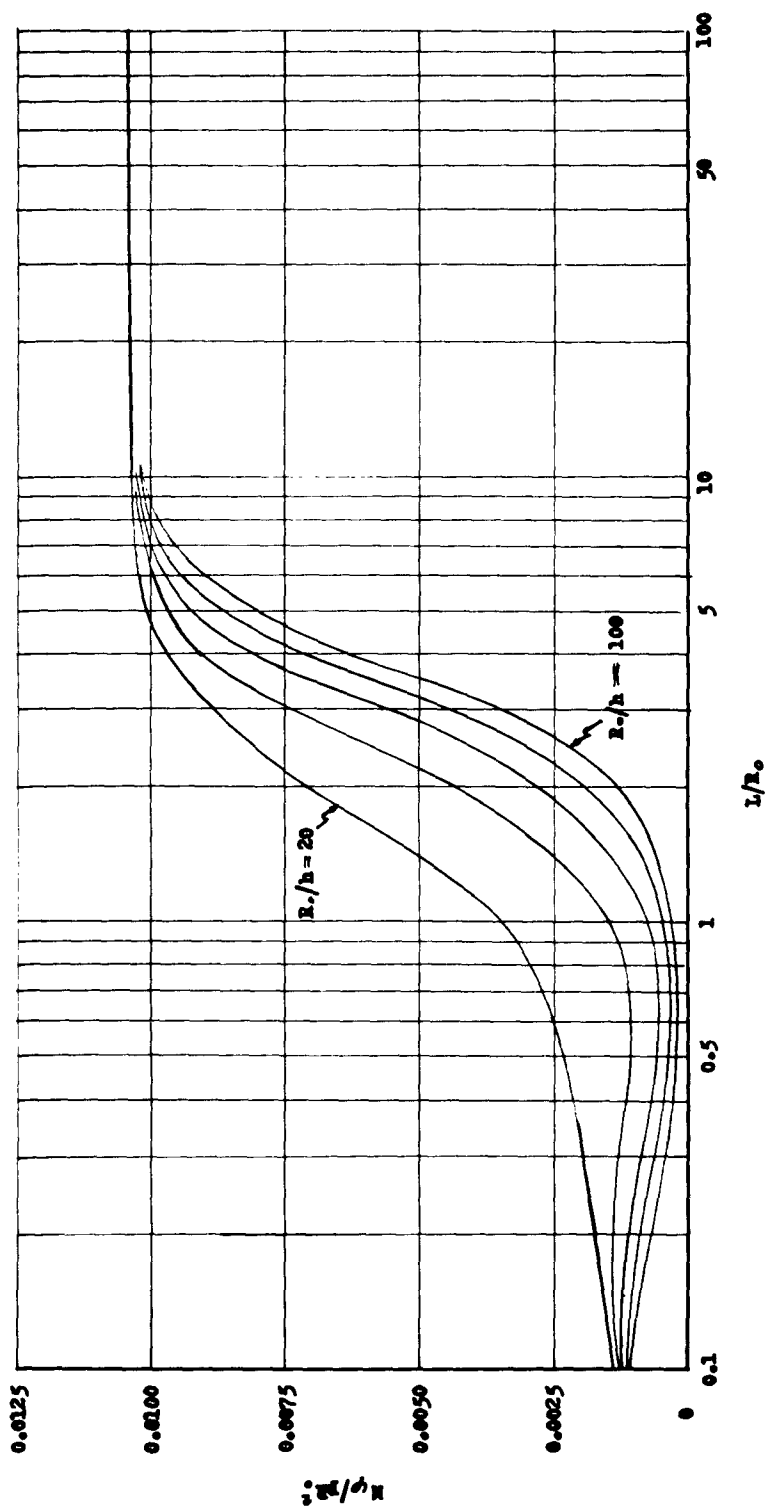
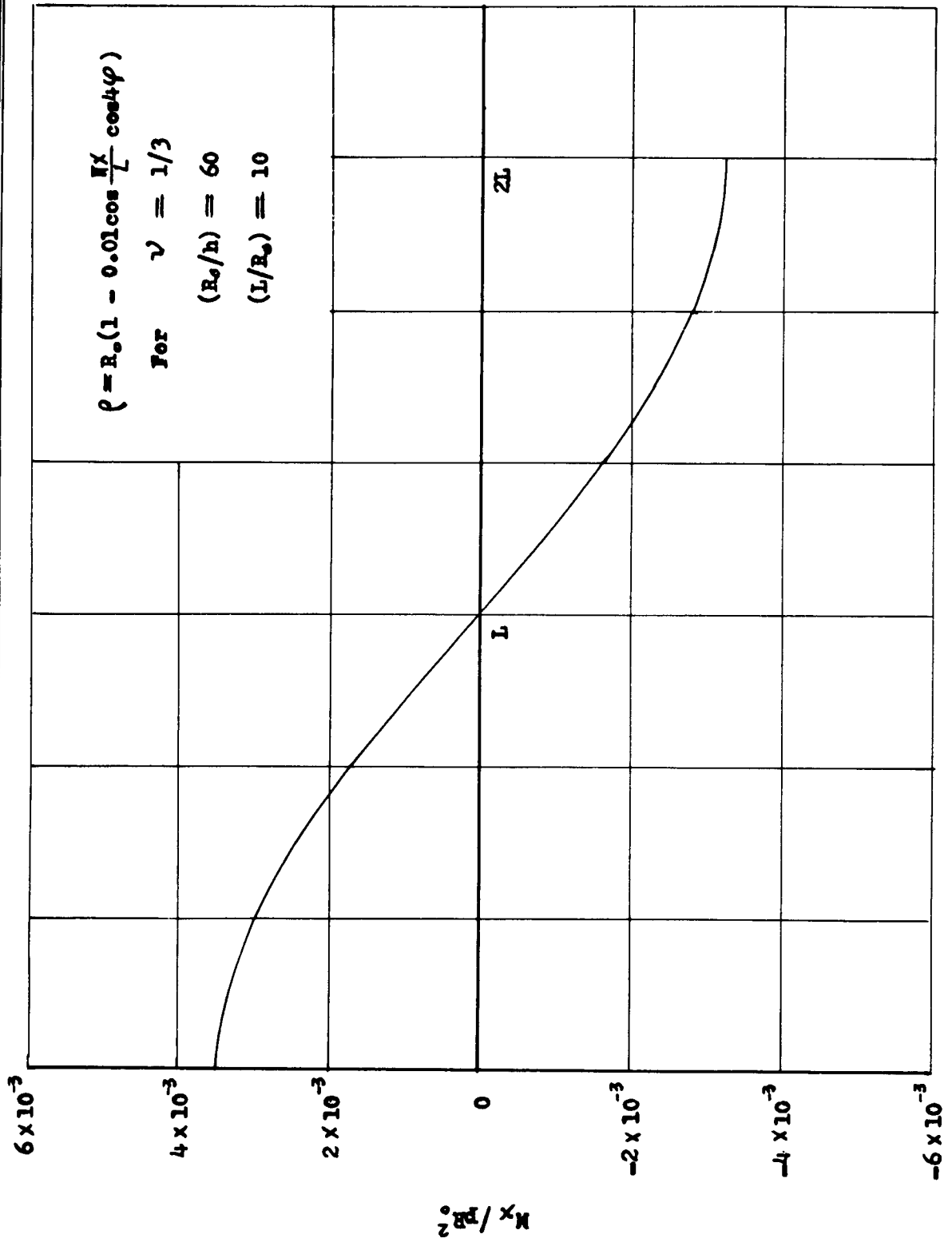
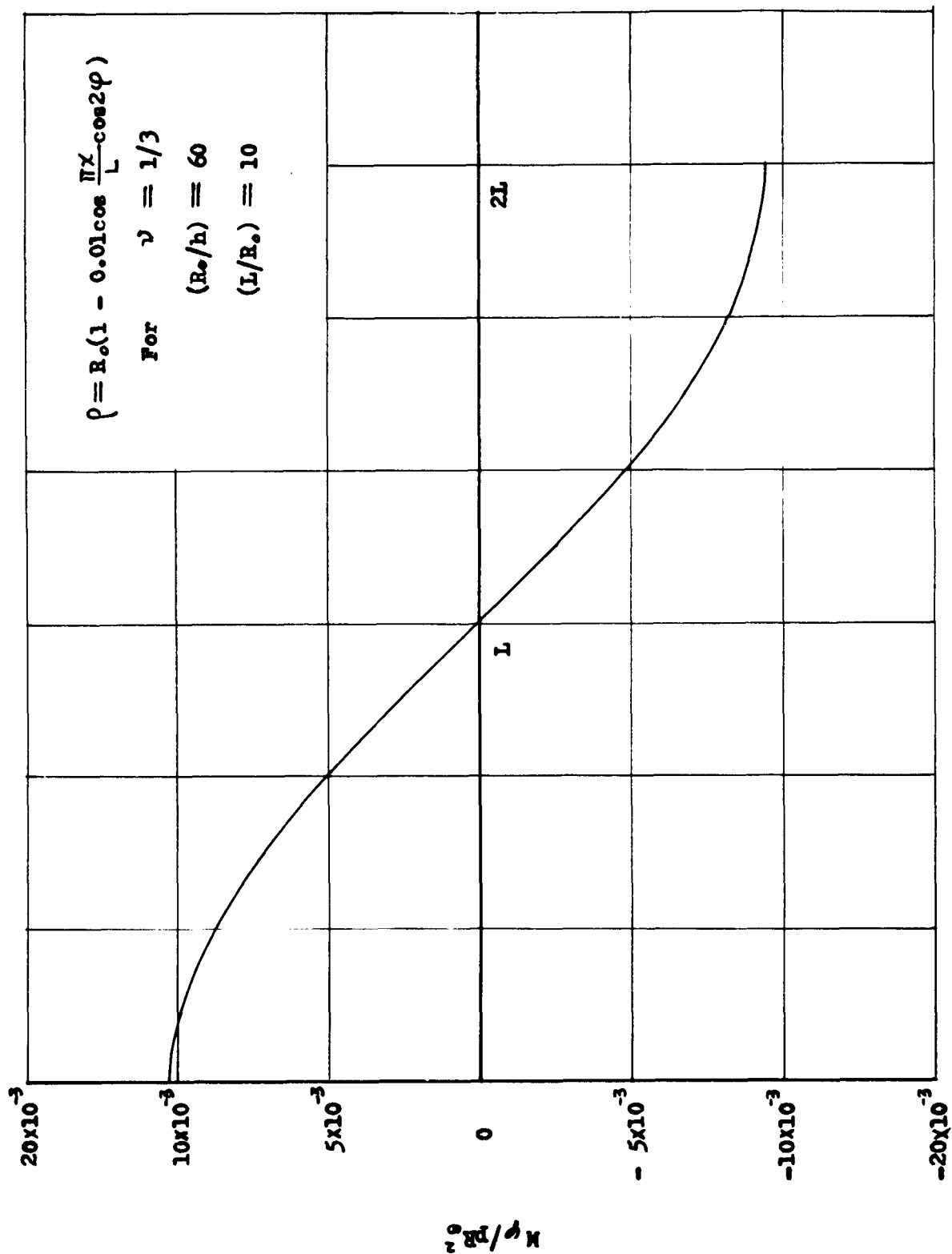


FIG. 3.6.10  $\mu/\eta = 0$  &  $\phi = 0$

FIG. 3.6.11  $M_x$  at  $\varphi = 0$

FIG. 3.6.12  $w_\varphi$  at  $\varphi=0$

## 4. CONCLUSIONS

### 4.1. Summary

Investigations of circular rings with initial out-of-roundness and local dents are presented using both small-deflection (approximate) and large-deflection ('exact') theories.

In the small-deflection case, a method due to Marbec is recommended as the most simple and convenient one for the prediction of bending moments and stresses due to dents and initial out-of-roundness in rings under hydrostatic pressure. When the initial imperfection in a circular ring is small, the bending moment at any point on the ring can be obtained by multiplying the amount of irregularity at that point, measured with reference to a 'node circle' defined in the text, by the constant force ( $pR_0$ ) in the ring.

A numerical approach which is a combination of two well-known procedures, is developed for the 'exact' or large-deflection analysis of circular rings with initial imperfections, taking into consideration the deflections and the extension of the ring axis. A method of successive approximations is used in conjunction with the numerical procedure of integration due to

N. M. Newmark (16). Although it requires a considerable amount of numerical work, this procedure has the merit of simplicity, wide adaptability and a straightforward arrangement of computations. The results of illustrative examples reveal that for that practical problems the effect of the extensibility of the ring axis is negligible; also, changes in direction of the external loads due to the deflection of the ring axis do not materially affect the final stresses. In the case of a thin ring with small imperfections they can be disregarded without introducing appreciable error. However, due to the small deviation of the ring axis from its original shape, the presence of axial forces contributes substantially to the stresses produced in the ring.

A rapid method of analysis taking into account the effect of axial forces is developed. By means of this procedure the bending moments or stresses produced in rings with small initial irregularities, under hydrostatic pressure, can easily be predicted. This simplification is obtained by multiplying the bending moments or stresses determined by small-deflection theory, by factors proportional to the relative amplitudes of the various buckling mode shapes present in the original dent. The shape of a ring with initial out-of-roundness can be expressed as a Fourier series. If the imperfection of the ring is small, the zero'th term in the Fourier series gives the difference of the radii of the circular ring and the node circle of Marbec's method. The coefficient of the  $n$ 'th term in the series represents the amount of irregularity of the  $n$ 'th buckling mode shape measured with reference to the node circle.

The range of validity of the simplified procedure has been verified by the foregoing numerical method. In case the maximum amount of initial irregularity of a circular ring ranges from  $1/100$  to  $1/10$  of its original radius, results obtained by these two methods check quite well. If the initial irregularity becomes large, appreciable error will be involved in the result obtained by the simplified method. When the maximum amount of initial imperfection reaches two tenths of the radius, the maximum bending moment predicted by the rapid method of analysis is thirty per cent greater than that calculated by the numerical method. However, for most practical problems the maximum amount of initial imperfection will hardly be more than one tenth of the radius. Furthermore, if the imperfection is very large, residual stresses, which are assumed to be negligibly small in the present investigation, might be of prime importance.

A small initial irregularity greatly reduces the strength of a circular ring. In small-deflection theory, when the maximum amount of imperfection is equal to  $1/100$  of the radius, the maximum fiber stress due to bending moment is from four to seven times the hoop stress, depending on the ratio of the nominal radius to the thickness. The foregoing figures are for values of  $R_0/h$  ranging from 50 to 100. Taking into account the deflection of the ring axis, the effect of such an irregularity on the strength of a circular ring under uniform external pressure becomes even more pronounced in most practical cases.

The bending moments and hence the stresses developed in an elliptical ring (using the simplified method) are obtained by

multiplying those predicted by small-deflection theory by a factor  $1/(1 - p/p_{cr.})$ . The bending moments developed in a ring having local dents depends not only on the magnitude of the external pressure but also on the geometrical shape of the dented portion. For a particular dented shape illustrated in Fig. (2.1.2.2), the maximum bending moment was found to be about 18% greater than that predicted by small-deflection theory. It may also be concluded that if the shape of a ring is similar to that of the lower buckling modes the effect of the deflection of the ring axis on the stresses will be of primary significance. For example, the worst case examined is that of a ring having an initial ellipticity under hydrostatic pressure.

Since the foregoing solution is two-dimensional in nature, a question arises as to the limits of its validity when applied to localized dents in cylindrical shells. This question has been answered (at least partially) by the solution of the shell equations for a dent varying in magnitude along the longitudinal axis of the shell. Due to the complexity of the general shell equations, some simplifications have been made in order to make the problem solvable. The results of analysis indicate that when the wave-length of the dent is large compared with the initial radius of the cylindrical shell, the solution coincides with the two-dimensional case. As the wave-length decreases, bending moments decrease and membrane stresses predominate. As the wave-length decreases still further and the dent becomes more localized in character, bending moments again increase. The method of analysis, presented in this dissertation, however, is

not accurate in the vicinity of a highly localized dent.

## APPENDIX I

Nomenclature

The following nomenclature, used in this report, conforms as nearly as possible to the conventional symbols of applied mechanics. The quantity in parentheses represents the dimension units corresponding to the symbol.

$E$  = Young's modulus of elasticity (  $MT^{-2} L^{-1}$  ).

$A$  = Area of cross section (  $L^2$  ).

$h$  = Thickness of either a ring or a shell (  $L$  ).

$R_0$  = Radius of a circular ring or a circular cylindrical shell (  $L$  ).

$x, y$  = Coordinates of any point on the ring axis with respect to the principal axes of the ring (  $L, L$  ).

$x', y'$  = Coordinates of any point on the ring axis with respect to any arbitrary axes  $X'$  and  $Y'$  (  $L, L$  ).

$a, b$  = Coordinates of the center of the node circle with respect to the principal axes (  $L, L$  ).

$\rho, \varphi$  = Coordinates of any point in polar coordinates (  $L, \text{Rad.}$  ).

$r_c$  = Radius of the node circle (  $L$  ).

$\rho_c$  = Distance between any point on the ring axis and the center of the node circle (  $L$  ).

$\rho^{(n)}$  = Component of  $\rho$  for  $n$ 'th buckling mode shape (  $L$  ).

$R, R'$  = Radii of curvature of the ring in the unstrained and strained states respectively ( L ).

$B$  = Curved length factor,  $-(ds/d\varphi) = [r^2 + (dr/d\varphi)^2]^{1/2}$  ( L ).

$I$  = Moment of inertia of the section of the ring having unit width (  $L^4$  ).

$ds, ds'$  = Curved length of an element in the undeformed and deformed states respectively ( L ).

$\Delta ds$  = Total extension of the ring axis ( L ).

$\xi, \eta$  = Deflections of the ring axis in X- and Y- directions respectively ( L ).

$d\xi, d\eta$  = Changes of length of  $dx$  and  $dy$  respectively ( L ).

$p$  = Uniform external pressure per unit length of the ring of the shell (  $MT^{-2}$  ).

$p_{cr.}$  = Critical pressure of a circular ring subjected to uniform external pressure,  $= (n^2 - 1)EI/R_o^3$ ,  $n = 2, 4, \dots$  (  $MT^{-2}$  ).

$H, V$  = Horizontal and vertical components of force per unit length (  $MT^{-2} L$  ).

$N$  = Normal force, per unit length, acting through the centroidal axis (  $MT^{-2} L$  ).

$Q$  = Shearing force, per unit length, parallel to the cross section (  $MT^{-2} L$  ).

$M$  = Bending moment, per unit length, acting at any point (  $MT^{-2} L^2$  ).

$M^{(n)}$  = Component of  $M$  for  $n$ 'th buckling mode shape (  $MT^{-2} L^2$  ).

$m_s$  = Static moment, per unit length, due to external loads only (  $MT^{-2} L^2$  ).

$\Delta m_s$  = Increment of  $m_s$  resulting from the deflection of the ring axis (  $MT^{-2} L^2$  ).

$\sigma_M, \sigma_N$  = Unit fiber stresses, per unit length, due to bending moment and normal force respectively (  $MT^{-2} L^{-1}$  ).

$(\Delta d\theta)_1, (\Delta d\theta)_2$  = Rotations of cross section due to the extension of the ring axis and due to bending moment respectively ( Rad. ).

$\Delta d\theta$  = Total rotation of cross section of an element ( Rad. ).

$\Delta\theta$  = Angle-change from a reference point to any point ( Rad. ).

$\theta$  = Angle between the tangent and X-axis at any point ( Rad. ).

$2\phi$  = Angular amplitude of a local dent in a ring ( Rad. ).

$\delta$  = Relative amplitude of initial irregularity of either a ring or a shell ( Dimensionless ).

$\epsilon$  = Unit deformation of the central line ( Dimensionless ).

$e$  = Ellipticity of an ellipse, equal to 1 minus the ratio of minor axis to major axis ( Dimensionless ).

$n$  = Number of buckling mode shape ( Dimensionless ).

$\lambda$  = A constant,  $= pR_0/EI$  ( Dimensionless ).

$\nu$  = Poisson's ratio ( Dimensionless ).

$F^{(n)}$  = Magnification factor for n'th buckling mode shape,  
 $= 1/(1 - p/p_{cr.})$  ( Dimensionless ).

$a_n, b_n$  = Coefficient in Fourier Series ( Dimensionless ).

$D$  = Flexural rigidity of the section, per unit length, of a shell,  $= Eh^3/12(1 - \nu^2)$  (  $MT^{-2} L^2$  ).

$K$  = A constant,  $= (1 - \nu^2)/Eh$  (  $M^{-1} T^2$  ).

$A$  = Curved length factor in longitudinal direction,  $= [1 + (d\phi/dx)^2]^2$  ( Dimensionless ).

$F =$  A constant,  $= 12(R_o/h)^2$  (Dimensionless) .

$x, \varphi =$  Cylindrical coordinates ( L, Rad. ) .

$m =$  A constant,  $= \pi / L$  (  $L^{-1}$  ) .

$2L =$  Wave-length of the dent ( initial imperfection ) along  
the longitudinal axis of a shell ( L ) .

$X', Y', Z' =$  Pressure acting on the shell element in the  
directions of coordinate axes X, Y, and Z  
respectively (  $MT^{-2}$  ) .

$\alpha, \beta, \gamma =$  Coefficients of deflection configurations w, v,  
and u of the middle surface of the shell  
( Dimensionless ) .

Strains, Displacements, Stresses, forces and moments in cylindrical coordinates follow the notations used in "Theory of Plates and Shells" by S. Timoshenko (20) .

## BIBLIOGRAPHY

1. A. G. Greenhill: "The Elastic Curve under Uniform Normal Pressure," Math. Annalen, Vol. 52, 1899, p. 465.
2. S. Timoshenko: "Buckling of Compressed Ring and Curved Bar," Chapter IV; "Buckling of Shells," Chapter IX, Theory of Elastic Stability, First Edition, McGraw Hill Book Company, New York, 1936.
3. M. Marbec: "Théorie de l'équilibre d'une lame élastique soumise à une pression uniforme," Bulletin de L'association Technique Maritime, No. 19, session de 1908, p. 181.
4. S. Timoshenko: "Working Stresses for Column and Thin-walled Structures," Journal of Applied Mechanics, Vol. 1, No. 4, 1933, p. 173.
5. M. A. Thuloup: "Remarques sur le calcul des tuyaux minces sous pression," Bull. Ass. Tech. Marit. Aero., No. 41, 1937, p. 317.
6. G. Salet: "Flambement, déformations élastiques non proportionnelles au chargement, application aux bouteilles ovalisées, analogies entre flambement et vibration," Bull. Ass. Tech. Marit. Aero., No. 46, 1947, p. 393.

7. A. E. H. Love: "General Theory of Thin Plates and Shells," Chapter XXIV, A Treatise on the Mathematical Theory of Elasticity, Fourth Edition, Dover Publications, New York, 1944.
8. W. R. Osgood and J. A. Joseph: "On the General Theory of Thin Shells," Journal of Applied Mechanics, Vol. 17, No. 4, 1950, p. 396.
9. H. Neuber: "General Theory of Shells I and II," Z. angew. Math. Bd. 29, No. 4, April & May 1949, pp. 97 and 142.
10. J. Barthelemy: "Sur la possibilité de calculer au moyen du principe de Lagrange la pression critique de flambement des enveloppes de révolution," Bull. Ass. Tech. Marit. Aero., No. 48, 1949, p. 849.
11. A. L. Goldenweiser: "Approximate Calculation of Thin Shells of Zero Gauss Curvature," Prikl. Mat. i. Mekh., Vol. 11, July-August, 1947, p. 409.
12. V. Z. Vlasov: "Some New Problems on Shells and Thin Structures," Nat. Adv. Comm. Aero. Tech. Memo., No. 1204, March, 1949, p. 1.
13. H. L. Langhaar: "A Strain Energy Expression for Thin Elastic Shells," Journal of Applied Mechanics, Vol. 16, No. 2, June, 1949, p. 183.
14. P. S. Epstein: "On the Theory of Elastic Vibrations in Plates and Shells," Journal of Mathematics and Physics, Vol. 21, 1942, p. 198.
15. E. F. Burmistrov: "Symmetrical Deformation of A Nearly Cylindrical Shell," Prikl. Mat. Mekh., No. 13, 1949, p. 401.

16. N. M. Newmark: "Numerical Procedure for Computing Deflections, Moments and Buckling Loads," Transactions, Amer. Soc. of C. E., No. 108, 1943, p. 1161.
17. R. Mayer: "Über Elastizität und Stabilität des geschlossenen und offenen Kreisbogens," Zeitschrift für Mathematik und Physik, Bd. 61, 1912, p. 246.
18. H. Heuber: "Vereinfachtes Verfahren zur Spannungsberechnung in dünnwandigen prismatischen Hohlkörpern unter Innendruck," Z. angew. Math. Mech., Bd. 28, 1948, p. 187.
19. R. V. Churchill: Fourier Series and Boundary Value Problems, First Edition, McGraw Hill Book Company, New York, 1941.
20. S. Timoshenko: "General Theory of Cylindrical Shells," Chapter XI, Theory of Plates and Shells, First Edition McGraw Hill Book Company, New York, 1940.

DISTRIBUTION LIST - PROJECT NR 064-183Administrative, Reference and Liaison Activities

|  |                   |   |     |
|--|-------------------|---|-----|
| Chief of Naval Research<br>Department of the Navy<br>Washington 25, D.C.<br>ATTN: Code 438<br>: Code 432                               | (2)<br>(1)        | Commanding Officer<br>Office of Naval Research<br>Branch Office<br>801 Donahue Street<br>San Francisco 24, California                     | (1) |
| Director, Naval Research Laboratory<br>Washington 25, D.C.<br>ATTN: Tech. Info. Officer<br>: Technical Library<br>: Mechanics Division | (9)<br>(1)<br>(2) | Commanding Officer<br>Office of Naval Research<br>Branch Office<br>1030 Green Street<br>Pasadena, California                              | (1) |
| Commanding Officer<br>Office of Naval Research<br>Branch Office<br>495 Summer Street<br>Boston 10, Massachusetts                       | (1)               | Contract Administrator, SE Area<br>Office of Naval Research<br>Department of the Navy<br>Washington 25, D.C.<br>ATTN: R. F. Lynch         | (1) |
| Commanding Officer<br>Office of Naval Research<br>Branch Office<br>346 Broadway<br>New York City 13, New York                          | (1)               | Officer in Charge<br>Office of Naval Research<br>Branch Office, London<br>Navy No. 100<br>FPO, New York City, New York                    | (5) |
| Office of Naval Research<br>The John Crerar Library Bldg.<br>Tenth Floor, 86 East Randolph St.<br>Chicago 1, Illinois                  | (2)               | Library of Congress<br>Washington 25, D.C.<br>ATTN: Navy Research Section   | (2) |
| Commander<br>U.S. Naval Ordnance Test Station<br>Inyokern, China Lake, California<br>ATTN: Code 501                                    | (1)               | Commander<br>U.S. Naval Ordnance Test Station<br>Pasadena Annex<br>3202 East Foothill Blvd.<br>Pasadena 8, California<br>ATTN: Code P8087 | (1) |
| Commander<br>U.S. Naval Proving Grounds<br>Dahlgren, Virginia  | (1)               |   |     |

Department of Defense  
Other Interested Government Activities  
GENERAL

Research and Development Board  
 Department of Defense  
 Pentagon Building  
 Washington 25, D.C.  
 ATTN: Library (Code 3D-1075)

(1)

Engineering Research and  
 Development Laboratory  
 Fort Belvoir, Virginia  
 ATTN: Structures Branch

(1)

Armed Forces Special Weapons Project  
 P.O. Box 2610  
 Washington, D.C.  
 ATTN: Col. G. F. Blunda

(1)

The Commanding General  
 Sandia Base, P.O. Box 5100  
 Albuquerque, New Mexico  
 ATTN: Col. Canterbury

(1)

Operation Research Officer  
 Department of the Army  
 Ft. Lesley J. McNair  
 Washington 25, D.C.  
 ATTN: Howard Brackney

(1)

ARMY

Chief of Staff  
 Department of the Army  
 Research and Development Division  
 Washington 25, D.C.  
 ATTN: Chief of Res. and Dev.

(1)

Office of Chief of Ordnance  
 Research and Development Service  
 Department of the Army  
 The Pentagon  
 Washington 25, D.C.  
 ATTN: ORDTB

(2)

Office of the Chief of Engineers  
 Assistant Chief for Public Works  
 Department of the Army  
 Bldg. T-7, Gravelly Point  
 Washington 25, D.C.  
 ATTN: Structural Branch  
 (R. L. Bloor)

(1)

Ballistic Research Laboratory  
 Aberdeen Proving Ground  
 Aberdeen, Maryland  
 ATTN: Dr. C. W. Lampson

(1)

Office of the Chief of Engineers  
 Asst. Chief for Military Const.  
 Department of the Army  
 Bldg. T-7, Gravelly Point  
 Washington 25, D.C.  
 ATTN: Structures Branch  
 (H. F. Carey)  
 : Protective Construction  
 Branch (I. O. Thorley)

(1)

(1)

Commanding Officer  
 Watertown Arsenal  
 Watertown, Massachusetts  
 ATTN: Laboratory Division

(1)

Commanding Officer  
 Frankford Arsenal  
 Philadelphia, Pa.  
 ATTN: Laboratory Division

(1)

Commanding Officer  
 Squier Signal Laboratory  
 Fort Monmouth, New Jersey  
 ATTN: Components and Materials  
 Branch

(1)

Office of the Chief of Engineers  
 Asst. Chief for Military Operations  
 Department of the Army  
 Bldg. T-7, Gravelly Point  
 Washington 25, D.C.  
 ATTN: Structures Dev. Brch. (W.F. Woollard)

(1)

Other Interested Government ActivitiesNAVY

Chief of Bureau of Ships  
Navy Department  
Washington 25, D.C.

ATTN: Director of Research (2)  
: Code 449 (1)  
: Code 430 (1)  
: Code 421 (1)

Director  
David Taylor Model Basin  
Washington 7, D.C.  
ATTN: Structural Mechanics  
Division (2)

Director  
Naval Engr. Experiment Station  
Annapolis, Maryland (1)

Director  
Materials Laboratory  
New York Naval Shipyard  
Brooklyn 1, New York (1)

Chief of Bureau of Ordnance  
Navy Department  
Washington 25, D.C.  
ATTN: Ad-3, Technical Library (1)  
: Rec., T. N. Girauard (1)

Superintendent  
Naval Gun Factory  
Washington 25, D.C. (1)

Naval Ordnance Laboratory  
White Oak, Maryland  
RFD 1, Silver Spring, Maryland  
ATTN: Mechanics Division (2)

Naval Ordnance Test Station  
Inyokern, California  
ATTN: Scientific Officer (1)

Naval Ordnance Test Station  
Underwater Ordnance Division  
Pasadena, California  
ATTN: Structures Division (1)

Chief of Bureau of Aeronautics  
Navy Department  
Washington 25, D.C.

ATTN: TD-41, Technical Library (1)  
: DE-22, C. W. Hurley (1)  
: DE-23, E. M. Ryan (1)

Naval Air Experimental Station  
Naval Air Material Center  
Naval Base  
Philadelphia 12, Pa.  
ATTN: Head, Aeronautical Materials  
Laboratory (1)

Chief of Bureau of Yards and Docks  
Navy Department  
Washington 25, D.C.  
ATTN: Code P-314 (1)  
: Code C-313 (1)

Officer in Charge  
Naval Civil Engr. Research and  
Eval. Lab, Naval Station  
Port Hueneme, California (1)

Superintendent  
Post Graduate School  
U. S. Naval Academy  
Monterey, California (1)

AIR FORCES

Commanding General  
U. S. Air Forces  
The Pentagon  
Washington 25, D.C.  
ATTN: Research and Development  
Division (1)

Commanding General  
Air Material Command  
Wright-Patterson Air Force Base  
Dayton, Ohio  
ATTN: MCAIDS (2)

Office of Air Research  
Wright-Patterson Air Force Base  
Dayton, Ohio  
ATTN: Chief, Applied Mechanics  
Group (1)

OTHER GOVERNMENT AGENCIES

|  |     |  |     |
|--|-----|--|-----|
| U. S. Atomic Energy Commission<br>Division of Research<br>Washington, D.C.                                       | (1) | National Advisory Committee for<br>Aeronautics<br>1724 F Street, N.W.<br>Washington, D.C.                                    | (1) |
| Argonne National Laboratory<br>P.O. Box 5207<br>Chicago 80, Illinois   | (1) | National Advisory Committee for<br>Aeronautics<br>Langley Field, Virginia<br>ATTN: Mr. E. Lundquist                          | (1) |
| Director,<br>National Bureau of Standards<br>Washington, D.C.<br>ATTN: Dr. W. H. Ramberg                         | (2) | National Advisory Committee for<br>Aeronautics<br>Cleveland Municipal Airport<br>Cleveland, Ohio<br>ATTN: J. H. Collins, Jr. | (1) |
| U. S. Coast Guard<br>1300 E Street, N.W.<br>Washington, D.C.<br>ATTN: Chief, Testing and<br>Development Division | (1) | U. S. Maritime Commission<br>Technical Bureau<br>Washington, D.C.<br>ATTN: Mr. V. Russo                                      | (1) |
| Forest Products Laboratory<br>Madison, Wisconsin<br>ATTN: L. J. Markwardt  | (1) |  |     |

CONTRACTORS AND OTHER INVESTIGATORS ACTIVELY ENGAGED IN RELATED RESEARCH

|  |     |   |     |
|--|-----|---|-----|
| Professor Jesse Ormendroyd<br>University of Michigan<br>Ann Arbor, Michigan  | (1) | Professor M. A. Sadowsky<br>Illinois Institute of Technology<br>Technology Center<br>Chicago 16, Illinois         | (1) |
| Dr. N. J. Hoff, Head<br>Department of Aeronautical<br>Engineering and Applied Mechanics<br>Polytechnic Institute of Brooklyn<br>99 Livingston Street<br>Brooklyn 2, New York | (1) | Dr. W. Osgood<br>Armour Research Institute<br>Technology Center<br>Chicago, Illinois                              | (1) |
| Dr. J. N. Goodier<br>School of Engineering<br>Stanford University<br>Stanford, California  | (1) | Professor R. L. Bisplinghoff<br>Massachusetts Inst. of Tech.<br>Cambridge 39, Massachusetts                       | (1) |
| Professor F. K. Teichmann<br>Department of Aeronautical Engr.<br>New York University<br>University Heights, Bronx<br>New York City, New York                                 | (1) | Professor B. Fried<br>Washington State College<br>Pullman, Washington   | (1) |
| Professor C. T. Wang<br>Department of Aeronautical Engr.<br>New York University<br>University Heights, Bronx<br>New York City, New York                                      | (1) | Professor E. Reissner<br>Department of Mathematics<br>Massachusetts Inst. of Tech.<br>Cambridge 39, Massachusetts | (1) |
|  |     | Dr. A. Phillips<br>School of Engineering<br>Stanford University<br>Stanford, California                           | (1) |

CONTRACTORS AND OTHER INVESTIGATORS ACTIVELY ENGAGED IN RELATED RESEARCH

|   |     |   |     |
|---|-----|---|-----|
| Professor E. Sternberg<br>Illinois Institute of Technology<br>Technology Center<br>Chicago 16, Illinois                                     | (1) | Professor L. S. Jacobsen<br>Stanford University<br>Stanford, California   | (1) |
| Dr. W. Prager<br>Grad. Div. Applied Mathematics<br>Brown University<br>Providence, Rhode Island   | (1) | Professor A. C. Eringen<br>Illinois Institute of Technology<br>Technology Center<br>Chicago 16, Illinois                            | (1) |
| Dr. W. H. Hoppmann<br>Department of Applied Mathematics<br>Johns Hopkins University<br>Baltimore, Maryland                                  | (1) | Professor B. J. Lazan<br>Engineering Experiment Station<br>University of Minnesota<br>Minneapolis 14, Minnesota                     | (1) |
| Professor W. K. Krefeld<br>College of Engineering<br>Columbia University<br>New York City, New York   | (1) | Commander<br>U. S. N.O.T.S.<br>China Lake, California   | (1) |
| Professor R. M. Hermes<br>University of Santa Clara<br>Santa Clara, California  | (1) | ATTN: Code 505  |     |
| Dr. W. A. McNair<br>Vice President, Research<br>Sandia Corporation<br>Sandia Base<br>Albuquerque, New Mexico                                | (1) | Professor George Lee<br>Dept. of Mechanics<br>Rensselaer Polytechnical Inst.<br>Troy, New York                                      | (1) |
| Dr. R. J. Hansen<br>Massachusetts Inst. of Technology<br>Cambridge 39, Massachusetts  | (1) | Professor Lloyd Donnell<br>Department of Mechanics<br>Illinois Institute of Technology<br>Technology Center<br>Chicago 16, Illinois | (1) |
| Dr. Francis H. Clauser<br>Chairman, Dept. of Aeronautics<br>The Johns Hopkins University<br>School of Engineering<br>Baltimore 18, Maryland | (1) | Professor Lynn Beedle<br>Fritz Engineering Laboratory<br>Lehigh University<br>Bethlehem, Pennsylvania                               | (1) |
| Dr. G. E. Uhlenbeck<br>Engineering Research Institute<br>University of Michigan<br>Ann Arbor, Michigan                                      | (1) | Dr. Bruce Johnston<br>301 West Engineering Bldg.<br>University of Michigan<br>Ann Arbor, Michigan                                   |     |
|   |     | Dr. Walter Bleakney<br>Department of Physics<br>Princeton University<br>Princeton, New Jersey                                       | (1) |

Library Engineering Foundation  
29 West 39th Street  
New York City, New York

(1)

Professor N. M. Newmark  
Department of Civil Engineering  
University of Illinois  
Urbana, Illinois

(2)

Dean W. L. Everitt  
College of Engineering  
University of Illinois  
Urbana, Illinois

(1)

Professor T. J. Dolan  
Dept. of Theoretical and Applied  
Mechanics  
University of Illinois  
Urbana, Illinois

(2)

#### TASK VI PROJECT - C. E. RESEARCH STAFF

W. H. Munse

J. E. Stallmeyer

R. J. Mosborg

W. J. Austin

L. E. Goodman

C. P. Siess

Research Assistants

(10)

Files

(5)

Reserve

(20)

Dr. C. B. Smith  
Department of Mathematics  
Walker Hall, University of Florida  
Gainesville, Florida

(1)

Dean. R. E. Johnson  
Graduate College  
University of Illinois  
Urbana, Illinois

(1)

Professor W. C. Huntington, Head  
Department of Civil Engineering  
University of Illinois  
Urbana, Illinois

(1)

Professor A. E. Green  
Kings College  
Newcastle on Tyne, 1  
England

(1)

Dr. L. Fox  
Mathematics Division  
National Physical Laboratory  
Teddington, Middlesex  
England

(1)

Professor W. J. Duncan, Head  
Dept. of Aerodynamics  
College of Aeronautics  
Cranfield, Bletchley  
Bucks, England

(1)

Professor R. V. Southwell  
Imperial College of Science  
and Technology  
Prince Consort Road  
South Kensington  
London S.W. 7, England

(1)